DOC.20041014.0007

OCRWM	DESIGN CALCULATION OR ANALYSIS COVER SHEET	1. QA: QA 2. Page 1

3. System	4. Document Identifier
Waste Isolation System	CAL-WIS-AC-000001 REV 00A

5. Title
Mechanical Assessment of the Waste Package Subject to Vibratory Motion

6. Group
Repository Integration Team - Seismic

7. Document Status Designation
☒ Preliminary ☐ Final ☐ Cancelled

8. Notes/Comments
An AP-2.14Q review of this document is not required as it produces no new calculations, and only summarizes the results of several previous calculations. The supporting calculations to this summary document are not superseded and still provide the references for waste package damage estimates.

Attachments	Total Number of Pages
N/A	N/A

RECORD OF REVISIONS

9. No	10. Reason For Revision	11. Total # of Pgs.	12. Last Pg. #	13. Originator (Print/Sign/Date)	14. Checker (Print/Sign/Date)	15. QER (Print/Sign/Date)	16. Approved/Accepted (Print/Sign)	17. Date
00A	Initial issue	166	6-6	Michael Gross 13 Oct 2004	Sreten Mastilovic 13Oct.2004	Daniel Tunney 10-14-2004	Mark Board For Paul R Dixon 10-14-04	

INTENTIONALLY LEFT BLANK

CONTENTS

Page

CONTENTS (Continued)

Page

CONTENTS (Continued)

Page

INTENTIONALLY LEFT BLANK

FIGURES

Page

FIGURES (Continued)

Page

TABLES

Page

TABLES (Continued)

Page

TABLES (Continued)

Page

TABLES (Continued)

Page

TABLES (Continued)

Page

INTENTIONALLY LEFT BLANK

ACRONYMS

21-PWR	21-pressurized water reactor
CS	carbon steel
FE	finite element
IV	inner vessel
OCB	outer corrosion barrier
PGV	peak ground velocity
PSHA	probabilistic seismic hazard analysis
SNF	spent nuclear fuel
SS	stainless steel
STN	software tracking number
Ti-7	Titanium Grade 7
TSPA-LA	Total System Performance Assessment - License Application

INTENTIONALLY LEFT BLANK

1. PURPOSE

The purpose of this document is to provide an integrated overview of the calculation reports that define the response of the waste package and its internals to vibratory ground motion. The calculation reports for waste package response to vibratory ground motion are identified in Table 1-1. Three key calculation reports describe the potential for mechanical damage to the waste package, fuel assemblies, and cladding from a seismic event. Three supporting documents have also been published to investigate sensitivity of damage to various assumptions for the calculations. While these individual reports present information on a specific aspect of waste package and cladding response, they do not describe the interrelationship between the various calculations and the relationship of this information to the seismic scenario class for Total System Performance Assessment-License Application (TSPA-LA). This report is designed to fill this gap by providing an overview of the waste package structural response calculations.

Table 1-1. Major References for Waste Package Damage Calculations

Damage Process	Calculation Report
Key Report for Kinematics and Structural Response of Waste Package:	
Damage to the waste package from vibratory ground motion	*Structural Calculations of Waste Package Exposed to Vibratory Ground Motion*, 000-00C-WIS0-01400-000-00A (BSC 2004 [DIRS 167083])
Key Report for Damage Caused by Side and End Impacts:	
Calculation of damaged area caused by end-to-end impacts of adjacent waste packages for a predefined set of impact velocities and impact angles	*21-PWR Waste Package Side and End Impacts,* 000-00C-DSU0-01000-000-00B (BSC 2003 [DIRS 162293])
Key Report for G-Loads on Fuel Assemblies Caused by End Impacts:	
Acceleration of the fuel assemblies from end-to-end waste package impacts	*Maximum Accelerations on the Fuel Assemblies of a 21-PWR Waste Package During End Impacts,* 000-00C-DSU0-01100-000-00A (BSC 2003 [DIRS 162602])
Supporting Documents to These Key Reports:	
Sensitivity of damaged area caused by end-to-end impacts of adjacent waste packages to mesh refinement	*21-PWR Waste Package End Impacts – A Mesh Study,* 000-00C-WIS0-02100-000-00A (BSC 2004 [DIRS 170844])
Sensitivity of damaged area to spectral matching and intercomponent variability of ground motion time histories for the 2.44 m/s PGV level	*Additional Structural Calculations of Waste Package Exposed to Vibratory Ground Motion,* 000-00C-WIS0-01700-000-00A (BSC 2004 [DIRS 168385])
Sensitivity of damaged area to interpolation scheme for impact angles between 0-degree and 1-degree	*Alternative Damaged Area Evaluation for Waste Package Exposed to Vibratory Ground Motion,* 000-00C-WIS0-01900-000-00A (BSC 2004 [DIRS 170843])
Other Reports Not Directly Relevant to the Seismic Abstractions:	
Sensitivity of damaged area to in-plane mesh refinement for waste package impact on the emplacement pallet	*Drop of Waste Package on Emplacement Pallet – A Mesh Study,* 000-00C-DSU0-002200-000-00A (BSC 2003 [DIRS 165497])
Analysis of spatial distribution of damaged area on the waste package for criticality analyses	*Spatial Distribution of Damage to Waste Package in Aftermath of Vibratory Ground Motion,* 000-00C-WIS0-01100-000-00A (BSC 2003 [DIRS 166247])
Define relative velocity time histories in the vertical direction between the waste package and emplacement pallet during vibratory ground motion	*Relative Vertical Velocity Between Waste Package and Emplacement Pallet During Vibratory Ground Motion,* 000-00C-WIS0-01800-000-00A (BSC 2004 [DIRS 170850])

21-PWR = 21-Pressurized Water Reactor spent nuclear fuel waste package; PGV = peak ground velocity

Of the nine reports listed in Table 1-1, three are not relevant to abstractions for the seismic scenario class and are not discussed further in this document. The general purpose of the remaining 6 design calculations is to determine the response of the waste package and/or its internals to the vibratory ground motion hazard at the proposed geologic repository at Yucca Mountain, Nevada. More specifically, the output data from the structural response of the waste package and its internals are the basis for development of damage abstractions for the seismic scenario class for TSPA-LA, as described in the *Seismic Consequence Abstraction* model report (BSC 2004 [DIRS 169183]). The results from the structural response calculations also address portions of integrated subissue Integrated Subissue for the Mechanical Disruption of Engineered Barriers, Mechanical Disruption of Engineered Barriers, including the acceptance criteria for this subissue defined in Section 2.2.1.3.2.3 of *Yucca Mountain Review Plan, Final Report* (NRC 2003 [DIRS 163274]).

The purpose of the first two key reports in Table 1-1 is to determine the damaged areas on the waste package from impacts between the waste package and emplacement pallet and from impacts between adjacent waste packages in response to vibratory ground motion. The purpose of the third key report in Table 1-1 is to determine the average and maximum g-loads on the fuel rod assemblies due to impacts between adjacent waste packages. These g-loads define the axial loads on fuel rod cladding, providing the basis for definition of cladding failure during end-to-end impacts of adjacent waste packages.

The three supporting documents in Table 1-1 provide supplemental analyses supporting the results and conclusions in the three key reports. The rationale and results from the supplemental analyses are as follows:

- It is always necessary to demonstrate that the results from a finite element (FE) analysis are insensitive to the level of mesh refinement. The first supporting document reports on a very detailed mesh refinement study for end-to-end impacts of adjacent waste packages, and demonstrates that the original damaged area calculations in *21-PWR Waste Package Side and End Impacts* (BSC 2003 [DIRS 162293]) are almost always conservative.

- Structural response calculations were based on the most current ground motions available at the time the analyses were performed. However, two aspects of the ground motions (intercomponent variability and spectral matching) have changed over time, as explained in Section 1.3.4. The second supporting document evaluates the effect of intercomponent variability and spectral matching for the ground motions at the 2.44 m/s peak ground velocity (PGV) level, and again demonstrates that the range of damaged area in the original calculations (BSC 2004 [DIRS 167083]) is conservative.

- The damaged area calculations for end-to-end impacts incorporate a simple interpolation scheme on impact velocity and impact angle. Damage at an impact angle of zero degrees is substantially less than damage at an impact angle of 1 degree because the impact load is uniformly distributed around the circumference, rather than concentrated at a point. In practice, a zero degree impact is very unlikely because it requires perfect alignment of waste package centerlines. The third supporting document reanalyzes the damaged areas for end-to-end impacts with an alternate interpolation scheme. This

alternate scheme holds damaged area constant at the 1-degree value for impact angles greater than zero degrees and less than 1 degree. This change in interpolation scheme produces only minor changes in total damaged area, in part because multiple impacts at angles greater than 1 degree tend to dominate the total damaged area.

The information in the calculation reports in Table 1-1 is not being superseded by this report. Although selected material from the key reports and supporting documents is repeated in this calculation report, the reports listed in Table 1-1 remain the basic references that document the analyses of waste package response to vibratory ground motion. In particular, the attachments to the reports in Table 1-1 are incorporated by reference, and are not repeated in this report.

This document is prepared in accordance with the applicable technical work plan: *Technical Work Plan For: Regulatory Integration Modeling of Drift Degradation, Waste Package and Drip Shield Vibratory Motion and Seismic Consequences* (BSC 2004 [DIRS 171520]), which directs the work identified in work package ARTM05. The technical work plan was prepared in accordance with AP-2.27Q, *Planning for Science Activities*. Although the underlying reports listed in Table 1-1 use qualified software to perform structural response calculations, no software of any kind has been used in the preparation of this report, so LP-SI.11Q-BSC, *Software Management,* is not applicable to this report. The 21-Pressurized Water Reactor spent nuclear fuel (SNF) waste package (21-PWR) is classified as a Safety Category item by the Q-List (BSC 2004 [DIRS 168361], page A-4). Therefore, this calculation is subject to the requirements of *Quality Assurance Requirements and Description* (DOE 2004 [DIRS 171539]). This document is prepared in accordance with AP-3.12Q, *Design Calculations and Analyses*.

1.1 SCOPE

The scope of this report is limited to summarizing the mechanical response of the waste package and its internals to vibratory ground motion during the postclosure period. All results are evaluated for the outer, Alloy 22 shell of the waste package or for the fuel rod assemblies that are internal to the waste package.

The damage abstractions for the waste package and cladding are not documented in this report; rather, the results from these design calculations provide the input data that the abstractions are based on. The damage abstractions for the seismic scenario class are developed and documented in the *Seismic Consequence Abstraction* model report (BSC 2004 [DIRS 169183]).

This report does not address the performance of naval SNF during seismic events. The Naval Nuclear Propulsion Program Technical Support Document for the License Application will provide the seismic analysis for naval SNF.

1.2 LIMITATIONS

The major limitations of these design calculations are as follows:

- The calculations include degradation of the waste package over a 20,000-year time frame, which includes the initial 10,000-year regulatory period (see Assumption 3.12). The 20,000-year duration for the seismic analyses is designed to demonstrate that repository performance remains robust well after the 10,000 year regulatory period has ended. Calculations of the seismic scenario class beyond 20,000 years will require new structural response calculations with additional levels of structural degradation.

- Calculations are performed for the 21-Pressurized Water Reactor (21-PWR) waste package type. This type of waste package is the most common package type in the repository, constituting 38 percent of the anticipated inventory by package type (BSC 2004 [DIRS 169472], Table 11).

- Structural response calculations for the waste package do not include any initial backfill around the drip shield at the time of the seismic event. This representation is consistent with the present design that does not include an engineered backfill, is consistent with the results from drift degradation analyses under nominal repository conditions, and is consistent with rockfall analyses that indicate complete drift collapse does not occur in the lithophysal zones until a peak ground velocity exceeds 2 m/s in most of the lithophysal zones of the repository (BSC 2004 [DIRS 166107], Section 6.4).

- The ground motion time histories[1] for structural response calculations were created using different approaches for intercomponent variability and for spectral matching. The results from a limited sensitivity study (Section 5.3.7) indicate that the original damage calculations using ground motion time histories for the 2.44 m/s PGV level are conservative. Section 1.3.4 provides a discussion on the methodology for defining the suites of ground motions that are used in the structural response calculations.

1.3 BACKGROUND INFORMATION ON SEISMIC SCENARIO CLASS

This section summarizes information about the seismic scenario class that is relevant to the structural response of the waste package and cladding under vibratory ground motion. This information includes:

- A description of the components of the engineered barrier system

- The anticipated failure mechanisms for these components under seismically-induced loads

- The residual stress damage threshold for failure of Alloy 22 from accelerated stress corrosion cracking

[1] A ground motion time history defines the three-dimensional motion of the earth during a seismic event. Each ground motion time history defines the displacement, velocity, and acceleration in three component directions as a function of time at a specific location in or near the repository.

- The Probabilistic Seismic Hazard Analysis that provides a framework for definition of ground motions at Yucca Mountain
- The procedure for developing site-specific ground motions
- The hazard levels and terminology that are relevant to these calculations.

The focus of this background discussion is on the response of the waste package and cladding to vibratory ground motion; the response of the drip shield to ground motion or to rockfall induced by ground motion and the response of engineered barrier system components to fault displacement is only mentioned in passing. A complete discussion of the technical basis for the seismic scenario class in TSPA-LA can be found in the *Seismic Consequence Abstraction* model report (BSC 2004 [DIRS 169183]).

Figure 1-1 illustrates the major components of the engineered barrier system in a typical emplacement drift. The major engineered barrier system components are the waste package, the drip shield, and the fuel rod cladding (the cladding is not shown in Figure 1-1). These are important components because they provide barriers to the release of radionuclides from the fuel rods into the unsaturated zone. The effectiveness of these barriers is potentially compromised by the direct effects from an earthquake, which include vibratory ground motion, fault displacement, and rockfall induced by ground motion. The effectiveness of these barriers is also potentially compromised by indirect effects after an earthquake, including changes in seepage, temperature, and relative humidity if an emplacement drift collapses completely during a very low probability earthquake.

The major engineered barrier system components are free standing structures. The drip shield and the emplacement pallet rest on top of the invert, while the waste package rests on top of the pallet. The invert consists of a framework of mild steel structural components that is filled with ballast from run-of-the-mine tunneling operations. Because the engineered barrier system components are unconstrained, impacts can occur between waste packages, drip shields, emplacement pallets, the invert, and the drift walls in response to significant ground motions.

1.3.1 Failure Mechanisms Under Seismic Loads

Mechanical processes that occur during a seismic event may compromise the functionality of the waste packages and drip shields as barriers to radionuclide release. These mechanical processes include impacts caused directly by vibratory ground motion during an earthquake, impacts caused by rock blocks and rockfall induced by vibratory ground motions, and mechanical loading from fault displacement.

Under vibratory ground motions, impacts can occur between adjacent waste packages and between the waste package and its emplacement pallet, the surrounding drip shield, and the invert. Impacts can also occur between the drip shield and the emplacement pallet, the invert, and even the drift wall. Rockfall induced by vibratory ground motions can result in impacts on the drip shield in the postclosure period and impacts on the waste packages in the preclosure period, when drip shields are not yet in place. Rockfall induced by vibratory ground motion in the lithophysal zones may collapse the drifts, resulting in static loads from the mass of rubblized

rock surrounding the drip shield. Finally, mechanical loads may be generated by fault displacement within the repository block. In this case, engineered barrier system components may become pinned if fault displacement is greater than the available clearances between components.

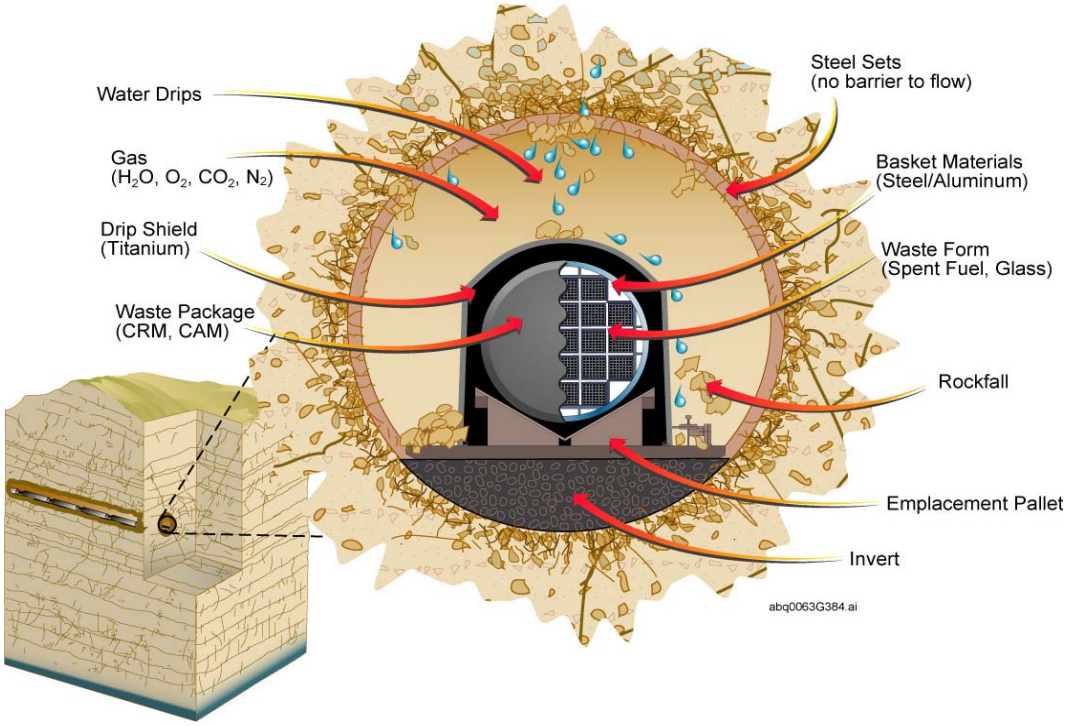

Source: BSC 2004 [DIRS 169183], Figure 6.1-1.

NOTE: CRM=Continuous Recording Monitor; CAM=Continuous Air Monitor.

Figure 1-1. Schematic Diagram of the Engineered Barrier System Components in a Typical Emplacement Drift

These mechanical processes are associated with a number of potential failure mechanisms for the waste package and cladding under vibratory ground motions:

- Peak dynamic loads have the potential to result in immediate puncture or tearing of an engineered barrier system component if the failure criterion is met. A puncture provides a potential pathway for flow into and radionuclide transport out of an engineered barrier system component.

- Impact-related dynamic loads may dent a component, resulting in permanent structural deformation with residual stress. High levels of residual tensile stress may lead to local degradation from accelerated corrosion processes. Areas that are breached from corrosion processes provide a potential pathway for flow into and radionuclide transport out of an engineered barrier system component.

- Impacts between adjacent waste packages, and other impacts involving waste package, impose dynamic loads on waste package internals. These dynamic loads may result in

deformed fuel rods and perforated cladding. Failure of cladding provides a potential pathway for release of radionuclides from fuel rods.

Immediate puncture or tearing of waste packages is unlikely because Alloy 22 is a highly ductile metal that requires very high dynamic loads to reach the tearing failure threshold. Additionally, the tearing failure of ductile material is, in general, accompanied by large distortion and significant expenditure of energy. Consequently, a small tear (through-wall macrocrack) is expected to be encompassed by a much larger highly-distorted region that is the preferable site for stress corrosion cracking. Therefore, a small tear is anticipated to be accounted for by the deformed area, which is defined and discussed in the following paragraph. The potential for immediate breach through tensile or shear failure is included in the nonlinear FE calculations supporting the seismic scenario class; however, the computational meshes are generally too coarse to realistically simulate a small, localized deformation. Supporting calculations for waste package drops on the emplacement pallet indicate that the maximum stress intensity[2] for the impact velocities observed in the vibratory ground motion calculations is significantly below the ultimate tensile strength (BSC 2003 [DIRS 165497]). In this situation, a localized puncture or tearing is very unlikely from impact processes caused by vibratory ground motions and is not included in the seismic scenario class.

On the other hand, the presence of high residual tensile stress has the potential to result in accelerated stress corrosion cracking. This combined mechanical-corrosion failure mechanism is expected to be the most likely cause of failure for the waste package and drip shield from impact processes caused by vibratory ground motions. The areas that exceed the residual tensile stress threshold are referred to as the damaged area throughout this document. The effective area for flow and transport through the damaged areas will be substantially less than the damaged area because the cross-sectional area of the stress corrosion cracks is much less than the total surface area that exceeds the residual stress threshold (BSC 2004 [DIRS 169183], Section 6.3.5).

Application of a residual tensile stress threshold for seismic failures is nonmechanistic in the sense that detailed calculations with accelerated corrosion rates or crack propagation are not used to determine the actual failure time after a seismic event. Rather, the waste package is assumed to fail immediately once the residual tensile stress threshold is exceeded, providing potential pathways for flow and transport through the areas exceeding the residual tensile stress threshold. The residual tensile stress threshold is often referred to as the residual stress threshold or more simply the stress threshold, with the understanding that the principal residual stress must always be tensile to initiate an accelerated corrosion process.

Figure 1-2 is a simplified illustration of how residual stress is generated by permanent (plastic) deformation in a simple uniaxial strain model. The loading path in Figure 1-2 has three phases: (1) elastic loading until reaching the elastic yield limit, (2) plastic loading above the elastic yield limit, and (3) elastic unloading when the external load reduces the local stress. Figure 1-2 also shows that plastic deformation does not always generate a damaged area because the final residual stress state may be compressive or, if tensile, may be below the threshold to

[2] The stress intensity used hereinafter is defined as the difference between the algebraically largest principle stress and the algebraically smallest principal stress at a given point. In other words, the stress intensity is defined as twice the maximum shear stress. It should not be confused with the stress intensity factor used commonly in Fracture Mechanics.

initiate accelerated localized corrosion or stress corrosion cracking. It should be recognized that propagation of a once nucleated stress corrosion crack could be arrested by an encounter with the residual stress field that is unfavorable for further propagation.

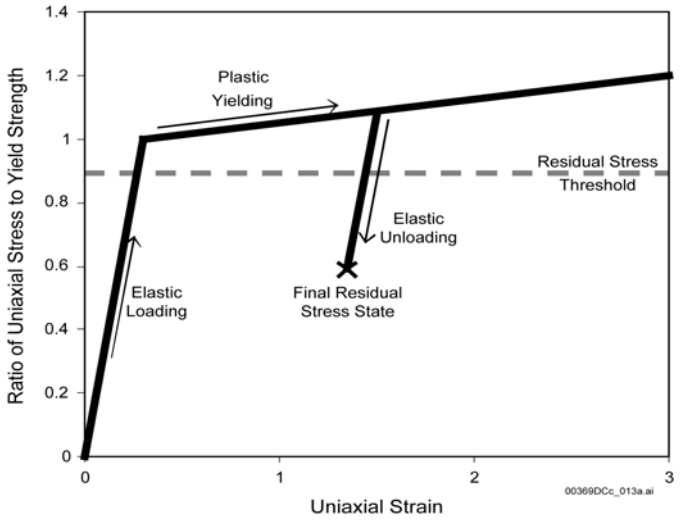

Source: BSC 2004 [DIRS 169183], Figure 6.3-1.

Figure 1-2. Permanent Deformation from Plastic Yielding Generates Residual Stress

The dynamic loads on fuel rods from end-to-end impacts of adjacent waste packages and from impacts between waste package and pallet (and, to a smaller degree, the drip shield) have the potential to fail the cladding. In the former case, direction of the fuel rods loading is predominantly axial while in the latter is transversal. The primary cladding failure mechanism is perforation due to acceleration (g-loads) in the axial and transversal direction of the fuel rods (BSC 2004 [DIRS 169183], Section 6.5.7). The primary deformation mode of axially loaded fuel rods (end-to-end impact of adjacent waste packages) is buckling and the resulting cladding failure mechanism is the only one considered in this study. The g-loads required to buckle fuel rods are estimated from a simple analytic model based on Euler buckling of a column (Chun et al. 1987 [DIRS 144357]). It is estimated that the cladding fails when the impact accelerations are in the range of 82 g to 252 g for axial impacts (and 63 g to 211 g for lateral impacts) (Chun et al. 1987 [DIRS 144357], Table 4).

1.3.2 Residual Stress Damage Threshold for the Waste Package

Accelerated stress corrosion cracking from high residual stress is expected to be the most likely cause of failure for the waste package from impact processes under vibratory ground motion. The residual stress thresholds for seismic response are similar to the criteria for initiation of stress corrosion cracking on smooth surfaces of Alloy 22 (BSC 2004 [DIRS 169042], Section 6.2.1), with thresholds defined on page 22). The use of a stress corrosion cracking initiation criterion is appropriate for seismic analysis because regions where the residual stress from mechanical damage exceeds the tensile failure criterion are expected to be severely cold-worked and, hence, potentially subject to enhanced stress corrosion cracking.

A residual stress threshold is a conservative failure criterion because detailed corrosion models will have a delay time until failure. A conservative approach is appropriate because it is

consistent with other tensile failure criteria (BSC 2004 [DIRS 169042], Section 6.2.1, second paragraph on page 22), because the residual stress failure criterion is transparent, and because it is easily applied to the output from structural response calculations.

The residual stress threshold for failure of the waste package is represented by a uniform distribution with a lower bound of 80 percent of the yield strength of Alloy 22 and an upper bound of 90 percent of the yield strength of Alloy 22. The upper bound is based on experimental data and conservatively incorporates a safety factor of 2.2 because of the very long lifetime of the waste package (BSC 2004 [DIRS 169042], Section 6.2.1, second paragraph on page 22). The lower bound is introduced to evaluate the sensitivity of damaged area to potential uncertainty in the residual stress threshold. This residual stress criterion (80 to 90 percent of the yield strength) is also consistent with the failure criterion for initiation of stress corrosion cracking in other waste package analyses.

In practice, the damage to the waste package has been evaluated at the extremes of the uniform distribution. The results from each structural response calculation are post-processed to determine the elements in the outer corrosion barrier (OCB) of the waste package whose residual stress exceeds 80 percent of the yield strength of Alloy 22 and to determine the elements in the OCB of the waste package whose residual stress exceeds 90 percent of the yield strength of Alloy 22. These elements are then converted into an area susceptible to accelerated stress corrosion cracking at the 80 and 90 percent criteria. The appropriate areas at intermediate values of the residual stress threshold can then be defined by linear interpolation between the extremes. The elements that exceed 90 percent of the yield strength are always a subset of the elements that exceed 80 percent of the yield strength. In other words, the damaged area for the 90 percent residual stress threshold is always less than or equal to the damaged area for the 80 percent residual stress threshold.

1.3.3 Probabilistic Seismic Hazard Analysis

A probabilistic seismic hazard analysis (PSHA) was performed to assess the seismic hazards of vibratory ground motions and fault displacement at Yucca Mountain. The PSHA (CRWMS M&O 1998 [DIRS 103731]) provides quantitative hazard results to support an assessment of the repository's long-term performance and to form the basis for developing seismic design criteria for the License Application. Key attributes of the PSHA methodology for Yucca Mountain are (1) utilization of an extensive geologic and seismologic database developed over a 20 year period in the Yucca Mountain region; (2) explicit consideration and quantification of uncertainties regarding alternative seismic-source, ground-motion, and fault-displacement models; and (3) use of a formal, structured expert elicitation process to capture the informed scientific community's views of key inputs to the PSHA.

The PSHA methodology for vibratory ground motions has become standard practice for deriving vibratory ground motion hazards for design purposes. Less commonly, probabilistic fault displacement analyses are conducted to provide quantitative assessments of the location and amount of differential ground displacement that might occur. Both analyses provide hazard curves, which express the probability of exceeding various amounts of ground motion (or fault displacement). The probability is usually expressed as a frequency of exceedance per year. The resulting seismic hazard curves represent the integration over all earthquake sources and

magnitudes of the probability of future earthquake occurrence and, given an occurrence, its effect at a site of interest.

The basic elements of a PSHA for vibratory ground motions are:

a) Identification of seismic sources that contribute to the vibratory ground motion hazard at Yucca Mountain and characterization of their geometry

b) Characterization of seismic sources by the recurrence rate of earthquakes of various magnitudes and the maximum magnitude

c) Attenuation relations that define a specified ground motion parameter (such as PGV) as a function of magnitude, source-to-site distance, local site conditions, and, in some cases, seismic source characteristics

d) Integration of the seismic source characterization and ground motion attenuation evaluations, including associated uncertainties, into a seismic hazard curve and associated uncertainty distribution.

The PSHA incorporates both variability and uncertainty. Variability, also termed randomness or aleatory variability, is the natural randomness in a process. For discrete variables, the randomness is parameterized by the probability of each possible value. For continuous variables, the randomness is parameterized by the probability density function. An example of variability is the amplitude of ground motion that would occur at a particular location from repeated earthquakes having exactly the same magnitude at exactly the same distance (magnitude 6 at 25 km distance). Variations in ground motion amplitude are expected due to unknowable complexities in earthquake-to-earthquake source properties and in the propagation path.

Uncertainty, also termed epistemic uncertainty, is the scientific uncertainty in the model of the process. It is due to limited data and knowledge. The uncertainty is characterized by alternative models. For discrete random variables, the epistemic uncertainty is modeled by alternative probability distributions. For continuous random variables, the uncertainty is modeled by alternative probability density functions. Examples of uncertainty are alternative ground motion attenuation relations that express the amplitude of ground motion at a particular site as a function of distance to the source and earthquake magnitude. Unlike variability, uncertainty is potentially reducible with additional knowledge and data.

Given the input evaluations, the hazard calculation method integrates over all values of the variables and estimates the annual probability of exceedance of any ground-shaking amplitude at the site. The hazard curve quantifies the variability of the earthquake occurrence and ground-shaking attenuation. In addition to the variability of the seismic hazard, however, is uncertainty about the seismotectonic environment of a site. Significant advances in development of methodology to quantify uncertainty in seismic hazard have been made in the past 20 years (Budnitz et al. 1997 [DIRS 103635]). These advances involve the development of alternative interpretations of the seismotectonic environment of a site by multiple experts and the structured characterization of uncertainty. Evaluations by multiple experts are made within a structured expert elicitation process designed to minimize uncertainty due to uneven or incomplete knowledge and understanding (Budnitz et al. 1997 [DIRS 103635]). The weighted alternative

interpretations are expressed by use of logic trees. Each pathway through the logic tree represents a weighted interpretation of the seismotectonic environment of the site for which a seismic hazard curve is computed. The result of computing the hazard for all pathways is a distribution of hazard curves representing the full variability and uncertainty in the hazard at a site.

The seismic scenario class for TSPA-LA uses the mean hazard curves for PGV and for fault displacement. Each mean hazard curve, which is defined as an average of the distribution of hazard curves referred to in the preceding paragraph, typically lies above the 80th percentile of the distribution because the average is dominated by the larger values of the distribution. The use of the mean hazard curves simplifies the Monte Carlo sampling process for TSPA. It is also appropriate for calculations of the mean dose to the reasonably maximally exposed individual, as required to demonstrate acceptable repository performance over 10,000 years (10 CFR 63.303 and 63.311 [DIRS 156605]). However, the use of the mean hazard curves does not propagate the epistemic uncertainty in the distributions of the hazard curves into TSPA.

1.3.4 Site-Specific Ground Motions

Site-specific ground motions are needed for the structural response calculations supporting postclosure performance assessment. Ground motion results from the PSHA are for a hypothetical reference rock outcrop and do not reflect site-specific soil and rock properties at the locations for which the ground motions are needed (e.g., the horizon where the emplacement drifts are located). The PSHA was conducted in this fashion because the site-specific rock and soil properties were not characterized at the time of the PSHA. Thus, further analyses are carried out to modify the PSHA results to reflect the appropriate site-specific conditions for the site of interest.

For analyses supporting postclosure performance assessment, site-specific ground motions are developed for the waste emplacement level. Selection of annual exceedance probabilities is motivated by the requirement to "*consider only events that have at least one chance in 10,000 of occurring over 10,000 years*" (10 CFR 63.114(d) [DIRS 156605]). To address this requirement, ground motions are developed for annual exceedance probabilities of 10^{-5}, 10^{-6}, and 10^{-7} per year. Analyses using the developed ground motions form the basis for evaluating repository performance for seismic events with annual exceedance probabilities from 10^{-4} per year to as low as 10^{-8} per year.

A detailed site response model provides the basis for development of seismic time histories at the emplacement drifts. Different approaches are used for developing time histories depending on how they will be used (e.g., in design or in evaluating postclosure repository performance). For Yucca Mountain, three approaches have been used to develop time histories: spectral matching, scaling to PGV, and scaling to PGV preceded by spectral conditioning. The spectral-matching approach is used primarily to develop time histories that will be used in design analyses and is not discussed further here.

The peak-ground-velocity scaling approaches are used to develop time histories for postclosure analyses, such as the calculations documented in this report. In addition to determining the consequences of these low-probability ground motions, another goal is to evaluate the variability

in the consequences. Because much of the variability in consequences will be driven by random variability in ground motion, the time histories for postclosure analyses are developed to capture and represent that random variability.

PGV is selected as the scaling parameter for the ground motions because damage to underground structures has been correlated with PGV (McGarr 1984 [DIRS 163996], page 206). PGV is appropriate for structural damage caused by sliding or impact under earthquake loads (Newmark and Rosenblueth 1971 [DIRS 151246], Section 11.3.5 and Section 11.4). Finally, PGV is also appropriate for the response of a rock mass to dynamic loading because the change in stress across a weak compression wave is directly proportional to the particle velocity. The abstractions in this document therefore use the horizontal PGV as the measure of the amplitude of the ground motion. Alternate measures, such as peak ground acceleration or the spectral acceleration at a given frequency, are anticipated to give similar results.

In the PGV-scaling approach, the earthquake recordings are scaled such that the PGV matches the PGV determined in the site-response analysis for a location of interest. The records may be scaled such that both horizontal components match the target horizontal PGV and the vertical component matches the target vertical PGV. Alternatively, one horizontal component may be scaled to the target horizontal PGV and the scaling of the other components done in a manner to maintain the intercomponent variability of the original recordings. Both of these methods have been used at Yucca Mountain.

For each annual exceedance probability of interest, 17 sets of time histories are developed. Each set of time histories consists of acceleration, velocity and displacement in each of two horizontal component directions and in the vertical component direction. The site-specific time histories are based on actual recordings of strong ground motion from earthquakes in the western United States and around the world (McGuire et al. 2001 [DIRS 157510], Appendix B). Recordings are selected to represent those earthquakes that dominate the seismic hazard at a given annual probability of exceedance. In other words, the recordings used as a basis for the time histories are selected to have a range of magnitudes and distances that corresponds to the magnitudes and distances of earthquakes contributing to the seismic hazard at the given annual exceedance probability. By basing the time histories on actual earthquake recordings and choosing records consistent with the seismic hazard, the resulting time histories will exhibit realistic phase characteristics and durations.

A variation of the PGV-scaling approach involves spectral conditioning of the original strong-ground-motion records before using them to develop time histories. Spectral conditioning modifies the original strong motion records such that their response spectra reflect to a greater degree the site conditions at Yucca Mountain. Conditioning can be done with respect to the PSHA reference rock outcrop conditions or to the waste emplacement level conditions that reflect the site response. Conditioning can be thought of as a weak spectral match. A strong spectral match is not desired in this case because it would tend to reduce the random variability of the original recordings.

For the annual exceedance probability of 10^{-6} per year, two suites of 17 sets of time histories each were developed. The 17 sets of recorded strong ground motion that form part of the basis for the time histories were selected to represent the range of magnitudes and distances consistent

with the range indicated by the PSHA. The first suite consists of time histories for which both horizontal components were scaled to the site-specific horizontal PGV and the vertical component was scaled to the site-specific vertical PGV. The observed intercomponent variability is therefore not maintained for the first suite. Also, the records used to generate the time histories were not spectrally conditioned prior to scaling.

A second suite of time histories for an annual probability of exceedance of 10^{-6} was developed by first spectrally conditioning the records to weakly match Yucca Mountain site conditions based on the response spectra for the PSHA reference rock outcrop. Specifically, the ratios between mean response spectra for average western U.S. conditions and mean response spectra for the PSHA reference rock outcrop at Yucca Mountain were determined. The western U.S. response spectra are considered typical of the strong motion records forming the basis for Yucca Mountain time histories. These ratios, or transfer functions, were then applied to the response spectrum for each of the strong ground motion records to be used in generating time histories. Finally, the modified response spectra formed targets for weak spectral matches of the original records. Following this conditioning, the records were scaled to the site-specific PGV. In this case, only one horizontal component was scaled to the PGV and the other components were scaled to preserve the intercomponent variability of the original records.

Two suites of 17 sets of time histories were also developed for an annual exceedance probability of 10^{-7}. For both of these suites, the records forming the basis for the time histories were spectrally conditioned prior to scaling. In one case, they were spectrally conditioned to weakly match the response spectra for the PSHA reference rock outcrop, similar to the approach for the second suite of ground motions for 10^{-6} annual exceedance probability. In the second case, they were conditioned to the site-specific response spectra for the waste emplacement area.

Analyses of waste package structural response used the most current suite of ground motions that were available when the calculations were performed. The waste package structural response calculations for the 10^{-6} per year ground motions were performed with the first suite of ground motions, wherein the time histories are scaled to the known values of PGV in the horizontal and vertical directions; intercomponent variability was not preserved. The waste package structural response calculations for the 10^{-7} per year ground motions were again performed with the first suite of ground motions that were spectrally conditioned to the reference rock outcrop and preserved the intercomponent variability of the original records.

1.3.5 Terminology for Ground Motion Level

The terminology for the ground motion hazard curves and for the suite of ground motions corresponding to a given exceedance frequency is explained here. A mean ground motion hazard curve defines the relationship between the mean estimate of the mean annual frequency of exceedance and the amplitude of the vibratory ground motion, measured by PGV. The mean annual exceedance frequency represents the mean value of the frequency in any year with which future seismic events will exceed a given value of the PGV or fault displacement.

The mean annual exceedance frequency spans many orders of magnitude, from a minimum of 10^{-8} per year to a maximum of 1 per year (or greater). The mean frequency is defined as the number of observed events, divided by the time interval of observation. It varies randomly from

one observation to the next. We use the mean of this random number as a measure of how likely an event is over any future year. When the mean annual exceedance frequency of interest is much less than 1, as it is here, the mean annual exceedance frequency and the annual exceedance probability are essentially equal[3]. This report uses the term exceedance frequency because it is more general, although the annual exceedance frequency and annual exceedance probability are interchangeable for the very infrequent seismic hazards considered in this study. The ground motion hazard curve for this report is based on the mean annual exceedance frequency.

The effect of vibratory ground motion on the engineered barrier system components is assessed for a set of ground motions with a given value of the horizontal PGV. Sets of 15 three-component ground motions have been developed for a PGV of 2.44 m/s and for a PGV of 5.35 m/s. These ground motion sets are often referred to as the 10^{-6} per year and the 10^{-7} per year ground motions (respectively) because PGV values of 2.44 m/s and 5.35 m/s correspond to these frequency values on the hazard curve at the emplacement drifts. Unfortunately, this convenient terminology is misleading because a seismic event with a PGV of 2.44 m/s will NOT occur with a frequency of 10^{-6} per year. The correspondence of 2.44 /s with 10^{-6} per year on the mean hazard curve means that all ground motion events with PGV greater than 2.44 m/s occur with a mean annual frequency of 10^{-6} per year. In other words, the ensemble of seismic ground motions with PGV exceeding 2.44 m/s will occur with a mean frequency of 10^{-6} per year. As an aside, the probability of encountering an earthquake with a PGV of exactly 2.44 m/s is infinitesimally small, and will certainly not occur with a frequency of 10^{-6} per year.

In this report, ground motions are identified by the appropriate value of PGV because the value of PGV provides a unique and unambiguous identifier for each set of ground motions, even when multiple hazard curves have been developed for a site. For the reader's convenience, the following list identifies the correspondence between the values of annual exceedance frequency at the emplacement drifts and the values of PGV in this report:

- PGV of 0.19 m/s corresponds to the 5×10^{-4} per year exceedance frequency.
- PGV of 0.384 m/s corresponds to the 10^{-4} per year exceedance frequency.
- PGV of 1.05 m/s corresponds to the 10^{-5} per year exceedance frequency[4].
- PGV of 2.44 m/s corresponds to the 10^{-6} per year exceedance frequency.
- PGV of 5.35 m/s corresponds to the 10^{-7} per year exceedance frequency.

[3] The probability of one or more events for a Poisson process with annual rate λ {1/year}over duration T {years} is given by $(1 - e^{-\lambda T})$. When λ is small enough, the probability that one or more events occur in an interval T becomes $(1 - e^{-\lambda T}) = 1 - (1 - \lambda T + (\lambda T)^2 - \ldots) \approx \lambda T$, so the annual probability for one or more events is given by $(\lambda T)/\mathrm{T} = \lambda$. A typical criterion for the accuracy of this expansion is for $\lambda T \leq 0.1$.

[4] Three preliminary ground motions corresponding to the 10^{-5} per year exceedance frequency were developed before the exact PGV value of 1.05 m/s was available. The approximate value of PGV corresponding to the 10^{-5} per year exceedance frequency was estimated to be 0.992 m/s, based on the scaled hazard curve (BSC 2004 [DIRS 169183], Figure 6.4-2 and Appendix A). The PGV value of 0.992 m/s is used to describe these preliminary ground motions, when appropriate.

2. METHOD

The waste package calculations presented in this overview document were conducted using commercial FE software. The FE method is a numerical technique in common use for analysis of engineering problems in structural dynamics. The method requires discretization of the structure as a number of elements that are interconnected by nodal points (the FE mesh). The governing equations of motion, subject to imposed boundary and initial conditions, are solved to provide the solution of the transient mechanical response of the structure. The boundary and initial conditions imposed on a waste package in this particular case are a result of the constraints supplied by the emplacement drift, adjacent waste packages, drip shield, and pallet; and from the applied dynamic loading conditions. The explicit FE method with the central difference method of time integration was employed in all calculations. Results are given in terms of the transient induced stresses, strains and displacements. Three-dimensional graphical representation of the motion of the waste package as well as the stress and strain states are used to aid in interpretation of the results.

The design of the 21-PWR waste package is used for all calculations and is defined in *Repository Design, Waste Package, Project 21-PWR Waste Package with Absorber Plates, Sheet 1 of 3, Sheet 2 of 3, and Sheet 3 of 3* (BSC 2001 [DIRS 157812]); exceptions are the gap between the inner vessel (IV) and the OCB, for which a value of 4 mm was used (Plinsky 2001 [DIRS 156800], Section 8.1.8), and the OCB thickness, for which a value of 18 mm was assumed (Assumption 3.12). The sketch in (BSC 2004 [DIRS 167083], Attachment I) provides additional information not included in *Repository Design, Waste Package, Project 21-PWR Waste Package with Absorber Plates, Sheet 1 of 3, Sheet 2 of 3, and Sheet 3 of 3* (BSC 2001 [DIRS 157812]).

The methods for the calculations in the three key reports identified in Table 1-1 are as follows:

- *Structural Calculations of Waste Package Exposed to Vibratory Ground Motion* (BSC 2004 [DIRS 167083])

  The structural response calculations were performed using off-the-shelf versions of commercially available FE programs. The FE mesh was created with the ANSYS V5.6.2 FE code (Software Tracking Number [STN] 10364-5.6.2-01, BSC 2002 [DIRS 159357]). Calculations were then performed with the LS-DYNA V960.1106 (STN 10300-960.1106-00, BSC 2002 ([DIRS 158898]) FE code or performed with the LS-DYNA V970.3858 (STN 10300-970.3858 D SMP-00, BSC 2003 [DIRS 166139]) FE code. All versions of LS-DYNA are simply referred to as LS-DYNA, unless it is necessary to distinguish features of different versions.

  These calculations also require design information for the emplacement pallet and drip shield. Design of the emplacement pallet (pallet, for brevity, throughout the document) is defined in *Emplacement Pallet* (BSC 2003 [DIRS 161520]); the sketch in *Structural Calculations of Waste Package Exposed to Vibratory Ground Motion* (BSC 2004 [DIRS 167083], Attachment II) provides additional information not included in (BSC 2003 [DIRS 161520]) (see also Assumption 3.8). Finally, design of the

interlocking drip shield (DS) used in this calculation is provided in *D&E / PA/C IED Interlocking Drip Shield and Emplacement Pallet* (BSC 2004 [DIRS 169220]).

A set of 15 structural response calculations is performed at each of two different ground motion amplitudes: 2.44 m/s PGV and 5.35 m/s PGV level, corresponding to the 10^{-6} and the 10^{-7} annual exceedance frequencies, respectively. One calculation is also performed at each of 0.19 m/s and 0.384 m/s PGV levels, corresponding to the 5×10^{-4} and 1×10^{-4} annual exceedance frequencies, respectively. Additionally, three simulations are performed using approximate time histories with a 0.992 m/s PGV level, corresponding to an annual exceedance frequency of 10^{-5} per year. These approximate time histories are created by scaling the three acceleration components for selected 2.44 m/s PGV level time histories, as explained in Section 1.3.5 and in *Structural Calculations of Waste Package Exposed to Vibratory Ground Motion* (BSC 2004 [DIRS 167083], Attachment XI).

Fifteen ground motion time histories are required for the calculations at the 2.44 m/s and 5.35 m/s PGV levels. The fifteen ground motions represent the uncertainty in the seismic sources and in seismic wave propagation through geologic media, as explained in Sections 1.3.3 and 1.3.4. The uncertainty in the ground motions is substantial. For example, at the 5.35 m/s PGV level, the first horizontal velocity component is scaled to always have a PGV of 5.35 m/s. However, the range in PGV values for the second horizontal velocity component is 1.72 m/s to 17.9 m/s, and the range in PGV values for the vertical velocity component is 2.27 m/s to 17.1 m/s (BSC 2004 [DIRS 166107], Appendix X). In fact, the uncertainty in the ground motions is the dominant uncertainty in the damaged areas from the structural response calculations, as shown by the results in Tables 5.3-22 and 5.3-55.

- *21-PWR Waste Package Side and End Impacts* (BSC 2003 [DIRS 162293])

  The structural response calculations were performed using off-the-shelf versions of commercially available FE programs. ANSYS V5.4 (CRWMS M&O 1998 [DIRS 153710]) was used to generate the FE meshes. The calculations were then performed with the commercially available LS-DYNA V950 FE code (CRWMS M&O 2000 [DIRS 149714]) or with the LS-DYNA V960.1106 FE code (BSC 2002 [DIRS 158898]).

  Ground motion time histories are not required for these calculations. Rather, the range of impact velocities and impact angles observed in the calculations for *Structural Calculations of Waste Package Exposed to Vibratory Ground Motion* (BSC 2004 [DIRS 167083]) provides the basis for developing a matrix of representative values of the impact velocity and impact angle. This matrix and the damaged areas associated with each representative impact provide a basis for determining damaged areas by interpolation for the multiple waste package-to-waste package impacts in each realization, as summarized in Sections 5.3, 5.3.1, 5.3.2, and 5.3.3 of this report.

- *Maximum Accelerations on the Fuel Assemblies of a 21-PWR Waste Package During End Impacts* (BSC 2003 [DIRS 162602])

  The structural response calculations were performed using off-the-shelf versions of commercially available FE programs. ANSYS V5.4 (CRWMS M&O 1998 [DIRS 153710]) was used to generate the FE meshes. The calculations were then performed with the commercially available LS-DYNA V950 FE code (CRWMS M&O 2000 [DIRS 149714]) or with the LS-DYNA V960.1106 FE code (BSC 2002 [DIRS 158898]).

  Ground motion time histories are not required for these calculations. Rather, the range of impact velocities and impact angles observed in the calculations for *Structural Calculations of Waste Package Exposed to Vibratory Ground Motion* (BSC 2004 [DIRS 167083]) provides the basis for developing a matrix of representative values of the impact velocity and impact angle. This matrix and the g-loads on the fuel rod assemblies for each representative impact provide a basis for determining cladding failure under the multiple waste package-to-waste package impacts summarized in Sections 5.3.1, 5.3.2, and 5.3.3 of this report.

The methods of the calculations in the supporting documentation for the seismic scenario are as follows:

- *21-PWR Waste Package End Impacts – A Mesh Study* (BSC 2004 [DIRS 170844])

  This calculation is a supplemental study of mesh sensitivity for the damaged area from end impacts. This study is based on the general approach and results for end impact calculations documented in *21-PWR Waste Package Side and End Impacts* (BSC 2003 [DIRS 162293]), with appropriate changes to the FE mesh. The design of the 21-PWR waste package is used for all calculations and is defined in *Repository Design, Waste Package, Project 21-PWR Waste Package with Absorber Plates, Sheet 1 of 3, Sheet 2 of 3, and Sheet 3 of 3* (BSC 2001 [DIRS 157812]); exceptions are the gap between the IV and the OCB, for which a value of 4 mm is used (Plinsky 2001 [DIRS 156800], Section 8.1.8), and the OCB thickness, for which a value of 18 mm is assumed (Assumption 3.12). All material properties are evaluated at 150ºC, which is the base case for structural response in the seismic scenario. Finally, ground motion time histories are not required for these calculations.

  The structural response calculations were performed using off-the-shelf versions of commercially available FE programs LS-DYNA Version (V) 970.3858 D SMP-00 and LS-DYNA V970.3858 D MMP-00 (BSC 2003 [DIRS 166139] and BSC 2003 [DIRS 166918]).

- *Additional Structural Calculations of Waste Package Exposed to Vibratory Ground Motion* (BSC 2004 [DIRS 168385])

  This calculation is a supplemental study of the sensitivity of damaged area to the conditioning of ground motion time histories. This study is based on the general

approach and results documented in *Structural Calculations of Waste Package Exposed to Vibratory Ground Motion* (BSC 2004 [DIRS 167083]), with appropriate changes for the ground motions.

Four additional calculations are performed with selected ground motions from the 2.44 m/s PGV level. The original ground motions (BSC 2004 [DIRS 167083]) did not preserve intercomponent variability in the original ground motion recordings and were not spectrally conditioned. The new ground motions (BSC 2004 [DIRS 168385]) preserved intercomponent variability in the original ground motion recordings and were spectrally conditioned for ground motions typical of the western United States. The issues of spectral conditioning and intercomponent variability are discussed in more detail in Section 1.3.4.

The structural response calculations were performed using an off-the-shelf version of commercially available FE program LS-DYNA Version (V) 970.3858 D SMP-00 (BSC 2003 [DIRS 166139]).

- *Alternative Damaged Area Evaluation for Waste Package Exposed to Vibratory Ground Motion* (BSC 2004 [DIRS 170843])

  This calculation is a supplemental study of the sensitivity of damaged area to the interpolation scheme for impact angles between zero degrees and one degree. The calculations documented in (BSC 2004 [DIRS 167083]) determine the timing, speed, and impact angle for multiple waste package-to-waste package impacts between adjacent waste packages exposed to ground motion time histories. The calculations documented in (BSC 2003 [DIRS 162293]) define the damaged areas on the waste package that result from individual end impacts at specific values of the impact speed and impact angle. This matrix of values provides a basis for predicting end-to-end damage under the complex kinematics of multiple impacts. The methodology in (BSC 2004 [DIRS 167083]) uses a linear interpolation on impact angle to estimate damaged area. However, ideal zero degree impacts are anticipated to be extremely unlikely because they require perfectly flat contact and because the centerlines of adjacent packages must be perfectly collinear. Since it will be very difficult to achieve the ideal zero degree impact, it may be more reasonable to estimate damage for low angle impacts (i.e., those below 1 degree) with the damaged area for a one-degree impact. In other words, all impact angles greater than zero and less than one degree are assumed to be one degree for purposes of damage estimation.

  This supplemental study consists entirely of recalculating by hand the damaged areas in (BSC 2004 [DIRS 167083]). No new structural response calculations were performed for this study. It follows that ground motion time histories are not required for this study and no qualified software is required for this study.

Damaged area is estimated from the residual stress distribution and a residual stress threshold for accelerated stress corrosion cracking of Alloy 22 in (BSC 2004 [DIRS 167083]) and (BSC 2003 [DIRS 162293]). The residual stress threshold is defined as a fraction of the yield strength of the OCB material, Alloy 22 [SB-575 N06022], at given temperature. Lower and

upper thresholds for Alloy 22 are based on 80 percent and 90 percent of the yield strength of Alloy 22 (see discussion in Sections 1.3.1 and 1.3.2). The yield strength and other material properties are generally evaluated at a temperature of 150°C. However, a few simulations use 100ºC (BSC 2003 [DIRS 162293], Tables 9 to 11) or 200°C (BSC 2004 [DIRS 167083], Attachments V and VIII, and BSC 2003 [DIRS 162293], Tables 7 and 8) for sensitivity purposes.

The residual stress distribution is evaluated from plots of the residual first principal stress in the OCB of the waste package. These plots are prepared by the postprocessing programs available with LS-DYNA. Analysis of the residual first principal stress in these plots identified those elements wherein the residual tensile stress exceeded the residual stress threshold for accelerated stress corrosion cracking. It is important to acknowledge that this failure criterion is applied in a very conservative manner. Namely if an element on either (inner or outer) surface of the OCB exceeds the residual stress threshold, then the area "fails" (i.e., it is considered damaged by accelerated stress corrosion cracking) regardless of the residual stress distribution across the thickness of the shell. If an element on the outer surface fails, then all elements beneath this element are assumed to fail, even though a compressive stress state may arrest crack propagation through the OCB.

INTENTIONALLY LEFT BLANK

3. ASSUMPTIONS

The following assumptions are made regarding the FE representations in *Structural Calculations of Waste Package Exposed to Vibratory Ground Motion* (BSC 2004 [DIRS 167083]) and in *Additional Structural Calculations of Waste Package Exposed to Vibratory Ground Motion* (BSC 2004 [DIRS 168385]). Assumptions related to calculation of material properties at 100°C, 150°C, and 200°C are not listed here, but can be found in Section 3 of the referenced documents.

3.1 The exact geometry of the waste package internals is simplified for this calculation. The waste package IV (including the IV lids) and its internals, including SNF, are represented by a thick-wall cylinder of 316 stainless steel (SS) with uniform thickness and circular cross section (see Section 5.2). The thickness of this cylinder is determined by the cumulative mass of these components. The rationale for this assumption is that the IV and the SNF affect the results of this calculation predominantly through their total mass and overall dimensions. This assumption is used in Section 5.2.1.2.

3.2 The friction coefficients for metal-to-metal contact and metal-to-rock contact are considered random parameters in this calculation. The range of values for both of these friction coefficients is 0.2 to 0.8. The rationale for this assumption follows:

Coefficients of static and sliding friction for various metals and other materials are provided in various handbooks (for example, Avallone and Baumeister 1987 [DIRS 103508], Table 3.2.1, page 3-26). However, the coefficients of friction for the specific materials in this calculation are not defined in this handbook. In addition, the potential for long-term corrosion to modify the sliding friction must also be considered in defining the friction coefficient. In this situation, the appropriate coefficients of friction for the repository components have high uncertainty. It is thus appropriate to pick a distribution of values for the coefficients of friction that encompass a range of materials and a range of mechanical responses from little or no sliding between components to substantial sliding between components.

A distribution of values for the friction coefficient between 0.2 and 0.8 will achieve these goals (DTN: MO0301SPASIP27.004. [DIRS 161869], Table I-4). First, this distribution is broad enough to encompass typical values of the dry sliding friction coefficients for a wide variety of metals and other materials (Avallone and Baumeister 1987 [DIRS 103508], Table 3.2.1, page 3-26). The appropriateness of this range is independently confirmed by seismic analyses for spent fuel storage racks (DiGrassi 1992 [DIRS 161539]). This distribution is also broad enough to represent a range of mechanical response for the waste package, pallet, and drip shield. A friction coefficient near 0.2 maximizes sliding of the waste package on the pallet, of the pallet on the invert, and of the drip shield on the invert. Similarly, a friction coefficient near 0.8 minimizes sliding among the various components. This assumption is used in Sections 5.2.1.2, 5.2.2.2.1 and 5.2.3.2.1.

3.3 The variation of functional friction coefficient between the static and dynamic values as a function of relative velocity of the contact surfaces is not available in the literature for the materials used in this calculation (see Section 5.2.1.2). The effect of relative velocity of the contact surfaces is neglected in these calculations by assuming that the functional friction coefficient and the static friction coefficient are both equal to the dynamic friction coefficient. The impact of this assumption on results presented in this document is anticipated to be negligible. The rationale for this conservative assumption is that it provides the bounding set of results by minimizing the friction coefficient within the given FE analysis framework. This assumption is used in Section 5.2.1.2 and corresponds to Mecham 2004 ([DIRS 170673], paragraph 5.2.14.2).

3.4 The FE representation of the drip shield is simplified in this analysis (see Section 5.2 for details), and the density of Titanium Grade 7 (Ti-7) is modified to conserve mass in the simplified representation. The impact of this assumption on results presented in this document is anticipated to be negligible. The rationale for this assumption is that it captures the essential kinematics of freestanding components in the drift while reducing the computer execution time. This assumption is used in Section 5.2.1.2.

3.5 Interactions with neighboring (adjacent) waste packages are represented by using a rigid longitudinal boundary that is attached to the invert. That is, for the purposes of calculating the damaged area on the waste package, the interaction between adjacent waste packages is assumed to be adequately described by a sequence of impacts of the waste package on a rigid wall (BSC 2003 [DIRS 162293]). The rationale for this assumption is that the initial longitudinal distance between adjacent waste packages is only 0.1 *m* (BSC 2004 [DIRS 168489], Table 1). In the course of the strong vibratory ground motions considered in this study, it is conceivable but very unlikely that the motion of the waste package-pallet assemblies would result in the local pile-up of the assemblies along the drift. In this situation, the impact of the adjacent waste package is represented by an unyielding, reflective boundary that is fixed to the invert. This assumption is used in Section 5.2.1.2.

This assumption provides a major simplification for the calculations, but is probably extremely conservative. Low frequency seismic waves have waste lengths that are much longer than the characteristic length scale of the waste package (about 5 meters). In this situation, adjacent waste packages are more likely to move in tandem. It follows that the damage from end-to-end impacts of adjacent waste packages is overestimated by the computational approach.

3.6 The interaction between the waste package and drip shield through lateral or side impacts is not taken into account for the calculation of the total damaged area of the waste package. The impact of this assumption on results presented in this document is anticipated to be negligible. The rationale for this assumption is twofold. First, the waste package is heavier than the drip shield (DS) by a factor of 10 (BSC 2004 [DIRS 167083], Attachments I and III); consequently, an impact between the waste package and drip shield results in the drip shield being pushed around by the waste package without significant deformation of the waste package OCB. Second, the interaction between waste package and drip shield takes place at the trunnion collar

sleeves, which is similar to the interaction from end-to-end impacts. Since the end-to-end impacts are much more frequent, and since the waste package is a much stiffer "target" than the drip shield, it is not likely that the side impacts would damage an area that is not already damaged by the end impacts (BSC 2003 [DIRS 162293], Tables 4 through 8, for impact angles). This assumption is used in Sections 5.3.1.3 and 5.3.2.3.

3.7 All interactions between the waste package and the longitudinal boundaries (representing the neighboring waste package) with impact velocity less than 1 m/s are not included in the calculation of damaged area. The impact of this assumption on results presented in this document is negligible. The rationale for this assumption is that the damaged area for an impact velocity of 1 m/s is either zero or negligible compared to higher impact velocities, as presented in Tables 5.3-56 through 5.3-64. This assumption is used in Section 5.3.1.2.

3.8 The longitudinal tubes in the emplacement pallet (Tube 1 in Attachment II of BSC 2004 [DIRS 167083]) are, for the purpose of this calculation, assumed to be made of Alloy 22. This assumption has a significant impact on the calculation results. The rationale for this assumption is that it is impossible to take structural credit for these tubes as long as they are made of 316 SS because of long-term corrosion. Thus, unless this design change is made, the pallet is going to fail due to an unacceptable performance (i.e., it would fail to support the waste package as intended). This assumption is used in Sections 2, 5.1, and 5.2.

3.9 The waste package rests on two "cradles" formed by the opposite ends of the emplacement pallet, and either cradle may damage the OCB of the waste package if the vertical impact velocity is large enough. However, the damaged area of the OCB due to the waste package-pallet interaction is evaluated only on one side of the waste package, in a finely meshed OCB region (see Section 5.2.1.2 for details). The total damaged area due to the waste package-pallet interaction is calculated by assuming that the damaged areas on either end of the waste package are the same (i.e., by multiplying by two the damaged area evaluated on one side). The rationale for this assumption is that the number and intensity of impacts on the two ends should be statistically similar. The rationale for this approach is that the waste package is symmetric, there is no spatial variability of friction coefficients, and the ground motion is uniformly applied to the invert, consequently the number and intensity of impacts on two ends should be similar. Obviously, the damaged areas on the two ends may be somewhat different due to the random nature of the event, but, on average, there should be no reason for a bias or preference. This assumption is used in Section 5.3.1.1 and Section 5.3.2.1.

3.10 The waste package is assumed to be symmetric about its mid-plane. Both waste package ends are represented based on the bottom-end configuration (BSC 2004 [DIRS 167083], Attachment I and BSC 2001 [DIRS 157812]). This simplification has no effect on the results, as obtained in this calculation. The rationale for this assumption is that it simplifies the FE representation, without affecting the calculation results. This assumption is used in Section 5.2.1.2.

3.11 The temperature of the waste package is assumed to be 150°C for temperature-dependent material properties. A temperature of 150°C is appropriate and reasonable for evaluation of material properties at the time of the seismic event. This value (150°C) is conservative for evaluation of material properties during 98.5 percent of the first 10,000 years after repository closure. This result is based on a thermal analysis for an open drift with three infiltration levels and five host-rock units (BSC 2004 [DIRS 169565], Figure 6.3-7 through Figure 6.3-11). The peak waste package temperature ranges from 147.4°C to 177.8°C (BSC 2004 [DIRS 169565], Table 6.3-8). The waste package temperature time histories demonstrate that temperature exceeds 150°C for, at most, the first 150 years after ventilation ceases. In some cases, the temperature never exceeds 150°C for certain infiltration levels and host rock units. Since the time period when temperature exceeds 150°C is never greater than 150 years, it follows that evaluating material properties such as the yield strength at 150°C is conservative for at least 98.5 percent of the 10,000 year regulatory period or 99.25 percent of the first 20,000 years after repository closure. This assumption is used in Sections 5.1 and 5.2.2.1.

3.12 The thickness of the waste package OCB is reduced by 2 mm to represent degradation of the package from general corrosion. The rationale for this assumption is that the thickness reduction of 2 mm over the period of 10,000 years to 20,000 years corresponds to very high rates of general corrosion. For example, the median general corrosion rate is 51.8 nanometers per year at 150°C (BSC 2004 [DIRS 169984], Section 8.1). This rate leads to a maximum thickness loss of 0.518 mm after 10,000 years or 1.036 mm after 20,000 years. Similarly, the maximum rate of general corrosion is 256 nanometers per year, based on the 99.99^{th} percentile corrosion rate at 150°C (BSC 2004 [DIRS 169984], Section 8.1). This rate leads to a maximum thickness loss of 2.56 mm after 10,000 years or 5.12 mm after 20,000 years. Both rates have a very conservative bias because (1) waste package temperature is significantly less than 150°C during 98.5 percent of the first 10,000 years after repository closure (see discussion for Assumption 3.11), and (2) the maximum corrosion rate is based on the 99.99^{th} percentile. Given the conservative biases in these estimates, a thickness reduction of 2 mm is a reasonable representation of degradation of the waste package OCB during the 10,000 year regulatory period or during the first 20,000 years after repository closure. This assumption is used in Sections 5.2.1.2, 5.2.2.2.1, 5.2.3.2.1, 5.2.4.2 and 5.2.5.2.

The calculations documented in *21-PWR Waste Package Side and End Impacts* (BSC 2003 [DIRS 162293]), in *Maximum Accelerations on the Fuel Assemblies of a 21-PWR Waste Package During End Impacts* (BSC 2003 [DIRS 162602]), and in *21-PWR Waste Package End Impacts – A Mesh Study* (BSC 2004 [DIRS 170844]) use assumptions 3.3 and 3.12, plus the following additional assumptions:

3.13 The exact geometry of the 21-PWR fuel assemblies is simplified for the purpose of this calculation in such a way that its total mass is assumed to be distributed within a bar of square cross section with uniform mass density. The rationale for this assumption is to simplify the FE representation while providing a set of bounding results. This assumption is used in Section 5.2.2.2.1, 5.2.3.2.1 and corresponds to Mecham (2004 [DIRS 170673], paragraph 5.2.9.1).

3.14 The material used to represent the fuel assemblies is 304 SS. The rationale for this assumption is that the end fittings are made of 304 SS (Punatar 2001 [DIRS 155635], Section 2.1, page 2-4) and they are the parts that will come in contact with other components. This assumption is used in Sections 5.1, 5.2.2.2.1, 5.2.3.2.1 and 5.2.4.2 and corresponds to Mecham (2004 [DIRS 170673], paragraph 5.2.9.2).

3.15 The following design parameters are assumed for the 21-PWR SNF assemblies to be loaded into a 21-PWR waste package: mass = 773.4 *kg*, width = 216.9 mm, and length = 4407 mm. The rationale for this assumption is that these parameters correspond to the B&W (Babcock & Wilcox) 15x15 fuel assembly, which is the heaviest 21-PWR fuel assembly available (BSC 2004 [DIRS 170803], Table 3-3). The mass of the B&W fuel assembly has been increased by 25 lbs (11.4 kg) to account for variations in fuel assembly mass. It should be noted that South Texas 21-PWR fuel assemblies will not be disposed in the 21-PWR waste package, and are therefore excluded from this assumption. This assumption is used in Section 5.2.2.2 and corresponds to Mecham (2004 [DIRS 170673], paragraph 5.2.9.5).

3.16 The target surface is assumed to be unyielding (i.e. elastic), and A 36 carbon steel (CS) is used to represent it in the FE analysis. The rationale for this assumption was that this material has a high modulus of elasticity compared to concrete and it is known that the use of an unyielding surface with high modulus of elasticity would ensure conservative results in terms of residual stresses in the waste package. This assumption is used in Section 5.1, 5.2.1.2, 5.2.2.2.1, 5.2.3.2.1, and 5.2.4.1 and corresponds to Mecham (2004 [DIRS 170673], paragraph 5.2.8.1).

3.17 It is assumed that the dynamic (sliding) friction coefficient is 0.5 for all contacts because the friction coefficients for the materials in this calculation are not available in the literature. The rationale for this assumption is that this friction coefficient represents a typical value for most metal-on-metal contacts (Avallone and Baumeister 1987 [DIRS 103508], Table 3.2.1, pp. 3-26). This assumption is used in Section 5.2.2.2.1 and 5.2.3.2.1.

The hand calculations documented in *Alternate Damaged Area Evaluation for Waste Package Exposed to Vibratory Ground Motion* (BSC 2004 [DIRS 170843]) require one additional assumption:

3.18 All impact angles between the waste package and the longitudinal boundary greater than zero and less than one degree are assumed to be one degree for the purpose of the damaged area calculation. The results from the single end impact calculations for the waste package (see Tables 5.3-56 and 5.3-57 in this report) demonstrate that the damaged area for a zero degree impact is substantially less than that for a one degree impact at the same impact speed. In this situation, a simple linear interpolation of damaged area values between zero and one degree may not be conservative. That is, the damaged area for a 0.2 degree impact may be more similar to the damaged area for a one degree impact because the load is not spread perfectly uniformly on the trunnion collar sleeve, as occurs for a zero degree impact.

Resetting impact angles that are greater than zero and less than one degree to one degree is conservative because damage is greater for the one-degree impact angle at a given impact velocity. The rationale for this approach is that it provides the bounding set of results. This assumption is used in Section 5.3.8.3.

4. USE OF COMPUTER SOFTWARE

Although the underlying reports listed in Table 1-1 and summarized in Section 2 use qualified software, no software has been used in the preparation of this report. For the reader's convenience, the software codes and versions used in the underlying reports are summarized in Table 4-1. The operating systems, CPU numbers, input files, and output files for all calculations are provided in the reports listed in Table 1-1, but are not repeated here.

Table 4-1. Software for Structural Response Calculations

Code Name	Version	Use	Documentation
ANSYS	V5.6.2	Mesh generation	BSC 2002 [DIRS 159357]
ANSYS	V5.4	Mesh generation	CRWMS M&O 1998 [DIRS 153710]
TrueGrid	V2.1.5	Mesh generation	N/A – Exempt Software
LS-DYNA	V950	Structural response	CRWMS M&O 2000 [DIRS 149714]
LS-DYNA	V960.1106	Structural response	BSC 2002 [DIRS 158898]
LS-DYNA	V970.3858 D SMP-00	Structural response	BSC 2003 [DIRS 166139]
LS-DYNA	V970.3858 D MMP-00	Structural response	BSC 2003 [DIRS 166918]
LSPOST	V2.0	Post-processing of computational results	N/A – Exempt Software
LS-PREPOST	V1.0	Post-processing of computational results	N/A – Exempt Software

INTENTIONALLY LEFT BLANK

5. CALCULATION

Throughout Section 5, ground motions are identified by the appropriate value of PGV because the value of PGV provides a unique and unambiguous identifier for each set of ground motions, even when multiple hazard curves have been developed for a site. Often, the original source information is given in annual exceedance frequency, which is then converted to PGV for use in this text. For the reader's convenience, the following list repeats the correspondence identified in Section 1.3.5:

- PGV of 0.19 m/s corresponds to the $5x10^{-4}$ per year exceedance frequency.
- PGV of 0.384 m/s corresponds to the 10^{-4} per year exceedance frequency.
- PGV of 1.05 m/s corresponds to the 10^{-5} per year exceedance frequency.
- PGV of 2.44 m/s corresponds to the 10^{-6} per year exceedance frequency.
- PGV of 5.35 m/s corresponds to the 10^{-7} per year exceedance frequency.

5.1 MATERIAL PROPERTIES

Material properties at room temperature and at elevated temperatures are defined in the individual design calculations listed in Table 1-1. Details of the assumptions for and the calculation of the material properties at 100°C, 150°C and 200°C are provided in the individual design calculations, and will not be repeated here because no calculations are performed in this document. The following summary identifies the major materials for the waste package structural response calculations:

- **SB-575 N06022 (Alloy 22)** (OCB of waste package, OCB lids, upper and lower trunnion collar sleeves, IV support ring, and pallet (see Assumption 3.8))
- **SA-240 S31600 (316 SS)** (IV, IV lids, shear ring, and shell interface ring)
- **SA-240 S30400 (304 SS)** (21-PWR fuel assemblies, see Assumption 3.14)
- **SA-516 K02700 (A 516 Grade 70 Carbon Steel [CS])** (basket guides and stiffeners, fuel basket plates and tubes)
- **SA-36 K02600 (A 36 Carbon Steel)** (unyielding surface for the side and end impact calculations; see Assumption 3.16)
- **SB-265 R52400 (Titanium Grade 7 [Ti-7])** (drip shield plates)
- **TSw2 Rock** (the drift walls).

Table 5.1-1 lists typical material properties of these materials at 150°C.

Table 5.1-1. Typical Material Properties at 150°C

	Alloy 22[a]	316 SS[a]	304 SS[b]	516 CS[b]	A 36 CS[b]	Ti-7[a]	TSw2[a]
Density (kg/m^3)	8690	7980	N/A	7850	7860	N/A	2370
Modulus of elasticity (GPa)	199	186	186	195	203	101	33.0
Poisson's ratio (-)	0.278	0.298	0.29	0.3	0.3	0.32	0.21
Yield strength (MPa)	310	161	154	232	N/A	N/A	N/A
Tangent modulus (GPa)[c]	1.77	1.94	1.69	3.08	N/A	N/A	N/A

[a] BSC 2004 [DIRS 167083], Sections 5.1, 5.1.1, and 5.3.
[b] BSC 2004 [DIRS 170844], Section 5.1.1 and Table 3 in Section 5.1.3.
[c] Tangent (hardening) modulus defines the slope of the stress-strain curve in the hardening (plastic) region.
TSw2 = Topopah Spring welded-lithophysal poor tuff

5.2 FE REPRESENTATIONS

5.2.1 FE Representation for Structural Calculations of Waste Package Exposed to Vibratory Ground Motion

5.2.1.1 Objective and Methodology

The objective of this calculation is to determine the residual stress distribution in the OCB of a waste package under vibratory ground motion, and to estimate the area of the waste package OCB for which the residual first principal stress exceeds the residual stress threshold. This area is called the "damaged area" in this document.

A set of 15 calculations for dynamic waste package structural response are performed for the suite of ground motions with a PGV of 2.44 m/s (BSC 2004 [DIRS 167083], Section 6.1). A similar set of calculations is also performed for a PGV of 5.35 m/s (BSC 2004 [DIRS 167083], Section 6.2). These values for PGV correspond to the peak of the first horizontal velocity component, which is always in a horizontal plane and perpendicular to the longitudinal direction for the structural response calculations (the longitudinal direction runs along the centerline of the drift). The stochastic (uncertain) input parameters for the 15 simulations are 15 sets of three-component ground motion time histories, the metal-to-metal friction coefficient, and the metal-to-rock friction coefficient. A Monte Carlo sampling scheme defines the appropriate combinations of ground motion and friction coefficients (BSC 2004 [DIRS 169999], Section 6.4) for each PGV level. The sampled values of these stochastic parameters are listed in Table 5.2-1, with the friction coefficients rounded to two significant figures.

Each FE simulation is performed in three steps. The first step calculates the transient vibratory motion and impacts. The goal of this step is to compute the deformation of the waste package during the dynamic impacts between package and emplacement pallet. During this computational phase the three components of ground-motion acceleration time history are simultaneously applied to all invert nodes. The stochastic (uncertain) input parameters for 15 simulations corresponding to the 2.44 m/s PGV level and for 15 simulations corresponding to the 5.35 m/s PGV level are listed in Table 5.2-1 (DTN: MO0301SPASIP27.004 [DIRS 161869], Table I-4). No system damping or contact damping is applied during the transient vibratory simulations. This admittedly conservative approach is used in order to prevent unwanted influence of damping on the rigid-body motion of unanchored structures.

Table 5.2-1. Values of Randomly Sampled Input Parameters for Each Realization

Realization Number	Ground Motion Number	Friction Coefficient (-)	
		Metal to metal	Metal to rock
1	7	0.80	0.34
2	16	0.33	0.49
3	4	0.50	0.62
4	8	0.60	0.22
5	11	0.20	0.24
6	1	0.27	0.69
7	2	0.71	0.60
8	13	0.56	0.54
9	10	0.55	0.36
10	9	0.36	0.41
11	5	0.42	0.67
12	6	0.65	0.73
13	12	0.75	0.31
14	14	0.29	0.45
15	3	0.46	0.78

Source: BSC 2004 [DIRS 167083], Table 6.1-1.

The second step of the simulation is the post-vibratory relaxation. The goal of this step is to obtain steady-state results (i.e., residual stresses) at the end of the ground motion. During this computational phase, the motion of the invert nodes is fixed in all three directions, and the only load applied to freestanding objects is the acceleration of gravity. In addition, system damping is applied globally (to all objects) to accelerate the convergence to steady-state results (see Section 5.2.1.4 for details). The specified duration of this post-vibratory relaxation part of simulation is such to allow for the steady-state stresses to establish; most of the time duration of 0.5 *s* suffices.

The third step of the analysis is comparison of the first principal residual stress with the residual stress threshold for accelerated corrosion cracking of Alloy 22. The goal of this step is to determine the "damaged areas" wherein the first principal stress exceeds the residual tensile stress threshold for Alloy 22. If an element on the surface of the waste package OCB exceeds this threshold, then its area is included in the total damaged area, independent of the stress state through the thickness of the waste package OCB. This is a conservative approach because it ignores the potential for a compressive stress profile through the thickness of the OCB to arrest crack propagation.

5.2.1.2 FE Representation

As seen in Figure 5.2-1, it represents the components of the three-dimensional FE representation for the vibratory ground-motion simulations. Figure 5.2-2 presents a cut-away view (portions of various parts are removed to offer a more revealing outlook) showing details of the waste package and emplacement pallet. As shown in these figures, the FE representation consists of the waste package mounted on its emplacement pallet, the surrounding drip shield, the invert surface, and the lateral and longitudinal boundaries. The longitudinal boundary represents the neighboring waste package/pallet assembly (Assumption 3.5), while the lateral boundary represents the drift walls. The FE representation is developed in ANSYS V5.6.2, based on the dimensions provided in the *Emplacement Pallet* report (BSC 2003 [DIRS 161520]), the *Repository Design, Waste Package, Project 21-PWR Waste Package with Absorber Plates, Sheet 1 of 3, Sheet 2 of 3, and Sheet 3 of 3* report (BSC 2001 [DIRS 157812]), and the *Structural Calculations of Waste Package Exposed to Vibratory Ground Motion* report (BSC 2004 [DIRS 167083], Attachments I, II, and III). The FE representations are then used in LS-DYNA V960.1106 and LS-DYNA V970.3858 to perform a transient analysis of the waste package exposed to vibratory ground motion.

The average waste package skirt-to-skirt spacing is 0.1 meters in the high temperature operating mode (BSC [DIRS 168489], Table 1). Thus, the distance between the waste package (specifically, the trunnion collar sleeve [i.e., the skirt]) and the longitudinal boundary (representing the neighboring package and emplacement pallet) is 0.1 meters.

Three components of the acceleration time history are simultaneously applied on the platform representing the top surface of the invert for each ground motion. The same acceleration time history is applied to all platform nodes simultaneously, resulting in zero deformation of the invert. The invert surface is represented in LS-DYNA as an elastic material.

The externally applied momentum from the ground motion is transferred to all freestanding (unanchored) objects solely by friction and impact. The lateral and longitudinal boundaries move synchronously with the platform and are rigid. In effect, these boundaries act like rigid members that are fixed to the platform.

Both ends of the waste package are represented as the bottom-end configuration (Assumption 3.10) (BSC 2004 [DIRS 167083], Attachment I and BSC 2001 [DIRS 157812]). The details of the waste package top end, such as the extended OCB lid and closure lid, are not explicitly represented and their mass is taken into account by increasing the thickness of the OCB lid. The thickness of the waste package OCB is reduced by 2 mm (from 20 mm to 18 mm; see Assumption 3.12) to represent degradation of the OCB over a 10,000 year to 20,000 year period. It needs to be emphasized that this is not a rigorous evaluation of shell thickness due to corrosion or potential corrosion-acceleration effects. Rather, a thickness reduction of 2 mm is a reasonable conservatism within the stated objective of this calculation.

The waste package OCB, the trunnion collar sleeve, and the boundary walls are represented by 8-node solid (brick) elements. The constant-stress 8-node solid element (Livermore Software Technology Corporation 2003 [DIRS 166841], p. 26.30) with one-point Gaussian quadrature (Hallquist 1998 [DIRS 155373], Section 3) is used for all vibratory ground motion calculations.

The part of the OCB that can come in contact with the pallet (see Figures 5.2-3 and 5.2-7; also identified by regions F and C in Fig. 5.2-4) is the most important area for these calculations. The FE representation for this region of the OCB is finely meshed on one side of the waste package (region F in Figure 5.2-4), with four layers of brick elements across the OCB thickness and a relatively dense in-plane mesh. The corresponding OCB region on the other side (region C in Figure 5.2-4) is more coarsely meshed with only two layers of brick elements across the thickness (see Figures 5.2-3 and 5.2-4). These two parts of the waste package OCB are represented as elastoplastic, with linear kinematic hardening.

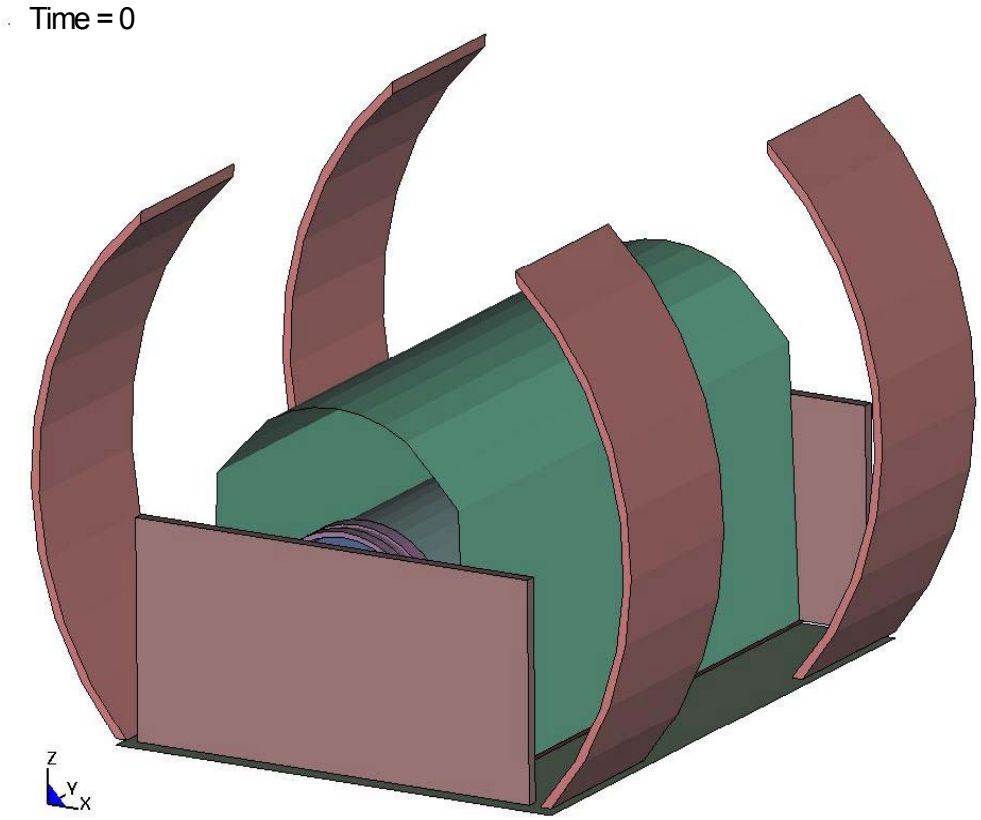

Source: BSC 2004 [DIRS 167083], Figure 1.

Figure 5.2-1. Initial Configuration for Waste Package Vibratory Simulations for Ground Motions at the 2.44 m/s PGV Level

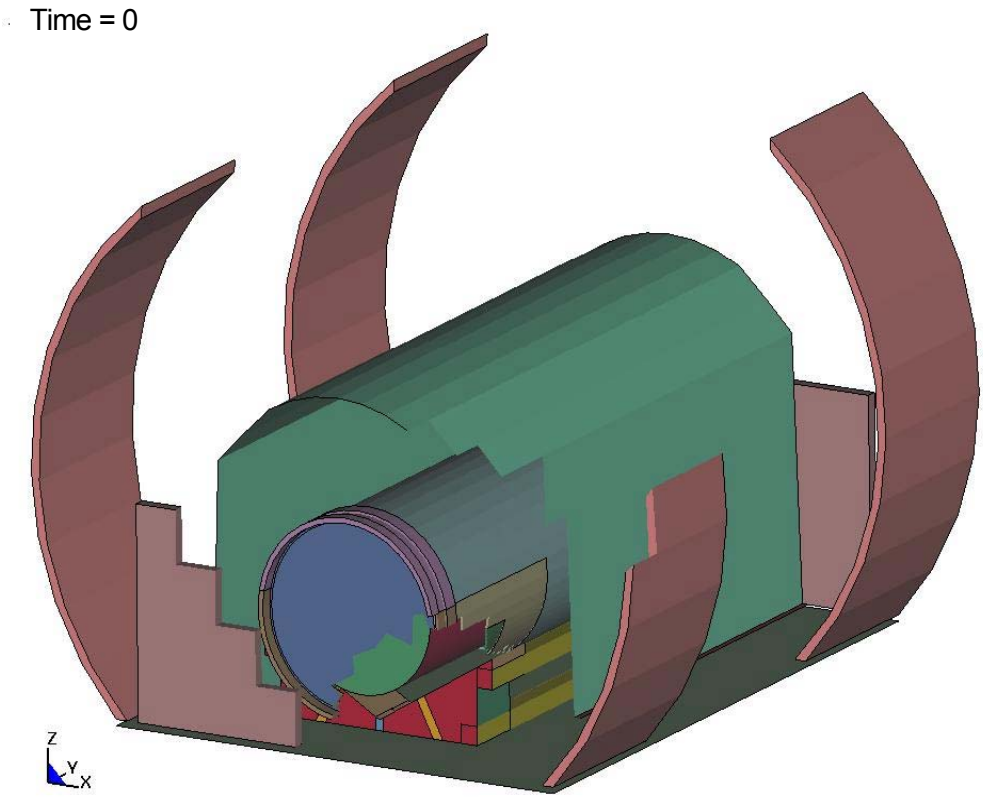

Source: BSC 2004 [DIRS 167083], Figure 2.

Figure 5.2-2. Cut-Away View of Initial Configuration for Waste Package Vibratory Simulations

Source: BSC 2004 [DIRS 167083], Figure 3.

Figure 5.2-3. The Emplacement Pallet and Two Regions on the Outer Surface of the Waste Package That Can Come in Contact with the Pallet

All damage resulting from the waste package-pallet interaction during the vibratory ground motion reported in this document are based on the part of the OCB designated by region F in Figure 5.2-4. The part of the OCB designated by region C (Figure 5.2-4), although coarsely meshed compared to region F, is still relatively finely meshed compared to the remaining part of the OCB (regions P and R in Figure 5.2-4) in order to ensure proper waste package-pallet interaction and the resulting rigid-body motions. The main purpose of the coarsely zoned parts of the mesh, designed P and R in Figure 5.2-4, is to provide appropriate boundary conditions for the more finely zoned F and C parts of the mesh. The main difference between parts of the OCB designated as P and R is that P is represented as elastoplastic (linear kinematic hardening) while R is rigid. The waste package components (excluding IV and IV lids) represented as rigid bodies are presented in Figures 5.2-5 and 5.2-7b.

Region F is especially important for the vibratory ground motion calculations because the stress state and damaged area are evaluated only for this region on the cylindrical surface of the waste package OCB. The two regions of the OCB that can contact the pallet, F and C, are connected to the remaining part of the OCB (P and R) by tied-interface contacts (Hallquist 1998 [DIRS 155373], Section 23.9; and Livermore Software Technology Corporation 2001 [DIRS 159166], page 6.29).

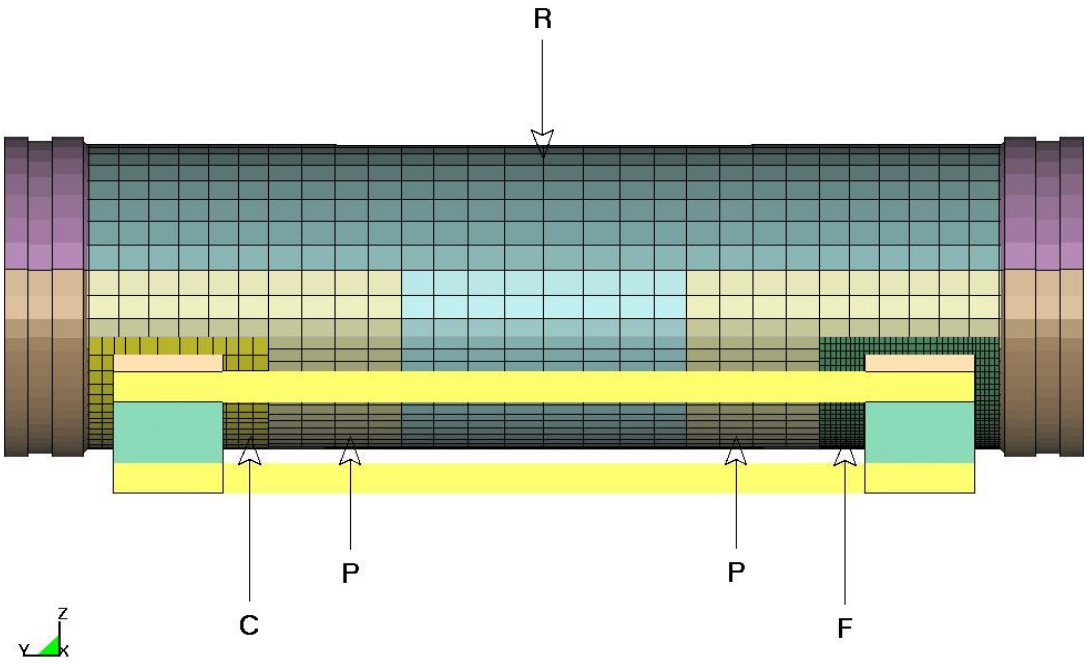

Source: BSC 2004 [DIRS 167083], Figure 4.

Figure 5.2-4. Side View of OCB of Waste Package, Showing Variations in FE Grid

The waste package IV and its lid, pallet, and drip shield are represented by shell elements. Shell elements provide an adequate representation of these components because their dominant mode of deformation is bending. Additionally, this analysis is focused on the waste package OCB, so the stress states in the IV, pallet, and drip shield are of secondary importance. The IV and IV lids, and drip shield are represented as rigid bodies (BSC 2004 [DIRS 167083], Attachment VI) in order to reduce the computer execution time while preserving all the features relevant for the solution. The shell element used for representation of the pallet is fully-integrated 4-node shell element with Gauss integration and three integration points through the shell thickness (Livermore Software Technology Corporation 2003 [DIRS 166841], p. 26.22).

The pallet is represented as elastoplastic but it is very coarsely meshed for the calculations at the 2.44 m/s PGV level (see Fig. 5.2-6). The coarse mesh of the pallet, necessitated by computer-execution-time considerations, results in an artificial increase of the pallet stiffness. In other words, the pallet is not as flexible as in reality and some of the cushioning effect of the pallet on the waste package is lost. The ultimate consequences of the coarse pallet mesh are an increase in the relative motion between the waste package and pallet, and an increase in deformation and residual stress in the OCB. Both of these effects are conservative for this analysis. Nonetheless, the pallet mesh has been refined (see Fig. 5.2-6b) for the calculations for the 5.35 m/s PGV level to prevent excessive relative motion and ensure more realistic results. This change is motivated by the much higher intensity of the ground motion at the 5.35 m/s PGV level in comparison to the 2.44 m/s level.

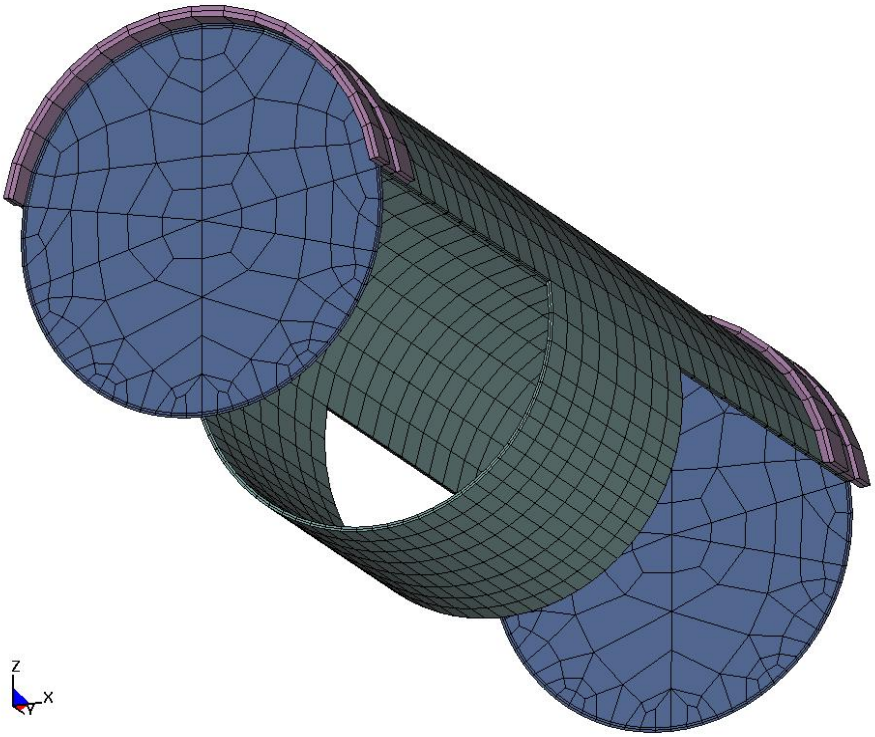

Source: BSC 2004 [DIRS 167083], Figure 5.

NOTE: IV and IV lids excluded.

Figure 5.2-5. Parts of the Waste Package Represented as Rigid Bodies

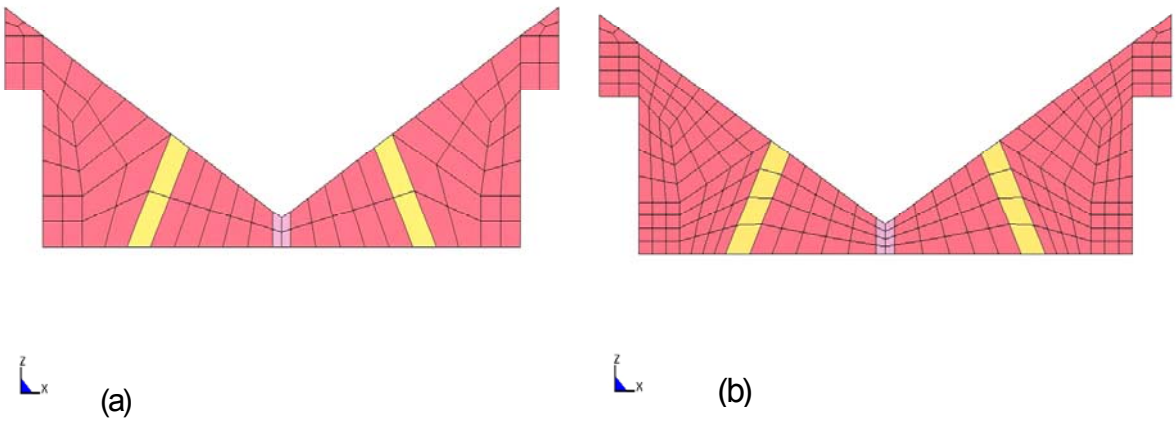

Source: BSC 2004 [DIRS 167083], Figure 6.

NOTE: (a) 2.44 m/s PGV calculations, (b) 5.35 m/s PGV calculations.

Figure 5.2-6. Front View of Pallet Mesh

The internal structure of the 21-PWR waste package is simplified by representing the IV and all waste package internals, including the fuel assemblies, as a thick-wall cylinder of circular cross section and uniform density (Assumption 3.1). The outside diameter of the IV is kept unchanged. The thickness of the IV is determined by using the material properties (including density) of 316 SS, and matching the total mass of the IV and internals as presented in *Structural Calculations of Waste Package Exposed to Vibratory Ground Motion* (BSC 2004 [DIRS 167083], Attachment I). The benefit of this approach is a reduction in the computer execution time while preserving all features of the problem relevant to the structural response.

The FE representation of the 21-PWR waste package maximizes the loose-fit gap between the IV and OCB to 4 mm (Plinski 2001 [DIRS 156800], Section 8.1.8). Consequently, the IV is free to move within the OCB. This maximized gap provides a conservatively bounding set of results, as demonstrated in *21-PWR Waste Package Side and End Impacts* (BSC 2003 [DIRS 162293], Attachment II).

The drip shield has a simplified FE representation (Assumption 3.4). The drip shield is represented as a rigid shell structure following the contour of the actual drip shield presented in *Structural Calculations of Waste Package Exposed to Vibratory Ground Motion* (BSC 2004 [DIRS 167083], Attachment III). All of the structural details of the drip shield are ignored. The drip shield is assumed to be made completely of Ti-7 and the density of Ti-7 is modified to match the total mass of the drip shield. These simplifications make it possible to capture the essential kinematics of freestanding components in the drift, while reducing the computer execution time. The impact of these simplifications in representation of the drip shield on the computational results presented in this document is anticipated to be negligible.

The most notable differences (in addition to the pallet mesh shown in Figure 5.2-6) between the two FE representations for the 2.44 m/s and 5.35 m/s PGV levels are that (1) the finely-meshed region is fully extended in the circumferential direction, and that (2) the configuration of the rigid OCB parts is changed for the 5.35 m/s PGV level calculations, as illustrated by Figure 5.2-7. These modifications are necessitated by the much more intense ground motion, causing much more relative (rigid-body) motion between the unanchored repository components, at the 5.35 m/s PGV level than at the 2.44 m/s PGV level. Figures 5.2-7(a) and 5.2-7(b) for the 5.35 m/s PGV calculations correspond to Figure 5.2-5 for the 2.44 m/s PGV calculations[5].

Contacts are specified between the OCB and IV, the OCB and pallet, the waste package (i.e., trunnion collar sleeve) and longitudinal and lateral boundaries, the pallet and invert, and the pallet and longitudinal and lateral boundaries, plus other components. The dynamic friction coefficients for all contacts are randomly sampled from a uniform distribution between 0.2 and 0.8 (see Assumption 3.2). One metal-to-metal friction coefficient and one metal-to-rock friction coefficient are sampled for each realization (see Table 5.2-1), and applied to all metal-to-metal and metal-to-rock contacts. In other words, the friction coefficients vary from realization to realization (random sampling) but all metal-to-metal contacts have the same friction coefficient in a specific realization regardless of the contact pair; the same applies to metal-to-rock contacts.

[5] Notice that Realization 6 was the only realization at the 2.44-m/s PGV level that was, due to high intensity of the ground motion and resulting rigid body kinematics, performed with the FE representation with the finely-meshed region fully extended in the circumferential direction.

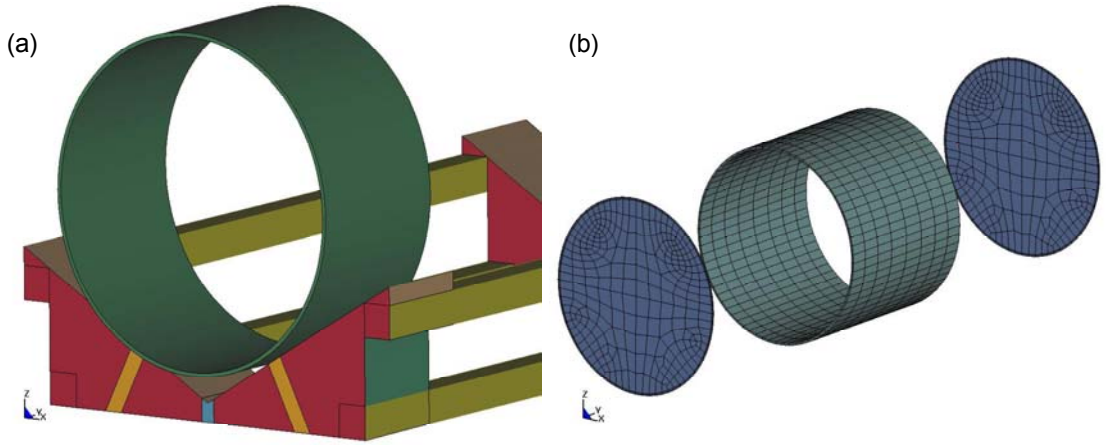

Source: BSC 2004 [DIRS 167083], Figure 7.

NOTE: (a) Extended finely-meshed OCB region; (b) Rigid parts.

Figure 5.2-7. Modifications in FE Representation for the 5.35 m/s PGV Calculations

The functional friction coefficient used by LS-DYNA is defined in terms of static and dynamic friction coefficients, and relative velocity of the surfaces in contact (Livermore Software Technology Corporation. 2001 [DIRS 159166], page 6.9). The effect of relative velocity between contact surfaces is represented by a fitting parameter, called the exponential decay coefficient. However, this parameter cannot be defined for these calculations because the variation of static and dynamic friction coefficients are not available for Alloy 22 and Ti-7. In this situation, the effect of the relative velocity between contact surfaces is neglected by assuming that the functional friction coefficient and the static friction coefficient are equal to the dynamic friction coefficient. This approach maximizes the relative motion of the unanchored repository components by minimizing the friction coefficient within the given FE analysis framework (Assumption 3.3). The friction coefficient affects the onset of sliding and dissipation of energy for the engineered barrier system components as a function of the ground motion intensity. However, the importance of friction is anticipated to diminish with increasing ground motion level because the engineered barrier system components begin to slide almost immediately for high-amplitude ground motions.

The mesh of the FE representation was appropriately generated and refined in the contact regions according to standard engineering practice. Thus, the accuracy and representativeness of the results of this calculation are deemed acceptable (BSC 2004 [DIRS 167083], Attachments V through IX for discussion of results). The uncertainties are taken into account by random sampling (from appropriate probability distributions) of the calculation inputs that are inherently stochastic (uncertain) and characterized by a large scatter of data (ground-motion time histories and friction coefficients).

5.2.1.3 Ground-Motion Time History Cutoff

The structural response calculations for the waste package are computationally intense because:

(1) The FE representation is quite detailed (Section 5.2.1.2)

(2) The calculations are highly nonlinear, with large deformation plasticity, friction, and impacts

(3) The computational time step is quite small to ensure numerical stability of the conditionally-stable explicit FE method (typically one microsecond or less)

(4) The ground motion duration is quite long, typically 30 to 40 seconds, relative to the time step.

Given these factors, it is attractive to reduce the duration of the calculations by considering only that portion of the ground-motion time history that causes changes in the damaged area.

For the ground motions at the 2.44 m/s PGV level, the computational duration is usually restricted to the 5 percent to 95 percent levels of ground motion energy, where energy is based on all three components of the ground motion. Measured by Arias Intensity - an estimate of energy delivered to structures. For a definition, see Kremer (1996 [DIRS 103337], Section 3.3.4). For brevity, the minimum time corresponding to the 5 percent level of the ground motion energy is called the "5 %-time", and the maximum time corresponding to the 95 percent level of the ground motion energy is called the "95 % time".

All simulations for ground motions at the 5.35 m/s PGV level are performed from the 5 percent-time to the 90 percent level of the ground motion energy, referred to as the "90 %-time". Thus, the starting times for the 2.44 m/s and 5.35 m/s PGV level coincide with the 5 percent-time, while the ending time for the 5.35 m/s PGV level has been reduced to the 90 percent-time.

Table 5.2-2 presents the characteristic times for the 2.44 m/s PGV level calculations (BSC 2004 [DIRS 167083], Table 5.2.1.1]). Table 5.2-2 lists the 5 percent-time, 95 percent-time, the start time and end time for the simulations (denoted as FE Start time and FE End time), and the duration of the FE simulations. The FE Start time is equal to the 5 percent-time for most simulations, and the FE End time is nominally the 95 percent-time. The duration of a specific simulation is determined by subtracting the FE End time from the FE Start time.

In five realizations, the starting time is ahead of the 5 percent-time to encompass some pertinent feature of the ground motion (see Table 5.2-2). Similarly, the FE End time has been varied from the 95 percent-time in a few realizations to examine the sensitivity of damage to cutoff time. Specifically, realizations 1, 2, 4, 9, and 12 are extended for a short time after the 95 percent-time for the purpose of examining the evolution of damage after the nominal cutoff (BSC 2004 [DIRS 167083], Attachment VII). On the other hand, realizations 3, 8, 13, and 14 are not run up to the 95 percent-time since – as indicated in *Structural Calculations of Waste Package Exposed to Vibratory Ground Motion* (BSC 2004 [DIRS 167083], Table VII-1) – it was unnecessary because damaged area becomes constant before the 95 percent-time.

Table 5.2-2. Characteristic Times and Duration of Simulations for 2.44 m/s PGV Ground Motion Level

Ground Motion Number	5%-Time (s)	FE Start Time (s)	95%-Time (s)	FE End Time (s)	Durations (s)		Realization Number
					5% to 95% Time	FE Run Time	
1	0.85	0.85	7.05	7.05	6.2	6.2	6
2	0.58	0.41	8.13	8.41	7.6	8.0	7
3	1.7	1.5	5.04	5.00	3.4	3.5	15
4	1.3	1.1	15.0	13.9	13.7	12.8	3
5	2.0	2.0	10.3	10.3	8.3	8.3	11
6	2.3	2.3	9.96	11.2	7.7	8.9	12
7	4.0	4.0	11.6	12.9	7.6	8.9	1
8	1.1	1.1	5.99	6.80	4.9	5.7	4
9	0.79	0.6	8.18	7.90	7.4	7.3	10
10	1.6	1.6	10.8	11.9	9.2	10.3	9
11	2.1	2.1	10.3	10.3	8.2	8.2	5
12	1.4	1.4	13.6	12.9	12.2	11.5	13
13	1.9	1.85	17.0	15.4	15.1	13.5	8
14	7.2	7.2	21.5	18.2	14.3	10.9	14
16	3.8	3.8	11.8	12.8	8.0	9.0	2

Source: BSC 2004 [DIRS 167083], Table 5.2.1.1.

Table 5.2-3 presents the characteristic times for the 2.44 m/s PGV level ground motions with a cutoff based on the 90 percent level of ground motion energy (BSC 2004 [DIRS 167083], Table 5.2.1.2). The durations in the fourth column (Duration of Simulation to 90 percent-time) represent the relative time in the simulation when the 90 percent level for ground motion energy is reached for all three components of ground motion. These data are used in *Structural Calculations of Waste Package Exposed to Vibratory Ground Motion* (BSC 2004 [DIRS 167083], Attachment VII, Table VII-5) to examine the sensitivity of damaged area to the time-history cutoff.

Table 5.2-3. Characteristic Times and Duration of Simulations for the 5 Percent-90 Percent Energy Range at the 2.44 m/s PGV Ground Motion Level

Ground Motion Number	FE Start Time (s)	90% Time (s)	Duration of Simulation to 90% Time (s)	Realization Number
1	0.85	5.21	4.36	6
2	0.41	6.05	5.47	7
3	1.5	3.64	1.94	15
4	1.1	10.2	8.90	3
5	2.0	7.46	5.46	11
6	2.3	9.20	6.90	12
7	4.0	11.1	7.10	1
8	1.1	5.12	4.02	4
9	0.6	6.98	6.19	10
10	1.6	7.66	6.06	9

Table 5.2-3. Characteristic Times and Duration of Simulations for the 5 Percent-90 Percent Energy Range at the 2.44 m/s PGV Ground Motion Level (Continued)

Ground Motion Number	FE Start Time (s)	90% Time (s)	Duration of Simulation to 90% Time (s)	Realization Number
11	2.1	8.30	6.20	5
12	1.4	12.2	10.8	13
13	1.85	12.7	10.8	8
14	7.2	19.8	12.6	14
16	3.8	9.57	5.77	2

Source: BSC 2004 [DIRS 167083], Table 5.2.1.2.

Table 5.2-4 presents the characteristic times for the 5.35 m/s PGV level calculations (BSC 2004 [DIRS 167083], Table 5.2.1.2). Table 5.2-4 lists the 5 percent time, the 90 percent time, and the duration of the FE simulations based on these times. Finally, Table 5.2-4 presents the duration of each simulation and characteristic times used to define the duration for the 5.35 m/s PGV level ground motions (BSC 2004 [DIRS 167083], Table 5.2.1.2). In this case, as discussed previously, the starting time presented in the second column coincides with the 5 percent time, rounded to two significant digits. The most pronounced difference between 2.44 m/s PGV and the 5.35 m/s PGV level ground motions is that the latter are run only up to the maximum of 90 percent energy of ground motion (i.e., the ending time coincides with the 90 percent time). The rationale is to reduce the simulation running time without significantly affecting the damaged area. This rationale is based on the results for the 2.44 m/s PGV level realizations (BSC 2004 [DIRS 167083], Attachment VII), and its appropriateness is confirmed to a large extent by the results of the 5.35 m/s PGV level realizations (see Section 5.3.2).

Table 5.2-4. Characteristic Times and Duration of Simulations for 5.35 m/s PGV Ground Motion Level

Ground Motion Number	5%-Time (s)	90% Time (s)	Duration of Simulation (s)		Realization Number
			5% to 95% Time	FE Run Time	
1	1.3	6.5	5.2	5.2	6
2	0.80	5.8	5.0	5.0	7
3	1.75	3.45	1.7	1.7	15
4	1.5	11.8	10.3	10.3	3
5	1.7	9.3	7.6	7.6	11
6	2.4	9.2	6.8	6.8	12
7	3.6	11.4	7.8	7.8	1
8	1.2	5.1	3.9	3.9	4
9	0.70	6.7	6.0	6.0	10
10	1.6	7.2	5.6	5.6	9
11	2.1	8.5	6.4	6.4	5
12	2.0	12.7	10.7	10.7	13
13	1.9	15.2	13.3	13.3	8
14	5.3	21.0	15.7	15.7	14
16	3.4	9.0	5.6	5.6	2

Source: BSC 2004 [DIRS 167083], Table 5.2.1.3.

5.2.1.4 System Damping

In order to obtain steady-state results (i.e., residual stresses) in a reasonable time, it is necessary to apply damping during the second post-vibratory relaxation step of the computational process. The system damping is strictly a numerical technique for accelerating convergence to the steady-state stress state after the transient simulation is completed. It is applied globally to all elements and nodes of the FE grid.

As discussed in Hallquist (1998 [DIRS 155373], Section 28.2), the most appropriate damping constant for the system is usually the critical damping constant. Therefore,

$$DC = 2 \cdot \omega_{\min} = 2 \cdot 350\, rad/s = 700\, rad/s,$$

where $\omega_{\min} = 2 \cdot \pi \cdot 56 \approx 350\, rad/s$ is the minimum non-zero frequency of the waste package OCB (BSC 2004 [DIRS 167083], Attachment X [*Modal Analysis/wpp6Bmod.out*, line #6517]). Since the engineered barrier system components are unanchored in these calculations, the damping constant is reduced to $DC = 200\, rad/s$ to avoid over-damping the system. Furthermore, the parametric study of various damping constants presented in *21-PWR Waste Package Side and End Impacts* (BSC 2003 [DIRS 162293]), confirms the appropriateness of this choice. The system is obviously not over-damped, and a steady state is reached in reasonable time (BSC 2003 [DIRS 162293], Figure 4, page 21).

5.2.2 FE Representation for 21-PWR Waste Package Side and End Impacts

5.2.2.1 Objectives and Methodology

The objective of these calculations is to determine the damage to a 21-PWR waste package from end-to-end impacts of adjacent waste packages and from side-on impacts of a waste package. These structural response calculations are based on a relatively detailed FE mesh to determine damaged areas more accurately than is possible in *Structural Calculations of Waste Package Exposed to Vibratory Ground Motion* (BSC 2004 [DIRS 167083]). In effect, it is more accurate and more computationally efficient to perform very detailed calculations of the (brief) impact process because the long duration of ground motions and the complexity of the FE representation in *Structural Calculations of Waste Package Exposed to Vibratory Ground Motion* (BSC 2004 [DIRS 167083]) precludes such a detailed analysis.

These calculations represent a parametric study of waste package impact as a function of six values of the impact velocity and up to four values of the impact angle (see Figures 5.2-8 and 5.2-9 below). The end-to-end impact calculations are performed with vertical rigid walls at 0.1 m spacing from the ends of the waste package. This boundary condition is used to represent the effects of the adjacent waste package as opposed to explicitly representing the waste package as a FE structure. The use of a rigid, unyielding surface is computationally efficient because it reduces the computational mesh by a factor of two and also provides a conservative representation of the damaged area. The damaged area with an unyielding surface will generally be greater than the damaged area with an adjacent waste package because the unyielding surface is infinitely stiff, maximizing impact stresses and deformation of the waste package for a given impact velocity and impact angle.

Material properties are based on three temperatures: 100ºC, 150ºC, and 200ºC. As noted in Assumption 3.11, a temperature of 150ºC is the base case for all calculations because it is conservative for 98.5 percent of the first 10,000 years and 99.25 percent of the first 20,000 years after repository closure. The calculations at 100ºC and 200ºC evaluate the sensitivity of damaged area (i.e., the area that exceeds the residual stress threshold) to temperature. The residual stress threshold is based on 80 percent, 90 percent, and 100 percent of the yield strength for Alloy 22 at the various temperature values. The variations in residual stress threshold evaluate the sensitivity of damaged area to this parameter.

The initial conditions for the impacts are as follows:

For end impacts: Initial velocity is 1 m/s, 2 m/s, 4 m/s, 6 m/s, 10 m/s, and 20 m/s; Initial angle between the axis of the waste package and the vertical (α in Figure 5.2-8) is 0 degrees, 1 degree, 5 degrees, and 8 degrees.

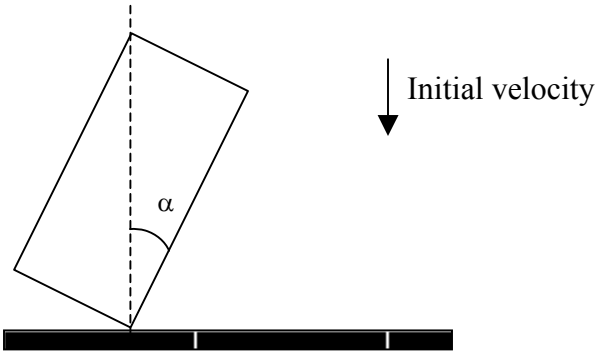

Source: BSC 2003 [DIRS 162293], Figure 2.

Figure 5.2-8. Initial Position of the Waste Package for the End Impacts

For side impacts: Initial velocity is 1 m/s, 2 m/s, 4 m/s, 6 m/s, 10 m/s, and 20 m/s; Initial angle between the axis of the waste package and the horizontal (α in Figure 5.2-9) is 0 degrees, 1 degree, and 8 degrees.

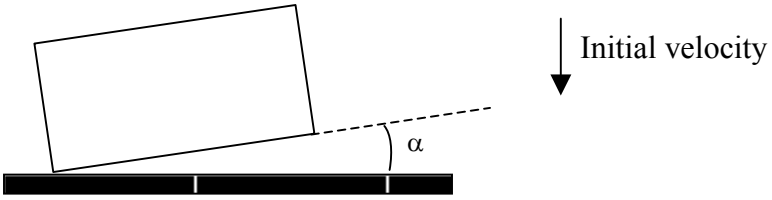

Source: BSC 2003 [DIRS 162293], Figure 3.

Figure 5.2-9. Initial Position of the Waste Package for the Side Impacts

The selected impact velocity range from 1 m/s to 20 m/s and impact angle range from 0 to 8 degrees were anticipated to be sufficiently wide to encompass all velocities and angles encountered during simulations of the vibratory ground motion. The appropriateness of this selection was confirmed by the results of the vibratory ground motion simulations (Tables 5.3-2 through 5.3-15 and Tables 5.3-24 through 5.3-38).

5.2.2.2 FE Representation

5.2.2.2.1 Description of FE Representation

There are ten different variations of the FE mesh (BSC 2003 [DIRS 162293], Table III-1 for a complete list) for an essentially same FE representation. The different meshes are used for the purpose of computational economy. Following a standard engineering practice, the mesh of the OCB is refined in the region where significant deformations and residual stresses are expected (i.e., "region of interest"). The remaining part of the mesh is coarser to reduce the simulation running time. The extent of the region of interest depends on the input parameters (the velocity and angle of impact). For example, B and C (BSC 2003 [DIRS 162293], Table III-1) have the same angle of impact (one degree), but C has more extended fine-mesh region than B to account for the greater damaged area extension due to the greater impact velocity. The initial configuration for 5-degree end impact of the 21-PWR waste package is illustrated in Figure 5.2-10.

A three-dimensional FE representation of the waste package was developed in ANSYS V5.4 using the dimensions provided in *21-PWR Waste Package Side and End Impacts* (BSC 2003 [DIRS 162293], Attachment I). The waste package OCB and lids, IV and lids, trunnion sleeves, and fuel assemblies were represented by solid (brick) elements. The constant-stress 8-node solid element (Livermore Software Technology Corporation 2003 [DIRS 166841], p. 26.30) with one-point Gaussian quadrature (Hallquist 1998 [DIRS 155373], Section 3) was used for all end and side impact calculations. As indicated by Figure 5.2-11 the number of the solid element layers in key regions of the OCB and its bottom lid is four.

The internal structure of the waste package was simplified in several ways:

1. The 21-PWR fuel assemblies were reduced to bars of square cross section of uniform mass density, and assumed to be constructed of 304 SS (Assumptions 3.13 and 3.14).

2. The geometric dimensions of the fuel assemblies were modified to keep the value of the gap between the fuel assemblies and the nearest element consistent with the gap defined using the elements found in *21-PWR Waste Package Side and End Impacts* (BSC 2003 [DIRS 162293], Attachment I).

3. The mass density of the fuel assemblies was modified so that the total mass of the loaded waste package equals the mass given in *21-PWR Waste Package Side and End Impacts* (BSC 2003 [DIRS 162293], Attachment I).

4. The fuel basket tubes were not represented in the FE mesh for end impacts.

5. The thickness of the OCB was reduced by 2 mm on its outer surface (see Assumption 3.12). The target surface was conservatively assumed to be unyielding (Assumption 3.16), and its density was rounded up to 8000 kg/m^3. A static and dynamic friction coefficient of 0.5 was taken into account between all parts (Assumption 3.2 and Assumption 3.17). The value of 0.5 is an average value for the range of friction coefficient, 0.2 to 0.8, defined in Assumption 3.2 and used for the structural response calculations described in Section 5.2.1. The use of an average friction coefficient of 0.5 is reasonable here because this is a single, discrete impact on an unyielding surface, so frictional forces should have a very minor effect in determining damaged area on the waste package.

5.2.2.2.2 Gap Between the IV and OCB

As shown in *Repository Design, Waste Package, Project 21-PWR Waste Package with Absorber Plates, Sheet 1 of 3, Sheet 2 of 3, and Sheet 3 of 3* (BSC 2001 [DIRS 157812], Section B-B'), a tight fit between the IV and the OCB is indicated. However, Plinski (2001 [DIRS 156800], Section 8.1.8) describes the fit between the two shells as "loose". In order to determine which configuration was more conservative for this study, two of the cases (end impacts, α = 5°, v = 4 *m/s* and α = 1°, v = 2 *m/s*, material properties for 150°C) were each run with a tight fit and the maximum loose fit for the gap. The results are presented in *21-PWR Waste Package Side and End Impacts* (BSC 2003 [DIRS 162293], Attachment II) and show that the configuration with a 4-mm gap is conservative. Consequently, all other cases were run with a 4-mm gap between the IV and the OCB.

5.2.2.2.3 Mesh Refinement Study

The FE mesh was generated and refined in the contact region according to standard engineering practice. This mesh was then further refined in the higher-stress region to verify that the results are not mesh sensitive. The volume and stress for the element of highest stress (at the end of the calculation) were compared, according to the method described in Mecham (2004 [DIRS 170673], Section 6.2.3). The results are presented in *21-PWR Waste Package Side and End Impacts* (BSC 2003 [DIRS 162293], Attachment III). Since the criterion defined in Mecham (2004 [DIRS 170673], Section 6.2.3) is met, the accuracy and representativeness of the mesh are deemed acceptable for this calculation. Additional studies documented in Sections 5.2.4 also confirm the adequacy of the FE mesh for estimating damaged area.

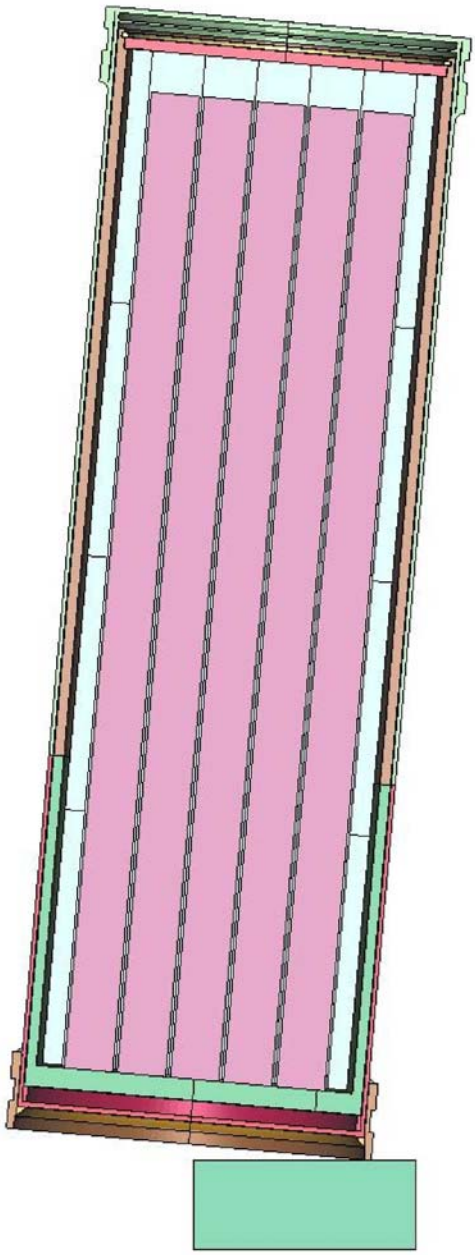

Source: BSC 2004 [DIRS 170844], Figure 1.

Figure 5.2-10. Schematic of Initial Configuration for 5-Degree End Impact of the 21-PWR Waste Package

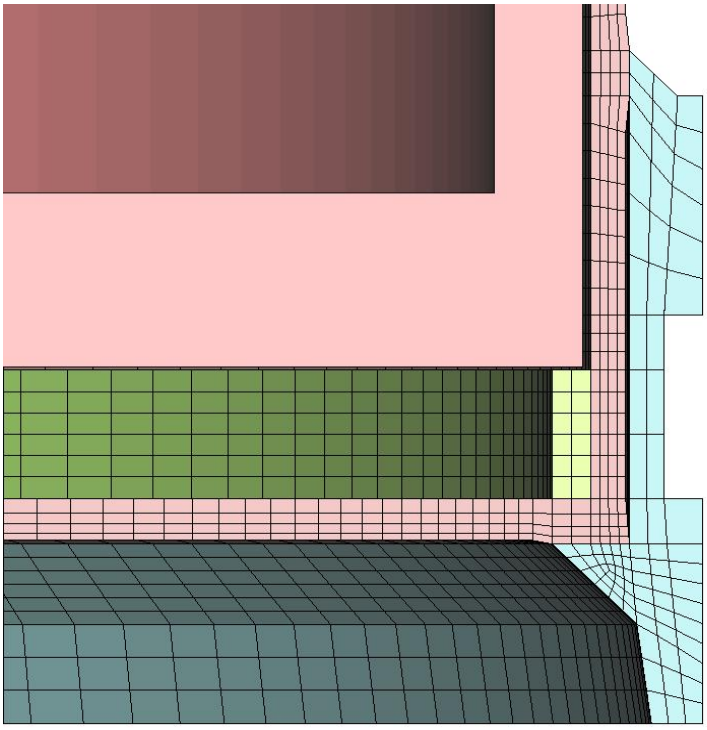

Source: BSC 2004 [DIRS 170844], Figure 2.

Figure 5.2-11. Detail of the Base FE Representation of 21-PWR Waste Package for Ideal (0 degree) End Impact

5.2.2.2.4 System Damping

The duration for all the impact calculations, 0.05 seconds, was chosen to establish a stable residual first principal stress after the waste package impact. In order to calculate residual stresses efficiently, system damping (Hallquist 1998 [DIRS 155373], Section 28.2) is applied after the first impact between the waste package and the unyielding surface (i.e., after 0.03 seconds), until the termination of the simulation at 0.5 seconds. The value of the damping coefficient is 200. This value was determined by running 3 test cases: first with a damping coefficient of 0 (no system damping); second with a coefficient of 50; and third with a coefficient of 200. The variation of maximum first principal stress with time is presented in Figure 5.2-12. Based on these results, a damping coefficient of 200 was considered adequate for this calculation.

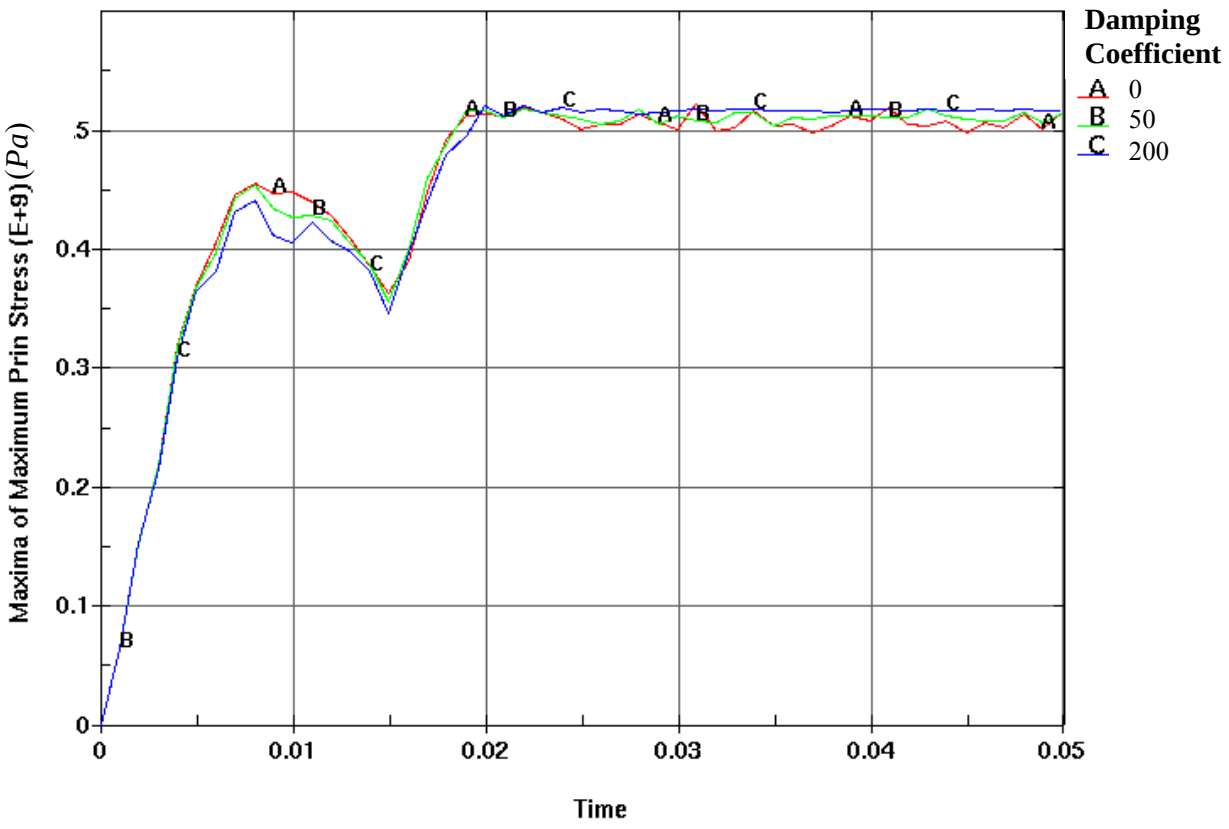

Source: BSC 2003 [DIRS 162293], Figure 4.

NOTE: Time in seconds.

Figure 5.2-12. Variation of Maximum First Principal Stress with Time for Different Values of the Damping Coefficient

5.2.2.2.5 Post-Processing

An element where the residual first principal stress is above the residual stress threshold is called a damaged element. If an element has its first principal stress below this threshold, it is referred to as an undamaged element.

In order to determine the damage, the results obtained in the last time step of each simulation are post-processed with LS-POST V2 as follows: the undamaged elements of the OCB are "blanked out" (dark blue color in Figure 5.2-13). The damage on the OCB outer surface is estimated by calculating the area of each damaged element's face that coincides with the OCB outer surface. Since the number of damaged elements can be very large, the area of neighboring elements is calculated as the area of a rectangle containing these elements. However, if the damaged elements do not form a perfect rectangle, outside elements can be accounted for as shown in Figure 5.2-13 (count these 2 elements/do not count these 2 elements).

Once the damage on the outer surface of the OCB is calculated, the inner surface of the OCB is treated in the same way. If the damaged area on the outer and inner surfaces overlap, the corresponding area is counted only once.

Finally, in the area where the OCB and the OCB bottom lid join, only the more damaged side of the junction is taken into account. For example, in Figure 5.2-14, the damaged area in region A is larger than the damaged area in region B. Thus, only the damaged area in region A will be taken into account to avoid excessive conservatism.

The angle defining the maximum extension of the damage in the circumferential direction (Figure 5.2-13) is reported in Section 5.3.

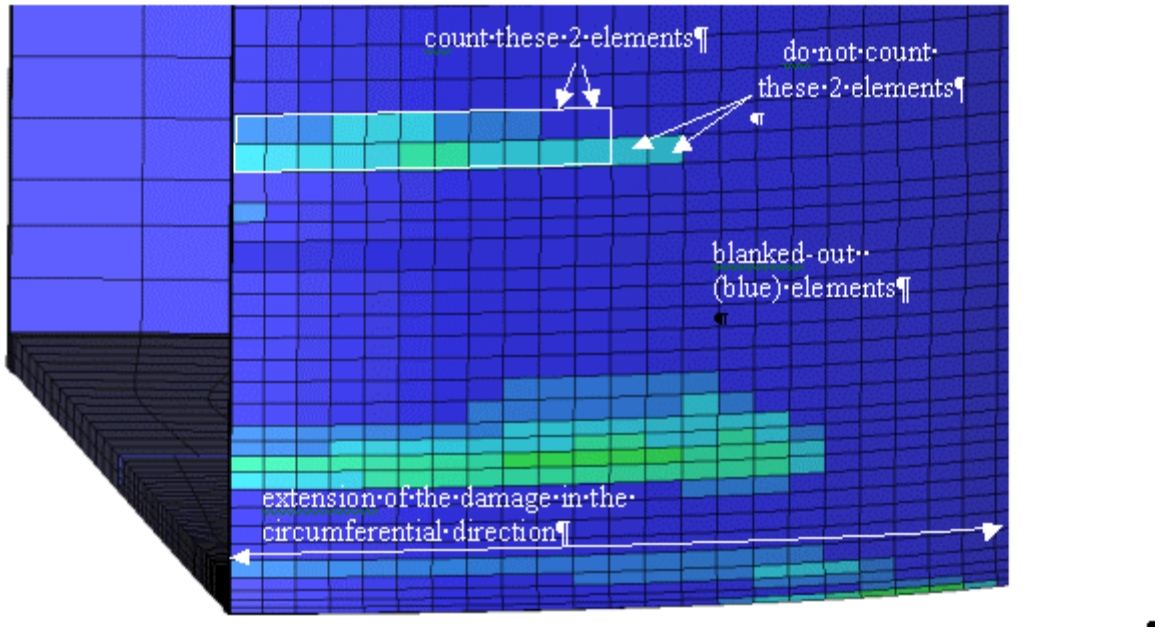

Source: BSC 2003 [DIRS 162293], Figure 5.

NOTE: Color is irrelevant; graphic appears for reference only.

Figure 5.2-13. Determination of Damaged Area – An Example

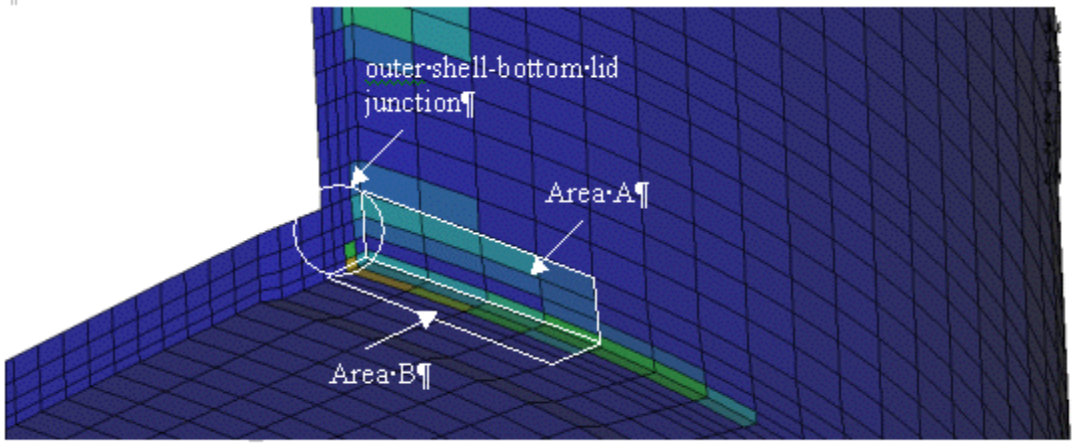

Source: BSC 2003 [DIRS 162293], Figure 6.

NOTE: Color is irrelevant; graphic appears for reference only.

Figure 5.2-14. Determination of the Damaged Area for the Bottom Lid Junction of the OCB

5.2.3 FE Representation for Maximum Accelerations on the Fuel Assemblies of a 21-PWR Waste Package During End Impacts

5.2.3.1 Objective and Methodology

The objective of this calculation is to determine the acceleration of the fuel assemblies contained in a 21-PWR waste package during impact on an unyielding surface. More specifically, the average acceleration and the maximum acceleration of the fuel assemblies are defined by two successive differentiations of the appropriate displacement time history. All accelerations are expressed in units of *g*, the acceleration of gravity (= 9.81 m/s).

These calculations represent a parametric study for average and maximum fuel rod accelerations in response to end-to-end impacts of waste packages. The calculations are performed for five impact velocities at a 1-degree impact angle. The impact calculations are performed with a rigid, unyielding boundary, rather than a detailed FE representation of the adjacent waste package. The use of a rigid, unyielding surface is computationally efficient because it reduces the computational mesh by a factor of two. The use of an unyielding surface also provides a conservative representation of the damaged area. The damaged area with an unyielding surface will generally be greater than the damaged area with an adjacent waste package because the unyielding surface is infinitely stiff, maximizing impact stresses and deformation of the waste package for a given impact velocity and impact angle.

Material properties are based on two temperatures: 150ºC, and 200ºC. A temperature of 150ºC is the base case for all calculations because it is conservative for 98.5 percent of the first 10,000 years and 99.25 percent of the first 20,000 years after repository closure. Two calculations for impact velocities of 1 m/s and 4 m/s are also performed with material properties at 200ºC to evaluate the sensitivity of fuel assembly accelerations at temperature.

The initial conditions for the calculations are an initial velocity of 0.5 m/s, 1 m/s, 2 m/s, 4 m/s, or 6 m/s, and an initial angle between the axis of the waste package and the vertical of 1 degree (i.e. $\alpha = 1^{o}$ in Figure 5.2-15). Additional calculations at multiple impact angles were not performed because the g-loads from these initial analyses were generally sufficient to fail most if not all fuel rod cladding. In this situation, a more limited set of analyses provided sufficient data for developing the damage abstraction for the fuel rod cladding.

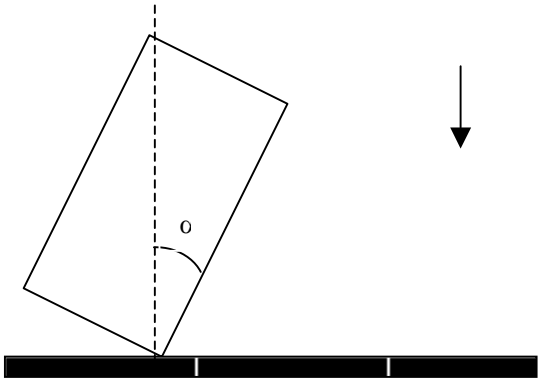

Source: BSC 2003 [DIRS 162293], Figure 2.

Figure 5.2-15. Initial Position of the Waste Package for the End Impacts

5.2.3.2 FE Representation

5.2.3.2.1 Description of FE Representation

A half-symmetry, three-dimensional FE representation of the waste package was developed in ANSYS V5.4 using the dimensions provided in *Maximum Accelerations on the Fuel Assemblies of a 21-PWR Waste Package During End Impacts* (BSC 2003 [DIRS 162602], Attachment I). The waste package OCB and lids, IV and lids, trunnion sleeves, and fuel assemblies were represented by solid (brick) elements. The constant-stress 8-node solid element (Livermore Software Technology Corporation 2003 [DIRS 166841], p. 26.30) with one-point Gaussian quadrature (Hallquist 1998 [DIRS 155373], Section 3) was used for all calculations. The FE mesh is illustrated in Figure 5.2-16.

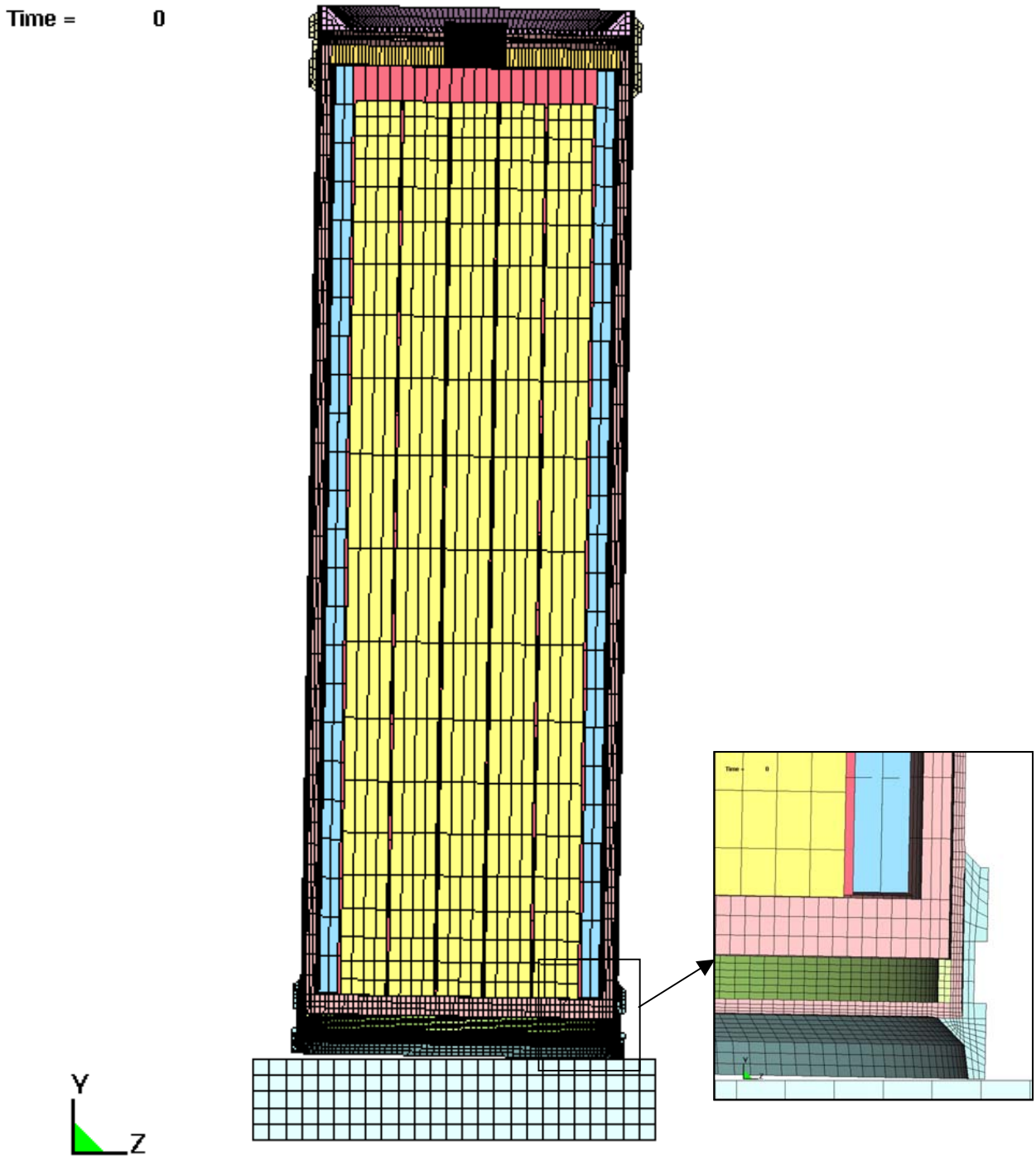

Source: BSC 2003 [DIRS 162602], Figure III-4.

Figure 5.2-16. Standard Mesh for Determination of Fuel Assembly Accelerations

The internal structure of the waste package was simplified in several ways:

1. The 21-PWR fuel assemblies were reduced to bars of square cross section of uniform mass density, and assumed to be constructed of 304 SS (Assumptions 3.13 and 3.14).

2. The geometric dimensions of the fuel assemblies were modified to keep the value of the gap between the fuel assemblies and the nearest element consistent with the gap defined using the elements found in *Maximum Accelerations on the Fuel Assemblies of a 21-PWR Waste Package During End Impacts* (BSC 2003 [DIRS 162602], Attachment I).

3. The mass density of the fuel assemblies was modified so that the total mass of the loaded waste package equals the mass given in *21-PWR Waste Package Side and End Impacts* (BSC 2003 [DIRS 162293], Attachment I).

4. The fuel basket tubes and fuel basket plates are not represented in the FE mesh for end impacts.

5. The mass density of the basket stiffeners is modified so that the total mass of the loaded waste package equals the mass given in *Maximum Accelerations on the Fuel Assemblies of a 21-PWR Waste Package During End Impacts* (BSC 2003 [DIRS 162602], Attachment I).

6. The thickness of the OCB was reduced by 2 mm on its outer surface (Assumption 3.12). The target surface was conservatively assumed to be unyielding (Assumption 3.16), and its density was rounded up to 8000 kg/m^3. A static and dynamic friction coefficient of 0.5 was taken into account between all parts (Assumption 3.2 and Assumption 3.17). This value of friction coefficient represents the average value of the distribution (0.2 to 0.8) used in *Structural Calculations of Waste Package Exposed to Vibratory Ground Motion* (BSC 2004 [DIRS 167083]). The effect of the friction coefficients on the deceleration of the fuel rods is expected to be a second-order effect. Since the resulting fuel rod accelerations exceeded the cladding failure threshold, the more detailed inquiry was unnecessary. Finally, no system damping or contact damping are applied during the simulations.

5.2.3.2.2 Initial Gap between the Fuel Assemblies and the IV Bottom Lid

The fuel assembly accelerations may vary with the initial gap between the fuel assemblies and the bottom lit of the IV. The sensitivity of acceleration to gap size is analyzed in *Maximum Accelerations on the Fuel Assemblies of a 21-PWR Waste Package During End Impacts* (BSC 2003 [DIRS 162602], Attachment II). These results show that the configuration with the minimum gap results in the highest maximum acceleration. Consequently, all cases were run with the minimum gap between the fuel assemblies and the bottom lid of the IV.

5.2.3.2.3 Mesh Refinement Study

The FE mesh was generated and refined in the contact region according to standard engineering practice. This mesh was then further refined in the region of contact (fuel assemblies and the

bottom lid of the IV) to verify that the results are not mesh sensitive. The variation in volume of a representative element and the variation in acceleration of the fuel assemblies are compared in *Maximum Accelerations on the Fuel Assemblies of a 21-PWR Waste Package During End Impacts* (BSC 2003 [DIRS 162602], Attachment III), based on the method described in Mecham (2004 [DIRS 170673], Section 6.2.3). The accuracy and mesh representativeness are deemed acceptable for this calculation because the criterion in Mecham (2004 [DIRS 170673], Section 6.2.3) is met.

5.2.3.2.4 Output Period

Computational results are saved at a user-defined output period. This output period is small enough to accurately capture the maximum values of acceleration. An output period of one nanosecond ensures stable values for the maximum acceleration, as demonstrated in *Maximum Accelerations on the Fuel Assemblies of a 21-PWR Waste Package During End Impacts* (BSC 2003 [DIRS 162602], Attachment IV). This output period is used for all results reported in Section 5.3.

5.2.4 FE Representation for 21-PWR Waste Package End Impacts – A Mesh Study

5.2.4.1 Methodology

Selected end impact calculations have been rerun to determine the sensitivity of damaged area to the refinement of the FE mesh. The selected calculations are representative of the range of calculations that were previously performed with a coarser mesh, as identified in Section 5.2.2.1 for end impacts. Furthermore, the selected calculations are representative of the contribution to damaged area from various impact velocities encountered during the simulations for a waste package exposed to vibratory ground motion, identified in Tables 5.3-2 through 5.3-16 and Tables 5.3-24 through 5.3-39 in this report. Based on these data, two simulations with refined meshes are performed with impact velocity of 2 m/s, three with 4 m/s and 6 m/s, and one with 10 m/s. The rationale for this selection follows:

First, high-velocity impacts contribute more to the total damaged area than the low-velocity impacts (see Tables 5.3-56 and 5.3-57). The impacts at 1 m/s are not rerun because their damaged areas are almost an order of magnitude smaller than the corresponding damaged areas at 2 m/s (see data in Tables 5.3-56 and 5.3-57). On the other hand, there are only two end impacts exceeding 6 m/s for the calculations documented in Sections 5.3.1.2 and 5.3.2.2. Impacts 6.4 m/s (Table 5.3-29) and 6.5 m/s (Table 5.3-33), and the damaged area for these two realizations is primarily determined by the 6-m/s impacts. Given these facts, the emphasis in this sensitivity study is on impacts at 2 m/s, 4 m/s, and 6 m/s. Only one 10 m/s end impact is rerun to examine mesh sensitivity in an extreme case, and no calculation is run with an impact velocity of 20 m/s. Only material properties evaluated at 150°C are used in this calculation.

5.2.4.2 FE Representation

The three-dimensional FE representation for these structural response calculations is described in detail in Section 5.2.2.2 of this report. The mesh-sensitivity of the stresses from end impacts was initially analyzed in *21-PWR Waste Package Side and End Impacts* (BSC 2003 [DIRS 162293], Attachment III). The current mesh refinement calculations are an addendum to the initial

mesh-refinement study in *21-PWR Waste Package Side and End Impacts* (BSC 2003 [DIRS 162293]). The FE representation developed for these calculations is identical to that used in *21-PWR Waste Package Side and End Impacts* (BSC 2003 [DIRS 162293]), except for increased mesh density (see Figures 5.2-11 and 5.2-17).

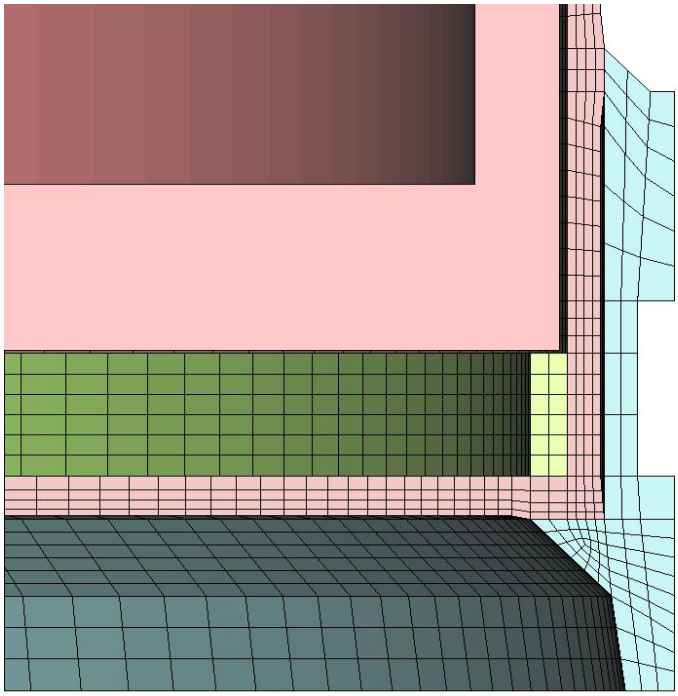

(a) the base mesh (BSC 2003 [DIRS 162293])

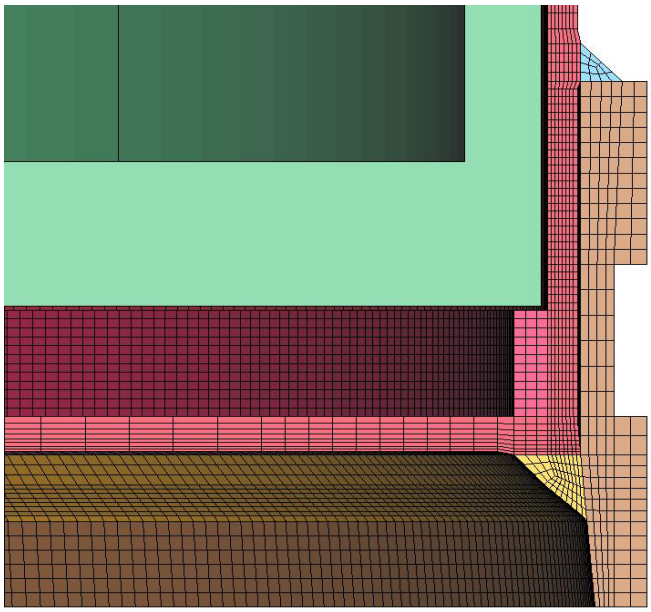

(b) the refined mesh

Source: BSC 2004 [DIRS 170844], Figure 2.

Figure 5.2-17. Detail of FE Representation of 21-PWR Waste Package for Ideal (0 degree) End Impact

Ten FE meshes were used in the original calculation to determine the damaged area for various impact configurations (BSC 2003 [DIRS 162293], Table III-1 has complete list). For the end-impacts rerun during this study, each FE mesh is refined by using the base mesh in *21-PWR Waste Package Side and End Impacts* (BSC 2003 [DIRS 162293]) as a starting point. It would be tedious and unnecessary to discuss all details of mesh refinement for each case. Instead, the general approach to mesh-refinement is explained using the FE mesh for a 0 degree impact. Figure 5.2-17 shows a detail of the base and refined FE meshes. As indicated by Figure 5.2-17, the number of the solid element layers in key regions of the OCB and its bottom lid is increased from four to eight. Such a significant increase is necessary because the damaged area is entirely contained within the OCB-lid junction for this impact case (see discussion in Section 5.3.1). The number of solid element layers across the OCB wall is increased from four to six for other impacts with more extended damage area (as in BSC 2004 [DIRS 170844], Figure I-4). The mesh refinement of the OCB surface is schematically illustrated by Figure 5.2-18. The red polygons superimposed on the base mesh outline the element contours of the refined mesh at the OCB surface.

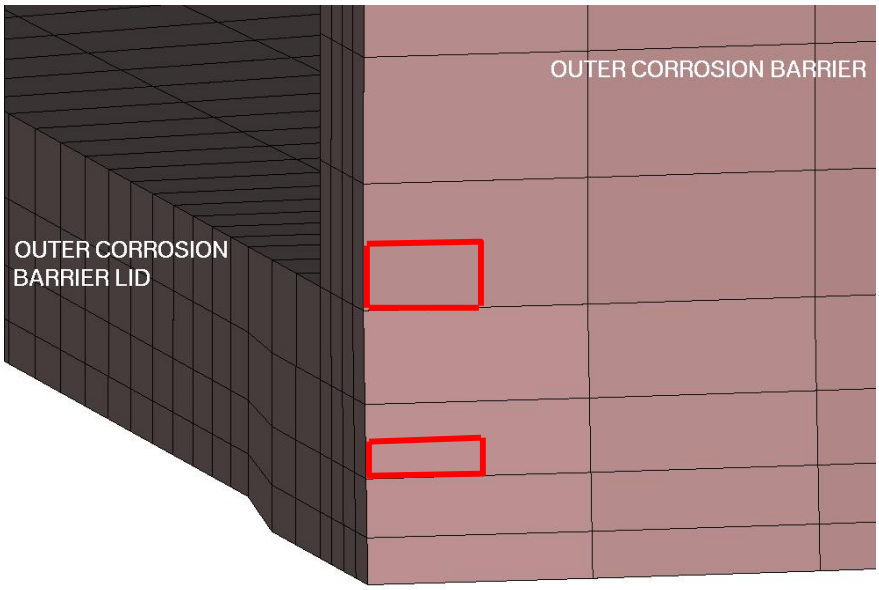

Source: BSC 2004 [DIRS 170844], Figure 3.

Figure 5.2-18. Schematic Illustration of Mesh Refinement of OCB Surface for Ideal (0 degree) End Impact

The elemental volume changes associated with the refined meshes are summarized in *21-PWR Waste Package End Impacts - A Mesh Study* (BSC 2004 [DIRS 170844], Tables 2, 3, 4, and 5]). Details of the base case FE meshes are available in *21-PWR Waste Package Side and End Impacts* (BSC 2003 [DIRS 162293], d3plot files in Attachment 2).

5.2.5 FE Representation for Additional Structural Calculations of Waste Package Exposed to Vibratory Ground Motion

5.2.5.1 Methodology

Calculations for four realizations have been repeated with revised ground motions at the 2.44 m/s PGV level. The original ground motions for the 2.44 m/s PGV level are not spectrally conditioned and do not preserve intercomponent variability in the ground motion recordings. The new ground motions for these calculations spectrally condition the ground motions for the western United States and preserve intercomponent variability in the ground motion recordings. The changes between the two ground motion sets for the longitudinal (along the tunnel, denoted as H2) and vertical (denoted as V) components of PGV are summarized in Table 5.2-5 for four selected realizations. Input data and results labeled as "Old" and "New" refer to the ground motion time histories presented in *Structural Calculations of Waste Package Exposed to Vibratory Ground Motion* (BSC 2004 [DIRS 167083], Section 5.2.1) and *Additional Structural Calculations of Waste Package Exposed to Vibratory Ground Motion* (BSC 2004 [DIRS 168385], Table 5.1), respectively.

Four realizations were selected to maximize the potential damage and maximize the changes in the H2 or V components of PGV. Note that the H1 component of PGV does not change between the two sets of ground motions because it is always scaled to 2.44 m/s. Realizations 3, 6, and 4 are characterized by the largest total damaged areas (in the descending order) at the 2.44 m/s PGV level (Table 5.3-22). Realizations 4 and 15 have large increases in the H2 component of PGV, and realizations 3 and 15 have large increases in the V component of PGV, as shown in Table 5.2-5. Realization 6 has the highest damaged area with significant decreases in both the H2 and V components. These realizations capture the potential changes from the revised ground motions with a bias toward high damaged area and large changes in individual components.

Realizations 3, 6, and 4, in addition to being characterized by the largest damaged areas, are also typical regarding the ground motion change between the two sets. Ground motion 4 (realization 3) and ground motion 1 (realization 6) are representative of a small increase and a moderate decrease in the PGV in both the longitudinal and vertical directions, respectively (BSC 2004 [DIRS 168385], Table 5-1). Ground motion 8 (realization 4) is representative of a moderate PGV increase in the longitudinal and decrease in the vertical direction. Finally, ground motion 3 (realization 15) is characterized by a dramatic PGV increase in both directions. Only material properties evaluated at 150ºC are used in this calculation.

Table 5.2-5. Change of PGV Between Ground Motion Sets

Realization	Ground Motion	Longitudinal (H2) PGV			Vertical (V) PGV		
		Old	New	Change	Old	New	Change
3	4	2.43 *m/s*	2.60 *m/s*	+7%	2.28 *m/s*	2.97 *m/s*	+30%
4	8	2.44 *m/s*	4.02 *m/s*	+65%	2.30 *m/s*	1.54 *m/s*	-33%
6	1	2.43 *m/s*	1.95 *m/s*	-20%	2.30 *m/s*	1.11 *m/s*	-52%
15	3	2.43 *m/s*	6.43 *m/s*	+165%	2.28 *m/s*	6.09 *m/s*	+167%

Source: BSC 2004 [DIRS 168385], Table 5-1.

5.2.5.2 FE Representation

The three-dimensional FE representation for these supplemental calculations is discussed in detail in Section 5.2.1.2. The only difference in the FE representation between these supplemental calculations and the representation in Section 5.2.1.2 is that the supplemental calculations are performed without any rigid elements in the waste package OCB. The potential effects of rigid elements in the FE representation of the OCB were analyzed in detail in *Structural Calculations of Waste Package Exposed to Vibratory Ground Motion* (BSC 2004 [DIRS 167083], Attachment VI), and it was demonstrated that this simplification had only a minor effect on the calculated damaged areas.

A ground motion time history cutoff is applied to the supplemental calculations, similar to that for the original calculations (Section 5.2.1.3). The 2.44 m/s PGV level, the computational duration for the supplemental calculations is restricted to the 5 percent to 95 percent levels of ground motion energy, where energy is based on all three components of the ground motion. The times corresponding to the 5 percent and 95 percent energy levels are defined in *Additional Structural Calculations of Waste Package Exposed to Vibratory Ground Motion* (BSC 2004 [DIRS 168385]) and summarized in Table 5.2-6. The effect of the time history cutoff on the results for the 2.44 m/s PGV level was demonstrated to be negligible in *Structural Calculations of Waste Package Exposed to Vibratory Ground Motion* (BSC 2004 [DIRS 167083], Attachment VII). In Table 5.2-6, the duration of each simulation is obtained by subtracting the starting (5 percent) time from the ending (95 percent) time.

5.3 RESULTS

Sections 5.3.1 through 5.3.3 present the results for damaged area on the waste package from vibratory ground motion, based on the calculations documented in *Structural Calculations of Waste Package Exposed to Vibratory Ground Motion* (BSC 2004 [DIRS 167083]). Section 5.3.4 presents the results for damaged area on the waste package due to side and end impacts, based on the calculations documented in *21-PWR Waste Package Side and End Impacts* (BSC 2003 [DIRS 162293]). Section 5.3.5 presents the results for maximum acceleration of fuel rod assemblies due to end impacts, based on the calculations documented in *Maximum Accelerations on the Fuel Assemblies of a 21-PWR Waste Package During End Impacts* (BSC 2003 [DIRS 162602]). A series of additional studies aimed at examining sensitivity of damage estimates to mesh refinement, alternative ground motions representation and methodology for damage estimates of end impacts are given in Sections 5.3.6 to 5.3.8. The stress time histories, residual stress distribution plots, impact parameters, and damaged areas presented in this section have been obtained by with the postprocessors LSPOST V2.0 and LS-PREPOST V1.0.

Table 5.2-6. Duration and Characteristic Times Corresponding to 5 Percent - 95 Percent Energy Range

	Ground Motion	5%- Time (s)	95%- Time (s)	Duration of Simulation (s)
3	4	1.48	17.29	15.81
4	8	1.21	6.48	5.27
6	1	1.28	7.47	6.19
15	3	1.75	4.73	2.98

Source: BSC 2004 [DIRS 168385], Table 5.2-1.

The stress intensity presented in this section is defined as the difference in the major principal stresses (ASME 2001 [DIRS 158115], Section 3, Division 1, NB-3000, Dieter 1976, [DIRS 118647], Chapter 3).

5.3.1 Damage From Vibratory Ground Motions at 2.44 m/s PGV Level

5.3.1.1 Interaction Between Waste Package and Pallet

The damaged area due to the waste package-pallet interaction is only evaluated on the half of the waste package with the finely-meshed region (see Figure 5.2-3, Figure 5.2-4, and the discussion in Section 5.2.1). The total damaged area from waste package-pallet interaction is calculated by multiplying the damaged area from the finely zoned region by two (Assumption 3.9).

The damaged area is presented as an area and as a fraction of the total OCB area (including the OCB lids) throughout this document. This approach is useful for scaling the current results to other waste package types. The surface area of 21-PWR waste package OCB is calculated to be 28.2 m^2 (BSC 2004 [DIRS 167083], Section 6.1.1).

Table 5.3-1 presents the damaged area resulting from the waste package-pallet interactions during the vibratory ground motion. The damaged area is based on the residual first principal stress plot, as computed by the postprocessor LSPOST V2.0.

Table 5.3-1. Damaged Area from Waste Package-Pallet Interaction at the 2.44 m/s PGV Level

Realization Number	Ground Motion Number	Damaged Area (m^2; % of total OCB area)	
		80% Yield Strength	90% Yield Strength
1	7	0.0029; 0.010%	0.0014; 0.0050%
2	16	0; 0	0; 0
3	4	0.0050; 0.018%	0; 0
4	8	0.030; 0.11%	0.0064; 0.023%
5	11	0.0015; 0.0053%	0; 0
6	1	0.025; 0.089%	0.0028; 0.0099%
7	2	0.017; 0.060%	0; 0
8	13	0; 0	0; 0
9	10	0.0035; 0.012%	0; 0
10	9	0; 0	0; 0
11	5	0.012; 0.043%	0.0037; 0.013%
12	6	0.0039; 0.014%	0; 0
13	12	0; 0	0; 0
14	14	0.010; 0.035%	0.0043; 0.015%
15	3	0.0078; 0.028%	0.0015; 0.0053%

Source: BSC 2004 [DIRS 167083], Table 6.1.1-1.

5.3.1.2 Interaction Between Waste Package and Longitudinal Boundary

This section presents the damaged area of the waste package OCB resulting from waste package-waste package interaction due to end-to-end impacts in the longitudinal direction. The damage is calculated by using the results in Tables 5.3-56, 5.3-57, 5.3-58 and 5.3-59, based on the speed, location, and angle for the individual end-to-end impacts calculated by these waste package simulations under vibratory ground motion. In other words, the current simulations define the kinematics of the impacts, while the damage from each impact is calculated using the impact velocity, impact location, and relative angle as interpolating parameters in the catalog of damaged areas in Tables 5.3-56, 5.3-57, 5.3-58 and 5.3-59.

The end-impact parameters presented in this section are evaluated with the postprocessor LSPOST V2. The "time" presented in the second column (Tables 5.3-2 through 5.3-15) is the time of impact, and it is obtained directly from the postprocessor. The impact speed (the third column) is relative speed between the longitudinal boundary (representing the neighboring waste package) and the first waste package (i.e., its trunnion collar sleeve) node that first comes in contact with the axial boundary at the time of impact. The impact angle presented in the fourth column defines the inclination of the waste package with respect to the longitudinal boundary; an angle of zero degrees corresponds to simultaneous contact everywhere on the trunnion collar sleeve.

The impact location (first column in table) is important for damage accumulation. The rationale for introducing the impact location is to prevent excessive conservatism that would result by simply adding the damage from individual impacts regardless of their location. The approach is based on purely geometrical arguments. If two impacts take place sufficiently close to each other, then their damage may overlap to a certain extent. The angular extent of the damaged area is a function of the impact speed and the impact angle (see Tables 5.3-56, 5.3-57, 5.3-59 and 5.3-60). The convention used to identify the impact locations is illustrated in Figure 5.3-1.

The impact location is defined with 12 discrete values (i.e., from 1 to 12 in 30° increments) equidistantly distributed in the clockwise direction (see the red numbers in Figure 5.3-1)[6]. Moreover, an end impact can take place on the waste package side corresponding to the finely meshed (identified as region "F" in Figure 5.2-4) or coarsely meshed (region "C") part of the OCB. Figure 5.3-2 presents a side view of the waste package that illustrates the naming convention for the "F" and "C" sides, only showing the designators closer to a viewer. That is, F9 is not shown to emphasize that it is behind F3 in this side view. Note that according to the outward looking convention, F12 corresponds to C12, F1 corresponds to C11, F2 corresponds to C10, and so on.

As an example, assuming that the impact between waste package and axial boundary takes place on the "coarse side" of the waste package OCB, the impact location marked by the blue arrow in Figure 5.3-1 would be designated as "C 2."

[6] Notice that the selection of 12 segments was arbitrary. The appropriateness of this choice was verified during post-processing. Namely, no need for more detailed discretization of impact locations was encountered in the process (Notice that if that need had arisen during post-processing, then it would be possible to use fractions [C12.5, F4.24, G7.1, and so on] to designate locations more precisely, without changing the number of selected segments.).

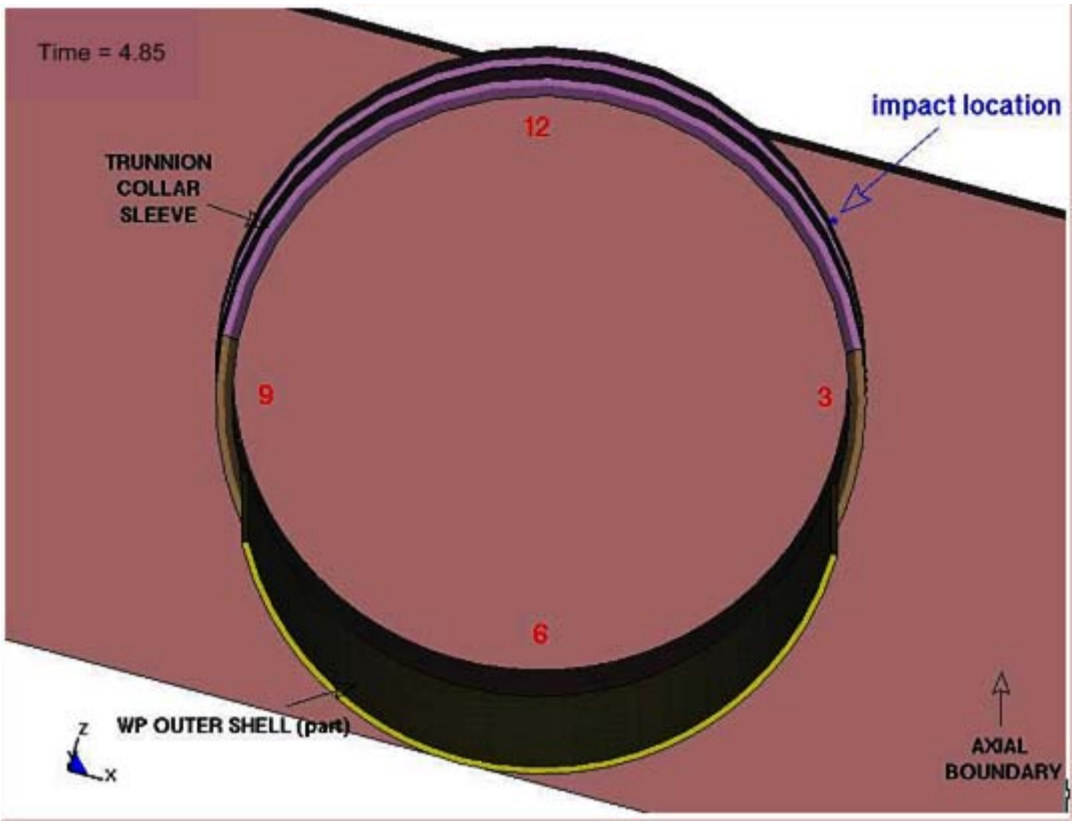

Source: BSC 2004 [DIRS 167083], Figure 8.

Figure 5.3-1. "Clock" Convention Used for Evaluation of Impact Location

Source: BSC 2004 [DIRS 168385], Figure 5.3.1-2.

Figure 5.3-2. Schematic Illustration of Waste Package Emplaced on Pallet Indicating Waste Package End Designation (Initial Position)

The damage contribution from each impact with a speed exceeding 1 m/s (Assumption 3.7) is accounted for in one of the three ways, depending of the location and the circumferential extent of damage. The damage contribution can be either fully taken into account, or just one-half of it (designated with "$\times 0.5$" in appropriate tables), or it may not be taken into account at all (designated as "NC" for "not counted"). Furthermore, if damage caused by two impacts partially overlap, the larger damage is fully taken into account while the smaller is reduced. As an example, the damage contribution from the impact at location "C 10" in Table 5.3-2 is taken into

account as one-half of the corresponding value, since the damage caused by impact at location "C 11" partially overlaps the "C 10" damage according to *21-PWR Waste Package Side and End Impacts* (BSC 2003 [DIRS 162293], Table 4 and Table 5). On the other hand, the "C 6" damage in Table 5.3-4 is not taken into account at all ("NC") since it is completely overlapped by "C 7" damage.

The end-impact parameters and corresponding damaged areas (calculated for both the lower and upper damage thresholds) are presented in Tables 5.3-2 through 5.3-15 for the 2.44 m/s PGV level.

Table 5.3-2. End-Impact Parameters and Damaged Area for Realization 1 at the 2.44 m/s PGV Level

Impact Location	Time (s)	Speed (m/s)	Angle (degree)	Damaged Area (m^2)	
				80% Yield Strength	90% Yield Strength
F 8	6.025	1.3	1.0	0.0089	0.0046
C 10	4.750	1.0	1.5	0.0031X0.5	0.0017X0.5
C 11	4.875	1.5	1.3	0.0122	0.0063
Total				0.023	0.012

Source: BSC 2004 [DIRS 167083], Table 6.1.2-1.

Table 5.3-3. End-Impact Parameters and Damaged Area for Realization 2 at the 2.44 m/s PGV Level

Impact Location	Time (s)	Speed (m/s)	Angle (degree)	Damaged Area (m^2)	
				80% Yield Strength	90% Yield Strength
F	0.750	1.2	0	0	0
F 8	3.150	1.8	0.5	0.0092X0.5	0.0047X0.5
F 9	5.000	1.5	1.0	0.0127	0.0065
Total				0.017	0.0089

Source: BSC 2004 [DIRS 167083], Table 6.1.2-2.

Table 5.3-4. End-Impact Parameters and Damaged Area for Realization 3 at the 2.44 m/s PGV Level

Impact Location	Time (s)	Speed (m/s)	Angle (degree)	Damaged Area (m^2)	
				80% Yield Strength	90% Yield Strength
F 1	6.050	1.3	1.3	0.0086	0.0045
F 6	3.500	3.9	3.4	0.0771	0.0374
F 9	0.675	1.5	1.1	0.0125	0.0064
F 11	3.100	2.4	0.9	0.0296	0.0124
C 4	0.975	1.1	1.6	0.0048	0.0026
C 6	2.625	1.1	1.6	0.0048 NC	0.0026 NC
C 7	3.225	3.6	0.9	0.0588	0.0192
C 8	4.575	1.5	1.6	0.0117 NC	0.0060 NC
C 8	7.350	1.1	1.1	0.0051 NC	0.0027 NC
Total				0.19	0.083

Source: BSC 2004 [DIRS 167083], Table 6.1.2-3.

Table 5.3-5. End-Impact Parameters and Damaged Area for Realization 4 at the 2.44 m/s PGV Level

Impact Location	Time (s)	Speed (m/s)	Angle (degree)	Damaged Area (m^2)	
				80% Yield Strength	90% Yield Strength
F 3	2.400	1.9	1.0	0.0202	0.0103
F 9	2.775	2.5	4.1	0.0307	0.0162
C 9	2.650	2.6	2.9	0.0354 NC	0.0166 NC
C 9	2.700	3.5	4.0	0.0650	0.0343
Total				0.12	0.061

Source: BSC 2004 [DIRS 167083], Table 6.1.2-4.

Table 5.3-6. End-Impact Parameters and Damaged Area for Realization 5 at the 2.44 m/s PGV Level

Impact Location	Time (s)	Speed (m/s)	Angle (degree)	Damaged Area (m^2)	
				80% Yield Strength	90% Yield Strength
F 2	0.425	1.6	1.2	0.0142 NC	0.0073 NC
F 2	2.025	2.0	1.7	0.0201 NC	0.0102 NC
F 2	2.075	4.2	1.4	0.0836 NC	0.0275 NC
F 3	3.425	1.3	2.9	0.0068 NC	0.0036 NC
F 3	5.025	1.8	3.0	0.0137 NC	0.0070 NC
F 3	5.075	4.4	2.5	0.0947	0.0385
F 3	5.900	1.3	1.0	0.0089 NC	0.0046 NC
F 9	1.325	1.2	1.7	0.0064	0.0034
F 9	2.500	1.0	3.8	0.0022 NC	0.0013 NC
C 2	3.125	1.2	0.2	0.0014	0.0007
C 3	0.800	1.2	1.7	0.0064X0.5	0.0034X0.5
C 4	1.650	1.7	2.9	0.0125	0.0064
C 9	2.325	2.4	4.7	0.0262	0.0145
C 11	0.200	1.4	0.2	0.0022	0.0011
Total				0.15	0.066

Source: BSC 2004 [DIRS 167083], Table 6.1.2-5.

Table 5.3-7. End-Impact Parameters and Damaged Area for Realization 6 at the 2.44 m/s PGV Level

Impact Location	Time (s)	Speed (m/s)	Angle (degree)	Damaged Area (m^2)	
				80% Yield Strength	90% Yield Strength
F 4	1.950	2.5	1.4	0.0344	0.0140
F 4	2.600	2.4	0.5	0.0186 NC	0.0090 NC
F 8	1.525	1.9	1.0	0.0202X0.5	0.0103X0.5
F 9	1.100	2.4	1.5	0.0315	0.0134
F 9	3.025	1.9	1.6	0.0187 NC	0.0095 NC
C 9	3.125	4.0	2.7	0.0692	0.0300
C 9	2.750	2.9	0.9	0.0418 NC	0.0152 NC
Total				0.15	0.063

Source: BSC 2004 [DIRS 167083], Table 6.1.2-6.

Table 5.3-8. End-Impact Parameters and Damaged Area for Realization 7 at the 2.44 m/s PGV Level

Impact Location	Time (s)	Speed (m/s)	Angle (degree)	Damaged Area (m^2)	
				80% Yield Strength	90% Yield Strength
F 2	2.350	1.4	0.4	0.0043	0.0022
F 9	3.700	2.7	0.5	0.0243	0.0116
F 10	2.925	2.1	2.5	0.0209 NC	0.0103 NC
C	3.150	2.2	0	0.0024	0.0024
C 3	4.150	1.2	0.8	0.0056 NC	0.0029 NC
C 3	4.200	4.5	0.4	0.0538	0.0265
C 8	2.775	2.4	3.0	0.0290	0.0139
Total				0.11	0.057

Source: BSC 2004 [DIRS 167083], Table 6.1.2-7.

An error in the specification of initial velocity components for realization 8 was identified after the simulation was completed. Specifically, the three initial velocity components do not correspond to the beginning of the acceleration time history. Consequently, the velocity and displacement time histories are not appropriately specified, and the results from this realization are not included in the tables summarizing results (Tables 5.3-18, 5.3-24, and 5.3-25).

Table 5.3-9. End-Impact Parameters and Damaged Area for Realization 9 at the 2.44 m/s PGV Level

Impact Location	Time (s)	Speed (m/s)	Angle (degree)	Damaged Area (m^2)	
				80% Yield Strength	90% Yield Strength
F 3	0.800	1.5	1.7	0.0116	0.0059
F 3	7.075	1.0	2.4	0.0027 NC	0.0016 NC
F 5	2.625	1.7	2.7	0.0129	0.0066
F 8	1.575	2.8	4.5	0.0408	0.0226
F 9	2.250	1.6	5.0	0.0072 NC	0.0038 NC
F 9	2.325	1.1	4.1	0.0021 NC	0.0013 NC
F 10	3.950	1.8	1.4	0.0174	0.0089
C 8	1.375	1.4	2.6	0.0086	0.0045
C 9	1.925	1.7	4.2	0.0098X0.5	0.0051X0.5
C 10	2.450	2.2	3.8	0.0210	0.0107
Total				0.12	0.062

Source: BSC 2004 [DIRS 167083], Table 6.1.2-9.

Table 5.3-10. End-Impact Parameters and Damaged Area for Realization 10 at the 2.44 m/s PGV Level

Impact Location	Time (s)	Speed (m/s)	Angle (degree)	Damaged Area (m^2)	
				80% Yield Strength	90% Yield Strength
F 3	5.425	1.1	2.7	0.0041	0.0022
C 3	5.050	1.5	0.3	0.0038 NC	0.0020 NC
C 3	5.175	1.6	3.8	0.0094	0.0049
Total				0.014	0.0071

Source: BSC 2004 [DIRS 167083], Table 6.1.2-10.

Table 5.3-11. End-Impact Parameters and Damaged Area for Realization 11 at the 2.44 m/s PGV Level

Impact Location	Time (s)	Speed (m/s)	Angle (degree)	Damaged Area (m^2)	
				80% Yield Strength	90% Yield Strength
F 6	4.150	1.7	1.5	0.0154	0.0079
F 10	1.275	1.5	0.3	0.0038 NC	0.0020 NC
F 10	2.125	1.6	1.7	0.0133	0.0068
C 3	0.975	1.1	0.5	0.0026	0.0014
C 8	3.400	1.6	1.9	0.0129 NC	0.0066 NC
C 9	2.000	1.7	1.6	0.0152 NC	0.0078 NC
C 9	2.225	2.8	1.3	0.0425	0.0158
Total				0.074	0.032

Source: BSC 2004 [DIRS 167083], Table 6.1.2-11.

Table 5.3-12. End-Impact Parameters and Damaged Area for Realization 12 at the 2.44 m/s PGV Level

Impact Location	Time (s)	Speed (m/s)	Angle (degree)	Damaged Area (m^2)	
				80% Yield Strength	90% Yield Strength
F 3	6.400	1.1	0.7	0.0036	0.0019
F 8	5.950	3.0	0.4	0.0264	0.0138
F 9	3.575	1.1	0.8	0.0041 NC	0.0022 NC
C 3	1.025	2.2	0.5	0.0148	0.0073
C 4	5.825	2.2	0.2	0.0074X0.5	0.0044X0.5
C 4	6.175	1.0	1.7	0.0030 NC	0.0017 NC
C 9	3.775	2.3	0.8	0.0246	0.0109
Total				0.073	0.036

Source: BSC 2004 [DIRS 167083], Table 6.1.2-12.

Table 5.3-13. End-Impact Parameters and Damaged Area for Realization 13 at the 2.44 m/s PGV Level

Impact Location	Time (s)	Speed (m/s)	Angle (degree)	Damaged Area (m^2)	
				80% Yield Strength	90% Yield Strength
F 4	2.300	1.9	0.6	0.0121	0.0062
C 3	2.025	1.2	0.5	0.0035 NC	0.0018 NC
C 3	2.450	2.0	3.2	0.0159	0.0081
C 3	7.625	1.1	0.9	0.0047 NC	0.0025 NC
C 9	9.875	1.1	0.7	0.0036	0.0019
Total				0.032	0.016

Source: BSC 2004 [DIRS 167083], Table 6.1.2-13.

Table 5.3-14. End-Impact Parameters and Damaged Area for Realization 14 at the 2.44 m/s PGV Level

Impact Location	Time (s)	Speed (m/s)	Angle (degree)	Damaged Area (m^2)	
				80% Yield Strength	90% Yield Strength
F 2	2.775	1.4	0.2	0.0022	0.0011
F 3	3.925	1.0	0.6	0.0020	0.0011
C 10	4.450	1.2	0.2	0.0014	0.0007
Total				0.0056	0.0029

Source: BSC 2004 [DIRS 167083], Table 6.1.2-14.

Table 5.3-15. End-Impact Parameters and Damaged Area for Realization 15 at the 2.44 m/s PGV Level

Impact Location	Time (s)	Speed (m/s)	Angle (degree)	Damaged Area (m^2)	
				80% Yield Strength	90% Yield Strength
F 8	1.125	2.0	1.7	0.0201	0.0102
Total				0.020	0.010

Source: BSC 2004 [DIRS 167083], Table 6.1.2-15.

Table 5.3-16 presents a summary of the total damaged areas for each realization, based on the information in Tables 5.3-2 through 5.3-15. Realization 8 is not included because of an input error in the analysis.

Table 5.3-16. Damaged Area from End Impacts (Waste Package-Waste Package Interaction) at the 2.44 m/s PGV Level

Realization Number	Ground Motion	Damaged Area (m^2; % of total OCB area)	
		80% Yield Strength	90% Yield Strength
1	7	0.023; 0.082%	0.012; 0.043%
2	16	0.017; 0.060%	0.0089; 0.032%
3	4	0.19; 0.67%	0.083; 0.29%
4	8	0.12; 0.43%	0.061; 0.22%
5	11	0.15; 0.53%	0.066; 0.23%
6	1	0.15; 0.53%	0.063; 0.22%
7	2	0.11; 0.39%	0.057; 0.20%
9	10	0.12; 0.43%	0.062; 0.22%
10	9	0.014; 0.050%	0.0071; 0.025%
11	5	0.074; 0.26%	0.032; 0.11%
12	6	0.073; 0.26%	0.036; 0.13%
13	12	0.032; 0.11%	0.016; 0.057%
14	14	0.0056; 0.020%	0.0029; 0.010%
15	3	0.020; 0.071%	0.010; 0.035%

Source: BSC 2004 [DIRS 167083], Table 6.1.2-16.

Although an attempt has been made to prevent excessive conservatism in the analysis of damaged areas from waste package-to-waste package impacts by using the damage accumulation technique described above, the results are still conservative. This conservatism is an unavoidable consequence of the FE representation. Two sources of conservatism need to be mentioned here:

- The damaged area from the waste package impacting the longitudinal boundary (representing the neighboring waste package) is calculated based on the end impacts on the surface that is not only unyielding but also completely constrained (BSC 2003 [DIRS 162293]). Consequently, the entire kinetic energy for each impact is transformed into the deformation of a single waste package. In reality, the part of the kinetic energy transferred into deformation energy is not only distributed between the two colliding waste packages but is also smaller than predicted because of elastic rebound during the impact.

- The damage accumulation technique is unable to represent relaxation of residual stress during subsequent impacts. In other words, the damaged area is not a monotonically increasing area, but can decrease if subsequent impacts relieve the stress from a previous impact. A region of the OCB that exceeded the residual stress threshold at time t_1 can be below that threshold following a "favorable" impact at time t_2 (where $t_2 > t_1$).

It is important to recognize that these aspects of the current FE representation lead to conservative estimates of the damage area.

5.3.1.3 Interaction Between Waste Package and Drip Shield

The impact velocity between the waste package and the drip shield is presented in this section. The interaction between the waste package (i.e., trunnion collar sleeves) and the drip shield occurred only in realizations 4, 7, 9, 11, and 15. In all other realizations there was no impact between the waste package and the drip shield.

It is clear from the results presented in Tables 5.3-17 through 5.3-21 that side impacts between the waste package and drip shield are infrequent events for ground motions at the 2.44 m/s PGV level and are characterized by relatively modest impact speeds, mostly between 1 *m/s* and 2 *m/s*. The impact speeds in this range do not contribute significantly to the total damaged area even when the waste package is impacting an unyielding surface (BSC 2003 [DIRS 162293], Table 4 through Table 8 (Side Impacts)). In this situation, these lateral impacts do not cause significant damage to the waste package, consistent with Assumption 3.6. Moreover, the drip shield was not constrained by the drift wall at any time of impact with the waste package. Consequently, the impact energy was not, after the impact, transformed entirely into deformation energy but also into kinetic energy of waste package and drip shield.

Table 5.3-17. Lateral-Impact Parameters for Realization 4 at the 2.44 m/s PGV Level

Impact Location	Time (s)	Speed (m/s)	Angle (degree)
F 3	2.700	2.9	3.0

Source: BSC 2004 [DIRS 167083], Table 6.1.3-1.

Table 5.3-18. Lateral-Impact Parameters for Realization 7 at the 2.44 m/s PGV Level

Impact Location	Time (s)	Speed (m/s)	Angle (degree)
C 3	2.800	1.2	3.4

Source: BSC 2004 [DIRS 167083], Table 6.1.3-2.

Table 5.3-19. Lateral-Impact Parameters for Realization 9 at the 2.44 m/s PGV Level

Impact Location	Time (s)	Speed (m/s)	Angle (degree)
C 3	1.000	1.3	3.4
F 3	1.575	2.1	4.4
F 3	2.225	2.0	4.8
F 3	2.300	1.2	4.4
F 9	2.600	4.1	0.2

Source: BSC 2004 [DIRS 167083], Table 6.1.3-3.

Table 5.3-20. Lateral-Impact Parameters for Realization 11 at the 2.44 m/s PGV Level

Impact Location	Time (s)	Speed (m/s)	Angle (degree)
C 9	2.500	1.8	4.8

Source: BSC 2004 [DIRS 167083], Table 6.1.3-4.

Table 5.3-21. Lateral-Impact Parameters for Realization 15 at the 2.44 m/s PGV Level

Impact Location	Time (s)	Speed (m/s)	Angle (degree)
F 3	1.125	1.2	1.0

Source: BSC 2004 [DIRS 167083], Table 6.1.3-5.

5.3.1.4 Summary of Results at the 2.44 m/s PGV Level

The damaged areas characterizing 14 different realizations for the ground motions at the 2.44 m/s PGV level are summarized in Table 5.3-22. The results in Table 5.3-22 show that the cumulative damage area is dominated by the contribution from end impacts. In all realizations, (with exception of realization 14) the damaged area from waste package pallet interaction is much smaller than the damaged area from waste package-waste package interaction. As a reminder, some of this difference is probably caused by the conservatisms in the damage accumulation procedure for the waste package-to-waste package impacts, as discussed at the end of Section 5.3.1.2.

The information in Table 5.3-22 is used directly in the development of the waste package damage abstraction for the seismic scenario class. These data are available through *D&E / PA/C IED Typical Waste Package Components Assembly* (BSC 2004 [DIRS 169990], Table 16).

Table 5.3-22. Damaged Area from Vibratory Ground Motion at the 2.44 m/s PGV Level

Realization Number[a]	Ground Motion Number	Damaged Area on the Waste Package					
		WP to Pallet Interaction (m^2; % of total OS[d] area)		WP to WP Interaction (m^2; % of total OS[d] area)		Cumulative Damage (m^2; % of total OS[d] area)	
		80% Yield Strength	90% Yield Strength	80% Yield Strength	90% Yield Strength	80% Yield Strength	90% Yield Strength
1	7	0.0029; 0.010%	0.0014; 0.0050%	0.023; 0.082%	0.012; 0.043%	0.026; 0.092%	0.013; 0.046%
2	16[b]	0; 0	0; 0	0.017; 0.060%	0.0089; 0.032%	0.017; 0.060%	0.0089; 0.032%
3	4	0.0050; 0.018%	0; 0	0.19; 0.67%	0.083; 0.29%	0.20; 0.71%	0.083; 0.29%
4	8	0.030; 0.11%	0.0064; 0.023%	0.12; 0.43%	0.061; 0.22%	0.15; 0.53%	0.067; 0.24%
5	11	0.0015; 0.0053%	0; 0	0.15; 0.53%	0.066; 0.23%	0.15; 0.53%	0.066; 0.23%
6	1	0.025; 0.089%	0.0028; 0.0099%	0.15; 0.53%	0.063; 0.22%	0.18; 0.64%	0.066; 0.23%
7	2	0.017; 0.060%	0; 0	0.11; 0.39%	0.057; 0.20%	0.13; 0.46%	0.057; 0.20%
9	10	0.0035; 0.012%	0; 0	0.12; 0.43%	0.062; 0.22%	0.12; 0.43%	0.062; 0.22%
10	9	0; 0	0; 0	0.014; 0.050%	0.0071; 0.025%	0.014; 0.050%	0.0071; 0.025%
11	5	0.012; 0.043%	0.0037; 0.013%	0.074; 0.26%	0.032; 0.11%	0.086; 0.30%	0.036; 0.13%
12	6	0.0039; 0.014%	0; 0	0.073; 0.26%	0.036; 0.13%	0.077; 0.27%	0.036; 0.13%

Table 5.3-22. Damaged Area from Vibratory Ground Motion at the 2.44 m/s PGV Level (Continued)

Realization Number[a]	Ground Motion Number	Damaged Area on the Waste Package					
		WP to Pallet Interaction (m^2; % of total OS[d] area)		WP to WP Interaction (m^2; % of total OS[d] area)		Cumulative Damage (m^2; % of total OS[d] area)	
		80% Yield Strength	90% Yield Strength	80% Yield Strength	90% Yield Strength	80% Yield Strength	90% Yield Strength
13	12	0; 0	0; 0	0.032; 0.11%	0.016; 0.057%	0.032; 0.11%	0.016; 0.057%
14	14	0.010; 0.035%	0.0043; 0.015%	0.0056; 0.020%	0.0029; 0.010%	0.016; 0.057%	0.0072; 0.026%
15	3	0.0078; 0.028%	0.0015; 0.0053%	0.020; 0.071%	0.010; 0.035%	0.028; 0.099%	0.012; 0.043%
				Mean Value[c, e]		0.310%	0.136%
				Standard Deviation[c]		0.237%	0.097%
				Minimum Value[c]		0.050%	0.025%
				Maximum Value[c]		0.710%	0.290%

Source: BSC 2004 [DIRS 169990], Table 16.

[a] Only 14 realizations are presented in this table. Results for realization 8 are not presented because of an error in the input file for this calculation.

[b] Calculations are performed with 15 ground motions numbered 1, 2, 3, …, 14, and 16. Seventeen sets of ground motion time histories were initially developed from which 15 sets were selected for postclosure analyses. Two extra sets were developed to allow for substitutions if any of the sets were found to be inappropriate. For example, the response spectrum for the vertical component of ground motion #15 is an outlier when plotted with the other 16 response spectra. It exhibits anomalously low values at high frequencies (greater than about 2 Hz) and anomalously high values at low frequencies (less than about 0.2 Hz). Ground motion #16 was substituted for ground motion #15 for all computational suites at 2.44 m/s PGV level and at 5.35 m/s PGV level because of its anomalous response spectrum.

[c] Mean, standard deviation, minimum and maximum damage areas calculated in Appendix B.

[d] Outer surface of waste package.

[e] The mean value of percent damaged area for end-to-end impacts is 0.278 percent and 0.130 percent at stress thresholds of 80 percent and 90 percent of yield strength, respectively. These values represent 89.7 percent and 95.7 percent, of the total mean cumulative mean damage for the two residual stress thresholds.

WP = waste package

5.3.2 Damage from Ground Motions at the 5.35 m/s PGV Level

The ground motions at the 5.35 m/s PGV level are much more intense than their counterparts at the 2.44 m/s PGV level. As an example, the maximum peak acceleration in ground motion 9 is approximately 34 *g* (*g* = 9.81 m/s, the acceleration of gravity), while the maximum PGV in ground motion 3 is approximately 16 *m/s* (BSC 2004 [DIRS 167083], Section 6.2). For comparison, the maximum peak ground acceleration is approximately 10 *g* at the 2.44 m/s PGV level (BSC 2004 [DIRS 167083]). As a consequence of the high-intensity ground motions at 5.35 m/s PGV level, the kinematics of the unanchored repository components are characterized by extreme rigid-body motion and numerous high-speed impacts (BSC 2004 [DIRS 167083], Figures 25 and 26).

5.3.2.1 Interaction Between Waste Package and Pallet

Table 5.3-23 presents the damaged area resulting from the waste package-pallet interaction during the vibratory ground motion.

Table 5.3-23. Damaged Area from Waste Package-Pallet Interaction at the 5.35 m/s PGV Level

Realization Number	Ground Motion Number	Damaged Area (m^2; % of total OCB area)	
		80% Yield Strength	90% Yield Strength
1	7	0.20; 0.71%	0.17; 0.60%
3	4	0.096; 0.34%	0.083; 0.29%
4	8	0.12; 0.43%	0.096; 0.34%
5	11	0.093; 0.33%	0.071; 0.25%
6	1	0.046; 0.16%	0.024; 0.085%
7	2	0.038; 0.13%	0.028; 0.099%
8	13	0.095; 0.34%	0.068; 0.24%
9	10	0.0052; 0.018%	0.0035; 0.012%
10	9	0.16; 0.57%	0.14; 0.50%
11	5	0.0016; 0.0057%	0; 0
12	6	0.062; 0.22%	0.041; 0.15%
13	12	0.027; 0.096%	0.018; 0.064%
14	14	0.020; 0.071%	0.016; 0.057%
15	3	0.0045; 0.016%	0; 0

Source: BSC 2004 [DIRS 167083], Table 6.2.1-1.

NOTE: Accuracy of the damaged area due to the Waste Package-pallet interaction is doubtful (see discussion in BSC 2004 [DIRS 167083], Section 6).

Results are not available for realization 2. This realization is one of four for which the simulation was performed with the FE representation for the 2.44 m/s PGV level calculations (compare Figures 5.2-3 and 5.2-7a, and see discussion in Section 5.2.1.2). Unfortunately, this approach failed because the areas of contact between the waste package and pallet extended beyond the finely meshed region of waste package OCB for realization 2 (see illustration in BSC 2004 [DIRS 167083], Figure VIII-2). The calculated damaged area for realization 2 is therefore of questionable accuracy and the results are not included in Table 5.3-23.

5.3.2.2 Interaction Between Waste Package and Longitudinal Boundary

This section presents the damaged area of the waste package OCB resulting from waste package-waste package interaction due to end-to-end impacts in the longitudinal direction. It is calculated by using the results in *21-PWR Waste Package Side and End Impacts* (BSC 2003 [DIRS 162293], Tables 5.3-56, 5.3-57, 5.3-59, and 5.3-60), based on the speed, location, and angle for the individual end-to-end impacts calculated by these waste package simulations under vibratory ground motion. In other words, the current simulations define the kinematics of the impacts, while the damage from each impact is calculated using the impact velocity, impact location, and relative angle as interpolating parameters in the catalog of damaged areas for individual impacts in *21-PWR Waste Package Side and End Impacts* (BSC 2003 [DIRS 162293], Tables 4, 5, 7, and 8).

The end-impact parameters and corresponding damaged areas (calculated for both the lower and upper damage thresholds) are presented in Tables 5.3-24 through 5.3-38 for all 15 realizations at the 5.35 m/s PGV level.

Table 5.3-24. End-Impact Parameters and Damaged Area for Realization 1 at the 5.35 m/s PGV Level

Impact Location	Time (s)	Speed (m/s)	Angle (degree)	Damaged Area (m^2)	
				80% Yield Strength	90% Yield Strength
F 3	4.825	2.0	2.6	0.0176	0.0090
F 7	2.725	1.4	2.7	0.0085	0.0044
F 8	4.025	1.0	7.2	0.0013 NC	0.0010 NC
F 8	7.100	1.2	3.7	0.0047	0.0025
F 9	2.350	1.0	3.9	0.0021	0.0013
C 2	4.900	4.5	5.3	0.1005	0.0556
C 3	5.400	1.8	1.0	0.0183 NC	0.0093 NC
C 7	2.100	1.8	2.1	0.0158	0.0080
C 10	4.525	1.2	6.6	0.0033	0.0020
C 11	6.900	1.3	4.0	0.0056	0.0030
Total				0.16	0.086

Source: BSC 2004 [DIRS 167083], Table 6.2.2-1.

Table 5.3-25. End-Impact Parameters and Damaged Area for Realization 2 at the 5.35 m/s PGV Level

Impact Location	Time (s)	Speed (m/s)	Angle (degree)	Damaged Area (m^2)	
				80% Yield Strength	90% Yield Strength
F 2	3.500	1.1	2.8	0.0040X0.5	0.0022X0.5
F 3	4.975	1.9	1.0	0.0202	0.0103
F 9	0.500	1.6	0.3	0.0044	0.0022
F 12	2.300	1.1	1.0	0.0052	0.0027
C 1	1.600	1.4	0.2	0.0022	0.0011
C 3	4.675	1.3	0.6	0.0054	0.0028
C 7	3.725	1.3	1.0	0.0089	0.0046
Total				0.048	0.025

Source: BSC 2004 [DIRS 167083], Table 6.2.2-2.

Table 5.3-26. End-Impact Parameters and Damaged Area for Realization 3 at the 5.35 m/s PGV Level

Impact Location	Time (s)	Speed (m/s)	Angle (degree)	Damaged Area (m^2)	
				80% Yield Strength	90% Yield Strength
F 1	1.225	1.3	1.7	0.0082 NC	0.0042 NC
F 1	2.650	2.4	1.4	0.0317	0.0133
F 4	5.600	3.4	1.3	0.0584	0.0196
F 5	0.925	1.7	2.2	0.0140 NC	0.0071 NC
F 5	2.900	3.7	2.5	0.0688 NC	0.0288 NC
F 7	3.100	4.0	3.6	0.0809	0.0404
F 8	6.600	1.5	0.3	0.0038 NC	0.0019 NC
F 8	8.450	1.7	1.4	0.0156 NC	0.0080 NC
F 9	1.700	2.2	1.7	0.0257X0.5	0.0118X0.5
F 9	4.725	2.2	0.2	0.0074 NC	0.0044 NC
F 9	9.000	1.1	5.0	0.0026 NC	0.0016 NC
F 10	3.975	2.3	3.2	0.0255	0.0125
F 10	10.275	1.7	3.1	0.0121 NC	0.0062 NC
C 2	1.875	2.7	0.8	0.0338 NC	0.0135 NC
C 3	0.375	2.5	2.8	0.0325	0.0151
C 3	3.825	2.5	0.4	0.0176 NC	0.0064 NC
C 3	8.650	2.0	1.3	0.0177 NC	0.0090 NC
C 4	6.750	1.7	5.2	0.0081 NC	0.0043 NC
C 5	6.075	1.5	0.6	0.0076 NC	0.0039 NC
C 6	6.950	1.3	1.9	0.0079 NC	0.0041 NC
C 7	1.350	1.1	1.8	0.0047 NC	0.0025 NC
C 7	2.825	4.7	1.4	0.1064	0.0357
C 7	7.300	1.8	4.8	0.0095 NC	0.0049 NC
C 8	1.525	1.0	1.4	0.0031 NC	0.0017 NC
C 8	5.425	1.4	1.0	0.0108 NC	0.0056 NC
C 8	9.825	1.5	2.4	0.0105 NC	0.0054 NC
C 9	4.125	2.4	2.5	0.0299 NC	0.0137 NC
C 10	2.150	1.3	1.9	0.0079 NC	0.0041 NC
C 10	3.200	2.2	1.5	0.0261 NC	0.0119 NC
C 10	4.100	2.1	2.6	0.0206 NC	0.0098 NC
C 11	2.225	1.2	2.2	0.0060 NC	0.0031 NC
C 11	3.000	3.8	2.4	0.0715	0.0293
C 11	5.900	1.2	4.7	0.0038 NC	0.0021 NC
C 11	6.150	1.8	0.6	0.0110 NC	0.0056 NC
Total				0.42	0.17

Source: BSC 2004 [DIRS 167083], Table 6.2.2-3.

Table 5.3-27. End-Impact Parameters and Damaged Area for Realization 4 at the 5.35 m/s PGV Level

Impact Location	Time (s)	Speed (m/s)	Angle (degree)	Damaged Area (m^2)	
				80% Yield Strength	90% Yield Strength
F 3	2.125	3.0	2.5	0.0478	0.0207
F 5	2.875	1.5	2.4	0.0105	0.0054
F 6	2.925	1.6	3.0	0.0109 NC	0.0056 NC
F 7	3.000	1.4	2.0	0.0095 NC	0.0049 NC
F 7	3.725	2.2	1.3	0.0266	0.0120
F 12	3.325	1.2	7.0	0.0033	0.0020
C 2	1.250	1.2	0.4	0.0028	0.0015
C 5	2.475	1.9	4.6	0.0110	0.0057
C 5	3.250	1.7	6.1	0.0082 NC	0.0045 NC
C 6	2.575	1.2	3.6	0.0048X0.5	0.0026X0.5
C 8	1.150	1.3	0.2	0.0018	0.0009
Total				0.11	0.050

Source: BSC 2004 [DIRS 167083], Table 6.2.2-4.

Table 5.3-28. End-Impact Parameters and Damaged Area for Realization 5 at the 5.35 m/s PGV Level

Impact Location	Time (s)	Speed (m/s)	Angle (degree)	Damaged Area (m^2)	
				80% Yield Strength	90% Yield Strength
F	3.675	1.8	0	0	0
F 1	1.925	2.0	4.1	0.0134	0.0069
F 1	4.850	1.4	1.6	0.0100 NC	0.0052 NC
F 5	1.300	2.7	0.9	0.0369	0.0141
F 6	2.700	1.8	1.7	0.0167 NC	0.0085 NC
F 6	5.000	1.2	0.4	0.0028 NC	0.0015 NC
F 7	3.425	1.4	2.6	0.0086	0.0045
F 10	0.350	2.1	1.6	0.0232	0.0111
F 12	5.900	1.3	3.0	0.0067X0.5	0.0035X0.5
C 2	0.525	1.6	1.3	0.0140	0.0072
C 3	5.375	1.7	0.1	0.0016X0.5	0.0008X0.5
C 4	0.825	1.2	0.7	0.0049 NC	0.0026 NC
C 4	3.950	1.2	1.0	0.0071X0.5	0.0037X0.5
C 5	3.000	1.9	2.4	0.0166	0.0085
C 8	1.650	3.4	0.8	0.0498	0.0180
C 8	2.300	1.5	1.3	0.0122 NC	0.0063 NC
C 11	6.225	1.3	2.0	0.0078	0.0041
C 12	0.100	1.4	0.2	0.0022	0.0011
C 12	3.125	1.4	0.2	0.0022 NC	0.0011 NC
Total				0.18	0.080

Source: BSC 2004 [DIRS 167083], Table 6.2.2-5.

Table 5.3-29. End-Impact Parameters and Damaged Area for Realization 6 at the 5.35 m/s PGV Level

Impact Location	Time (s)	Speed (m/s)	Angle (degree)	Damaged Area (m^2)	
				80% Yield Strength	90% Yield Strength
F 2	0.950	4.0	1.7	0.0754 NC	0.0264 NC
F 2	2.325	4.4	1.7	0.0933	0.0328
F 3	3.225	1.3	0.1	0.0009 NC	0.0004 NC
F 6	3.075	2.0	2.0	0.0193	0.0098
F 8	1.775	3.2	2.9	0.0541 NC	0.0246 NC
F 9	1.275	4.4	6.9	0.0863 NC	0.0455 NC
F 9	1.425	1.4	3.3	0.0077 NC	0.0040 NC
F 9	2.125	1.6	1.5	0.0137 NC	0.0070 NC
F 10	0.600	2.9	0.9	0.0418 NC	0.0152 NC
F 10	2.725	5.0	2.0	0.1200	0.0445
C 1	1.575	3.2	1.1	0.0529 NC	0.0176 NC
C 1	2.650	4.6	1.9	0.1024 NC	0.0374 NC
C 1	2.875	2.5	1.2	0.0347 NC	0.0139 NC
C 3	2.250	6.4	1.7	0.1572	0.0563
C 6	0.700	3.7	0.7	0.0522X0.5	0.0200X0.5
C 7	4.275	1.3	0.1	0.0009 NC	0.0004 NC
Total				0.42	0.15

Source: BSC 2004 [DIRS 167083], Table 6.2.2-6.

Table 5.3-30. End-Impact Parameters and Damaged Area for Realization 7 at the 5.35 m/s PGV Level

Impact Location	Time (s)	Speed (m/s)	Angle (degree)	Damaged Area (m^2)	
				80% Yield Strength	90% Yield Strength
F	0.325	1.9	0	0	0
F 1	2.400	6.0	8.4	0.1019 NC	0.0466 NC
F 1	4.150	1.8	0.7	0.0128 NC	0.0065 NC
F 2	4.350	2.3	2.2	0.0275X0.5	0.0126X0.5
F 6	1.700	1.5	1.2	0.0124 NC	0.0063 NC
F 7	4.075	3.4	1.3	0.0584	0.0196
F 9	3.250	3.8	3.7	0.0746 NC	0.0378 NC
F 11	2.175	5.4	1.4	0.1382	0.0472
F 12	2.225	3.1	3.2	0.0511 NC	0.0243 NC
C	2.100	2.0	0	0	0
C 3	2.700	3.3	2.5	0.0568	0.0242
C 3	2.900	1.9	3.3	0.0143 NC	0.0073 NC
C 4	2.000	4.0	0.5	0.0489 NC	0.0228 NC
C 4	3.675	1.6	0.3	0.0044 NC	0.0022 NC
C 6	2.325	1.5	8.0	0.0062	0.0038

Table 5.3-30. End-Impact Parameters and Damaged Area for Realization 7 at the 5.35 m/s PGV Level (Continued)

Impact Location	Time (s)	Speed (m/s)	Angle (degree)	Damaged Area (m^2)	
				80% Yield Strength	90% Yield Strength
C 9	3.375	2.3	1.9	0.0280	0.0126
C 10	4.550	2.0	1.5	0.0207 NC	0.0105 NC
C 11	0.900	1.7	1.3	0.0158	0.0081
Total				0.32	0.12

Source: BSC 2004 [DIRS 167083], Table 6.2.2-7.

Table 5.3-31. End-Impact Parameters and Damaged Area for Realization 8 at the 5.35 m/s PGV Level

Impact Location	Time (s)	Speed (m/s)	Angle (degree)	Damaged Area (m^2)	
				80% Yield Strength	90% Yield Strength
F	12.075	1.2	0	0	0
F 1	2.925	1.7	6.2	0.0082X0.5	0.0045X0.5
F 2	1.100	1.2	1.9	0.0063 NC	0.0033X0.5
F 3	7.025	1.9	4.0	0.0125 NC	0.0064 NC
F 3	9.300	2.0	1.5	0.0207	0.0105
F 4	1.975	1.7	2.5	0.0133 NC	0.0068 NC
F 4	1.550	1.7	1.6	0.0152 NC	0.0077 NC
F 4	5.375	2.2	6.2	0.0179 NC	0.0099X0.5
F 6	3.425	2.6	3.2	0.0351 NC	0.0169 NC
F 7	2.675	3.5	2.9	0.0634	0.0286
F 8	9.350	2.1	0.3	0.0423 NC	0.0254 NC
F 9	11.325	1.0	1.5	0.0031 NC	0.0017 NC
F 10	6.475	1.5	0.6	0.0076 NC	0.0039 NC
F 10	6.775	2.1	1.7	0.0229	0.0110
F 11	4.325	1.6	0.8	0.0117 NC	0.0060 NC
F 12	3.825	2.0	3.2	0.0159	0.0081
F 12	9.900	1.7	0.2	0.0033 NC	0.0017 NC
C 1	2.375	2.0	1.3	0.0213 NC	0.0108 NC
C 2	4.450	1.7	2.5	0.0071 NC	0.0038 NC
C 2	5.225	1.2	3.5	0.0049 NC	0.0026 NC
C 2	5.450	1.2	6.5	0.0033 NC	0.0020 NC
C 2	6.900	2.3	1.6	0.0286	0.0127
C 3	2.275	1.2	0.4	0.0028 NC	0.0015 NC
C 4	2.825	2.2	4.9	0.0185 NC	0.0102 NC
C 4	3.050	3.0	3.2	0.0479	0.0228
C 5	3.075	2.1	3.0	0.0196 NC	0.0098 NC
C 6	4.625	1.2	1.3	0.0068	0.0036
C 8	3.700	3.4	0.6	0.0416 NC	0.0178 NC
C 9	1.850	4.1	1.2	0.0786	0.0243

Table 5.3-31. End-Impact Parameters and Damaged Area for Realization 8 at the 5.35 m/s PGV Level (Continued)

Impact Location	Time (s)	Speed (m/s)	Angle (degree)	Damaged Area (m^2)	
				80% Yield Strength	90% Yield Strength
C 9	9.500	1.6	2.0	0.0127 NC	0.0065 NC
C 10	2.100	2.2	1.4	0.0263 NC	0.0120 NC
C 10	11.725	1.5	1.6	0.0117 NC	0.0060 NC
C 12	3.375	2.3	1.1	0.0296	0.0127
Total				0.32	0.14

Source: BSC 2004 [DIRS 167083], Table 6.2.2-8.

Table 5.3-32. End-Impact Parameters and Damaged Area for Realization 9 at the 5.35 m/s PGV Level

Impact Location	Time (s)	Speed (m/s)	Angle (degree)	Damaged Area (m^2)	
				80% Yield Strength	90% Yield Strength
F 1	1.725	1.7	0.3	0.0049	0.0025
F 8	3.425	1.1	1.0	0.0052	0.0027
C 4	1.475	1.2	0.1	0.0007 NC	0.0004 NC
C 4	3.100	1.4	1.3	0.0104	0.0054
C 11	1.900	1.8	3.2	0.0132	0.0068
Total				0.034	0.017

Source: BSC 2004 [DIRS 167083], Table 6.2.2-9.

Table 5.3-33. End-Impact Parameters and Damaged Area for Realization 10 at the 5.35 m/s PGV Level

Impact Location	Time (s)	Speed (m/s)	Angle (degree)	Damaged Area (m^2)	
				80% Yield Strength	90% Yield Strength
F 2	1.250	6.5	8.0	0.1079	0.0486
F 4	4.950	2.1	8.0	0.0143 NC	0.0081 NC
F 5	2.450	2.4	1.5	0.0315	0.0134
F 6	0.600	2.5	3.7	0.0312 NC	0.0159 NC
F 12	0.875	3.6	5.8	0.0673	0.0388
F 12	1.675	2.7	6.2	0.0241 NC	0.0132 NC
C 1	1.475	3.8	1.8	0.0701	0.0254
C 1	5.200	3.7	8.0	0.0626 NC	0.0322 NC
C 4	0.475	1.3	0.1	0.0009 NC	0.0005 NC
C 4	1.300	1.3	8.0	0.0042	0.0026
C 5	0.825	1.8	4.0	0.0114 NC	0.0057 NC
C 5	1.200	2.5	7.1	0.0273	0.0150

Table 5.3-33. End-Impact Parameters and Damaged Area for Realization 10 at the 5.35 m/s PGV Level (Continued)

Impact Location	Time (s)	Speed (m/s)	Angle (degree)	Damaged Area (m^2)	
				80% Yield Strength	90% Yield Strength
C 5	2.200	1.2	4.3	0.0042 NC	0.0023 NC
C 6	0.975	1.0	7.2	0.0013	0.0010
C 11	4.775	2.8	1.8	0.0422X0.5	0.0169X0.5
Total				0.33	0.15

Source: BSC 2004 [DIRS 167083], Table 6.2.2-10.

Table 5.3-34. End-Impact Parameters and Damaged Area for Realization 11 at the 5.35 m/s PGV Level

Impact Location	Time (s)	Speed (m/s)	Angle (degree)	Damaged Area (m^2)	
				80% Yield Strength	90% Yield Strength
F 2	4.950	1.7	1.9	0.0146	0.0075
F 4	2.950	1.7	3.7	0.0108 NC	0.0056 NC
F 4	3.325	1.2	0.8	0.0056 NC	0.0029 NC
F 4	3.875	1.5	3.3	0.0090 NC	0.0046 NC
F 4	5.800	1.6	0.9	0.0131NC	0.0067 NC
F 5	2.375	2.7	2.4	0.0389	0.0171
F 8	2.050	1.4	0.8	0.0087 NC	0.0044 NC
F 8	4.350	3.1	1.0	0.0503	0.0167
F 9	6.200	2.0	0.7	0.0155 NC	0.0078 NC
F 9	6.550	1.4	1.0	0.0108 NC	0.0056 NC
F 10	3.550	3.0	3.3	0.0479X0.5	0.0231X0.5
C 1	3.050	1.9	3.7	0.0133	0.0068
C 1	5.550	1.7	3.9	0.0104 NC	0.0054 NC
C 3	4.225	3.2	2.6	0.0539	0.0234
C 3	6.375	1.7	1.0	0.0165 NC	0.0084 NC
C 4	1.850	2.5	0.2	0.0147 NC	0.0084 NC
C 4	4.650	1.1	2.5	0.0042 NC	0.0023 NC
C 7	3.725	4.6	1.0	0.1013	0.0313
C 8	2.250	2.0	1.2	0.0215 NC	0.0109 NC
C 8	2.275	2.7	1.0	0.0401 NC	0.0147 NC
C 8	3.450	2.5	3.3	0.0318 NC	0.0155 NC
C 8	5.150	2.2	1.7	0.0257 NC	0.0118 NC
Total				0.30	0.11

Source: BSC 2004 [DIRS 167083], Table 6.2.2-11.

Table 5.3-35. End-Impact Parameters and Damaged Area for Realization 12 at the 5.35 m/s PGV Level

Impact Location	Time (s)	Speed (m/s)	Angle (degree)	Damaged Area (m^2)	
				80% Yield Strength	90% Yield Strength
F	0.275	1.8	0	0	0
F 1	5.775	2.1	4.8	0.0151	0.0081
F 1	6.225	1.5	5.9	0.0063 NC	0.0035 NC
F 2	3.750	1.9	4.2	0.0120 NC	0.0062 NC
F 2	5.350	1.4	1.4	0.0103 NC	0.0053 NC
F 2	6.750	1.8	3.4	0.0128X0.5	0.0065X0.5
F 10	1.425	1.2	1.3	0.0068	0.0036
F 12	3.450	2.0	0.6	0.0133X0.5	0.0067X0.5
C 3	3.875	1.6	7.2	0.0072	0.0042
C 5	5.600	1.3	5.4	0.0044 NC	0.0025 NC
C 6	1.150	3.5	0.9	0.0563	0.0187
C 6	3.650	2.2	1.5	0.0261 NC	0.0119 NC
C 7	0.875	2.2	1.5	0.0261 NC	0.0119 NC
C 10	5.125	1.1	2.3	0.0043	0.0024
Total				0.10	0.044

Source: BSC 2004 [DIRS 167083], Table 6.2.2-12.

Table 5.3-36. End-Impact Parameters and Damaged Area for Realization 13 at the 5.35 m/s PGV Level

Impact Location	Time (s)	Speed (m/s)	Angle (degree)	Damaged Area (m^2)	
				80% Yield Strength	90% Yield Strength
F 1	7.125	1.2	5.1	0.0035X0.5	0.0020X0.5
F 3	1.075	1.5	0.5	0.0064 NC	0.0033 NC
F 3	2.275	2.2	3.1	0.0225 NC	0.0111 NC
F 3	4.950	1.1	2.8	0.0040 NC	0.0022 NC
F 4	1.625	2.4	1.4	0.0317	0.0133
F 11	6.350	1.2	0.8	0.0056X0.5	0.0029X0.5
F 12	9.375	1.7	3.8	0.0106	0.0055
C 2	9.175	1.8	0.2	0.0037	0.0019
C 3	1.900	1.5	3.9	0.0081	0.0042
C 6	2.475	2.2	2.2	0.0246	0.0116
C 6	2.550	1.0	2.9	0.0025 NC	0.0015 NC
C 6	3.950	2.0	1.2	0.0215 NC	0.0109 NC
C 7	3.900	1.6	1.3	0.0140 NC	0.0072 NC
C 9	0.750	1.1	0.2	0.0010 NC	0.0005 NC
C 9	1.300	2.2	0.7	0.0198 NC	0.0093 NC
C 9	1.350	1.4	0.6	0.0065 NC	0.0033 NC
C 9	2.975	2.4	0.8	0.0269	0.0115
C 12	10.325	1.4	0.5	0.0054	0.0028
Total				0.12	0.053

Source: BSC 2004 [DIRS 167083], Table 6.2.2-13.

Table 5.3-37. End-Impact Parameters and Damaged Area for Realization 14 at the 5.35 m/s PGV Level

Impact Location	Time (s)	Speed (m/s)	Angle (degree)	Damaged Area (m^2)	
				80% Yield Strength	90% Yield Strength
F 1	7.150	1.3	2.1	0.0077	0.0040
Total				0.0077	0.0040

Source: BSC 2004 [DIRS 167083], Table 6.2.2-14.

Table 5.3-38. End-Impact Parameters and Damaged Area for Realization 15 at the 5.35 m/s PGV Level

Impact Location	Time (s)	Speed (m/s)	Angle (degree)	Damaged Area (m^2)	
				80% Yield Strength	90% Yield Strength
F 4	1.075	4.3	3.3	0.0921	0.0426
F 4	0.850	1.5	0.6	0.0076 NC	0.0039 NC
F 7	0.750	1.5	7.2	0.0062	0.0036
F 7	1.225	1.1	10.0	0.0018 NC	0.0014 NC
F 11	0.025	2.8	0.1	0.0130	0.0103
C 3	0.150	3.5	0.4	0.0352	0.0185
C 4	0.500	2.2	0.6	0.0173 NC	0.0083 NC
C 6*	1.400	8.6	5.2	0.0332	0.0133
C 9	0.925	4.1	2.7	0.0825	0.0353
C 11	0.600	1.6	0.8	0.0117 NC	0.0060 NC
C 11	1.200	2.4	7.8	0.0235X0.5	0.0128X0.5
C 12	0.325	1.6	1.9	0.0129	0.0066
Total				0.29	0.14

Source: BSC 2004 [DIRS 167083], Table 6.2.2-15.

* NOTE: Trunnion collar sleeve impacts the invert not the axial boundary.

Table 5.3-39 presents a summary of Tables 5.3-24 through 5.3-38.

Table 5.3-39. Damaged Area from End Impacts (Waste Package-Waste Package Interaction) at the 5.35 m/s PGV Level

Realization Number	Ground Motion	Damaged Area (m^2; % of total OCB area)	
		80% Yield Strength	90% Yield Strength
1	7	0.16; 0.57%	0.086; 0.30%
2	16	0.048; 0.17%	0.025; 0.089%
3	4	0.42; 1.49%	0.17; 0.60%
4	8	0.11; 0.39%	0.050; 0.18%
5	11	0.18; 0.64%	0.080; 0.28%
6	1	0.42; 1.49%	0.15; 0.53%
7	2	0.32; 1.13%	0.12; 0.43%

Table 5.3-39. Damaged Area from End Impacts (Waste Package-Waste Package Interaction) at the 5.35 m/s PGV Level (Continued)

Realization Number	Ground Motion	Damaged Area (m^2; % of total OCB area)	
		80% Yield Strength	90% Yield Strength
8	13	0.32; 1.13%	0.14; 0.50%
9	10	0.034; 0.12%	0.017; 0.060%
10	9	0.33; 1.17%	0.15; 0.53%
11	5	0.30; 1.06%	0.11; 0.39%
12	6	0.10; 0.35%	0.044; 0.16%
13	12	0.12; 0.43%	0.053; 0.19%
14	14	0.0077; 0.027%	0.0040; 0.014%
15	3	0.29; 1.03%	0.14; 0.50%

Source: BSC 2004 [DIRS 167083], Table 6.2.2-16.

Two important observations can be made by comparing the end-impact results for the 2.44 m/s PGV level (Tables 5.3-2 through 5.3-15) with the results for the 5.35 m/s PGV level (Tables 5.3-24 through 5.3-38). First, the end impacts for the 5.35 m/s PGV level are much more frequent and of higher intensity (as indicated by impact speed). Second, the damaged area that is not taken into account due to the damage overlap (as indicated by the designators x 0.5 and NC; see Section 5.3.1.2) is significantly larger.

5.3.2.3 Interaction Between Waste Package and Drip Shield

The impact velocity between the waste package and the drip shield is presented in this section. Unlike the 2.44 m/s PGV level, interaction between the waste package (i.e., trunnion collar sleeves) and the drip shield occurs in all realizations. It is assumed in this calculation that these lateral impacts do not cause any damage to the waste package (Assumption 3.6). Lateral impact parameters between the waste package and drip shield, in terms of location time, speed, and angles are given for all 15 realizations at 5.35 m/s in Table 5.3-40 through Table 5.3-54.

Table 5.3-40. Lateral-Impact Parameters for Realization 1 at the 5.35 m/s PGV Level

Impact Location	Time (s)	Speed (m/s)	Angle (degree)
F 3	4.050	3.3	6.1
F 9	3.675	3.6	0.2
F 9	4.650	10.0	5.6
C 3	3.625	4.6	2.3
C 4	4.450	2.1	6.1
C 9	3.275	1.6	1.7
C 11	7.375	1.9	0.2
C 12	5.825	1.8	0.2

Source: BSC 2004 [DIRS 167083], Table 6.2.3-1.

Table 5.3-41. Lateral-Impact Parameters for Realization 2 at the 5.35 m/s PGV Level

Impact Location	Time (s)	Speed (m/s)	Angle (degree)
F 1	4.700	3.3	0.1
F 1	5.350	1.9	6.3
F 9	3.800	2.1	0.1
C 1	3.675	2.6	1.3
C 3	4.075	1.2	0.3
C 4	2.900	2.4	1.7
C 5	5.225	4.8	2.5
C 6	5.500	1.9	6.3
C 9	2.150	2.7	0.3
C 10	4.725	2.5	0.6
C 10	4.775	4.7	0.2
C 12	3.550	3.0	1.1

Source: BSC 2004 [DIRS 167083], Table 6.2.3-2.

Table 5.3-42. Lateral-Impact Parameters for Realization 3 at the 5.35 m/s PGV Level

Impact Location	Time (s)	Speed (m/s)	Angle (degree)
F 2	5.550	3.9	1.4
F 2	6.900	8.1	1.8
F 3	0.450	3.4	0.6
F 4	2.125	2.6	0.8
F 4	3.400	2.1	4.6
F 9	2.875	2.5	0.1
F 10	1.100	2.3	0.1
C 1	6.775	1.4	1.0
C 2	1.250	1.7	0.8
C 2	1.450	2.4	1.6
C 3	1.000	3.9	1.0
C 3	2.925	3.5	0.2
C 3	3.050	2.4	0.1
C 3	3.150	2.9	0.9
C 9	5.625	1.6	0.2
C 11	6.950	4.7	0.1

Source: BSC 2004 [DIRS 167083], Table 6.2.3-3.

Table 5.3-43. Lateral-Impact Parameters for Realization 4 at the 5.35 m/s PGV Level

Impact Location	Time (s)	Speed (m/s)	Angle (degree)
F 4	2.500	4.2	0.8
F 9	2.875	2.9	0.6
C 3	2.275	3.8	2.7
C 4	2.925	6.3	0.2
C 8	2.500	4.2	1.5
C 10	3.225	6.1	4.6

Source: BSC 2004 [DIRS 167083], Table 6.2.3-4.

Table 5.3-44. Lateral-Impact Parameters for Realization 5 at the 5.35 m/s PGV Level

Impact Location	Time (s)	Speed (m/s)	Angle (degree)
F 9	0.475	1.0	0.2
C 3	0.425	2.1	1.6
C 10	0.675	1.0	2.7

Source: BSC 2004 [DIRS 167083], Table 6.2.3-5.

Table 5.3-45. Lateral-Impact Parameters for Realization 6 at the 5.35 m/s PGV Level

Impact Location	Time (s)	Speed (m/s)	Angle (degree)
C 2	3.325	1.2	1.2

Source: BSC 2004 [DIRS 167083], Table 6.2.3-6.

Table 5.3-46. Lateral-Impact Parameters for Realization 7 at the 5.35 m/s PGV Level

Impact Location	Time (s)	Speed (m/s)	Angle (degree)
F 2	2.800	7.8	1.0
F 3	3.500	5.2	2.4
F 4	4.275	8.0	1.7
F 9	2.550	6.1	0.1
F 9	4.025	5.9	0.8
F 10	4.95	3.3	0.6
C 1	2.325	4.0	9.2
C 1	2.475	1.5	10.2
C 2	4.550	6.3	4.9
C 3	1.450	1.8	1.5
C 8	4.250	7.1	1.5
C 8	4.300	1.7	0.6
C 9	1.900	3.0	1.2
C 10	2.875	1.8	2.5
C 10	3.600	1.8	2.5

Source: BSC 2004 [DIRS 167083], Table 6.2.3-7.

Table 5.3-47. Lateral-Impact Parameters for Realization 8 at the 5.35 m/s PGV Level

Impact Location	Time (s)	Speed (m/s)	Angle (degree)
F 1	4.700	1.1	0.4
F 2	3.575	3.4	0.4
F 7	5.100	1.8	2.8
F 8	4.075	2.7	0.3
F 9	9.575	2.8	0.1
F 9	9.675	1.2	0.3
F 9	10.050	1.0	0.3
F 10	2.000	2.0	2.2
C 1	2.075	3.1	0.4
C 2	0.925	1.3	0.1
C 3	9.550	1.1	0.1
C 4	3.950	2.9	2.0
C 4	4.050	2.5	0.2
C 4	5.225	4.5	0.9
C 8	1.450	1.2	4.0
C 9	2.850	1.8	4.1
C 9	3.075	1.6	1.8
C 10	3.525	4.8	0.2
C 11	4.650	2.2	0.5
C 11	4.725	4.1	0.5

Source: BSC 2004 [DIRS 167083], Table 6.2.3-8.

Table 5.3-48. Lateral-Impact Parameters for Realization 9 at the 5.35 m/s PGV Level

Impact Location	Time (s)	Speed (m/s)	Angle (degree)
F 1	2.150	2.4	2.8
F 2	1.550	4.0	0.9
F 8	2.550	3.9	0.3
C 3	1.125	2.4	1.8
C 4	2.475	3.9	1.3
C 11	2.225	5.5	1.0

Source: BSC 2004 [DIRS 167083], Table 6.2.3-9.

Table 5.3-49. Lateral-Impact Parameters for Realization 10 at the 5.35 m/s PGV Level

Impact Location	Time (s)	Speed (m/s)	Angle (degree)
F 5	1.025	3.8	6.3
F 9	3.425	3.3	3.4
F 9	4.250	1.5	5.3
F 9	4.875	9.0	2.4
F 10	0.525	3.0	0.5

Table 5.3-49. Lateral-Impact Parameters for Realization 10 at the 5.35 m/s PGV Level (Continued)

Impact Location	Time (s)	Speed (m/s)	Angle (degree)
F 10	4.950	7.2	10.5
F 11	3.550	5.7	6.1
F 12	0.575	5.4	3.9
C 9	3.725	1.5	4.9
C 10	5.175	1.3	2.6
C 10	5.575	2.9	3.7
C 12	0.900	2.6	6.0
C 12	1.200	4.9	7.3

Source: BSC 2004 [DIRS 167083], Table 6.2.3-10.

Table 5.3-50. Lateral-Impact Parameters for Realization 11 at the 5.35 m/s PGV Level

Impact Location	Time (s)	Speed (m/s)	Angle (degree)
F 2	3.075	1.8	0.2
F 2	3.100	1.1	0.6
F 9	3.825	4.5	2.0
F 9	5.325	3.4	2.1
F 9	5.400	1.8	3.3
C 4	2.550	5.2	2.4
C 10	2.750	5.9	3.5

Source: BSC 2004 [DIRS 167083], Table 6.2.3-11.

Table 5.3-51. Lateral-Impact Parameters for Realization 12 at the 5.35 m/s PGV Level

Impact Location	Time (s)	Speed (m/s)	Angle (degree)
F 3	0.550	1.2	0
F 6	6.175	3.6	4.1
F 7	1.100	1.8	1.8
F 7	5.350	2.6	0.9
F 12	3.475	7.0	0.2
C 2	0.875	2.8	1.5
C 2	0.925	1.5	1.8
C 9	0.475	2.7	1.1
C 12	0.775	2.1	2.6
C 12	1.750	1.5	1.5
C 12	3.450	1.7	0.5

Source: BSC 2004 [DIRS 167083], Table 6.2.3-12.

Table 5.3-52. Lateral-Impact Parameters for Realization 13 at the 5.35 m/s PGV Level

Impact Location	Time (s)	Speed (m/s)	Angle (degree)
F 1	6.675	2.8	2.3
F 2	9.150	2.4	0.6
F 7	8.775	1.1	0.1
F 8	5.025	1.8	1.8
F 9	1.475	2.3	1.8
F 9	3.125	2.0	4.6
C 10	2.750	1.6	1.1
C 10	3.700	2.0	2.3
C 10	10.625	1.3	0.2
C 11	6.800	2.2	1.9
C 11	10.000	3.1	0.2

Source: BSC 2004 [DIRS 167083], Table 6.2.3-13.

Table 5.3-53. Lateral-Impact Parameters for Realization 14 at the 5.35 m/s PGV Level

Impact Location	Time (s)	Speed (m/s)	Angle (degree)
C 9 & F 3	6.150	5.9	0
F 2	5.975	1.8	0.1
F 2	6.425	1.5	0.5
F 3	6.050	5.0	0.2
C 3	7.425	1.2	0.5
C 9	6.000	2.3	0.2
C 10	6.350	2.0	0.3

Source: BSC 2004 [DIRS 167083], Table 6.2.3-14.

Table 5.3-54. Lateral-Impact Parameters for Realization 15 at the 5.35 m/s PGV Level

Impact Location	Time (s)	Speed (m/s)	Angle (degree)
F 2	0.400	14.3	4.6
F 2	0.650	4.5	3.0
C 8	0.450	3.2	0.3
C 10	0.800	11.4	2.3

Source: BSC 2004 [DIRS 167083], Table 6.2.3-15.

While impacts between the waste package and drip shield are infrequent, low intensity events at the 2.44 m/s PGV level, these impacts are significantly more frequent and more intense at the 5.35 m/s PGV level. Not only is there no realization at 5.35 m/s PGV level for which a waste package-DS interaction does not occur, but also the impact speed is also significantly larger. Second, the waste package-DS interaction at the 2.44 m/s PGV level takes place exclusively between the trunnion collar sleeves and the side (vertical) plates of the drip shield. At the 5.35 m/s PGV level, the waste package can impact any part of the drip shield. Note that an

impact between the waste package and invert takes place only once – in realization 15 this waste package-invert impact is, for convenience, included among the end-impacts in Table 5.3-39.

5.3.2.4 Summary of Results at the 5.35 m/s PGV Level

The damaged areas characterizing 14 different realizations for the ground motions at the 5.35 m/s PGV level are summarized in Table 5.3-55. The results in Table 5.3-55 show that the cumulative damage area is dominated by the end-impact contribution. In most realizations the damaged area due to waste package-pallet interaction is much smaller than that due to waste package- waste package interaction. It should be kept in mind that the damaged areas due to waste package-waste package interactions are conservatively estimated (see discussion in Section 5.3.1.2). It is also noteworthy that the only two realizations conspicuous by the absence of the nonphysical damaged area at the boundary of the finely-meshed OCB region – realization 11 (BSC 2004 [DIRS 167083], Figure IV-46) and realization 15 (BSC 2004 [DIRS 167083], Figure IV-51) are characterized by an extremely small contribution from waste package to pallet impacts to the cumulative damaged area.

The information in Table 5.3-55 is used directly in the development of the waste package damage abstraction for the seismic scenario class. These data are available through *D&E / PA/C IED Typical Waste Package Components Assembly* (BSC 2004 [DIRS 169990], Table 17).

Table 5.3-55. Damaged Area from Vibratory Ground Motion at the 5.35 m/s PGV Level

Realization Number [a]	Ground Motion Number	Damaged Area on the Waste Package					
		WP to Pallet Interaction (m^2; % of total OS[c] area)		WP to WP Interaction (m^2; % of total OS[c] area)		Cumulative Damage (m^2; % of total OS[c] area)	
		80% Yield Strength	90% Yield Strength	80% Yield Strength	90% Yield Strength	80% Yield Strength	90% Yield Strength
1	7	0.20; 0.71%	0.17; 0.60%	0.16; 0.57%	0.086; 0.30%	0.36; 1.28%	0.26; 0.92%
3	4	0.096; 0.34%	0.083; 0.29%	0.42; 1.49%	0.17; 0.60%	0.52; 1.84%	0.25; 0.89%
4	8	0.12; 0.43%	0.096; 0.34%	0.11; 0.39%	0.050; 0.18%	0.23; 0.82%	0.15; 0.53%
5	11	0.093; 0.33%	0.071; 0.25%	0.18; 0.64%	0.080; 0.28%	0.27; 0.96%	0.15; 0.53%
6	1	0.046; 0.16%	0.024; 0.085%	0.42; 1.49%	0.15; 0.53%	0.47; 1.67%	0.17; 0.60%
7	2	0.038; 0.13%	0.028; 0.099%	0.32; 1.13%	0.12; 0.43%	0.36; 1.28%	0.15; 0.53%
8	13	0.095; 0.34%	0.068; 0.24%	0.32; 1.13%	0.14; 0.50%	0.42; 1.49%	0.21; 0.74%
9	10	0.0052; 0.018%	0.0035; 0.012%	0.034; 0.12%	0.017; 0.060%	0.039; 0.14%	0.021; 0.074%
10	9	0.16; 0.57%	0.14; 0.50%	0.33; 1.17%	0.15; 0.53%	0.49; 1.74%	0.29; 1.03%
11	5	0.032; 0.11%	0.0070; 0.025%	0.17; 0.59%	0.072; 0.26%	0.20; 0.70%	0.079; 0.28%

Table 5.3-55. Damaged Area from Vibratory Ground Motion at the 5.35 m/s PGV Level (Continued)

Realization Number [a]	Ground Motion Number	Damaged Area on the Waste Package					
		WP to Pallet Interaction (m^2; % of total OS[c] area)		WP to WP Interaction (m^2; % of total OS[c] area)		Cumulative Damage (m^2; % of total OS[c] area)	
		80% Yield Strength	90% Yield Strength	80% Yield Strength	90% Yield Strength	80% Yield Strength	90% Yield Strength
12	6	0.062; 0.22%	0.041; 0.15%	0.10; 0.35%	0.044; 0.16%	0.16; 0.57%	0.085; 0.30%
13	12	0.027; 0.096%	0.018; 0.064%	0.12; 0.43%	0.053; 0.19%	0.15; 0.53%	0.071; 0.25%
14	14	0.020; 0.071%	0.016; 0.057%	0.0077; 0.027%	0.0040; 0.014%	0.028; 0.099%	0.020; 0.071%
15	3	0.0045; 0.016%	0; 0%	0.29; 1.03%	0.14; 0.50%	0.29; 1.03%	0.14; 0.50%
				Mean Value[b, d]		1.011%	0.518%
				Standard Deviation[b]		0.567%	0.303%
				Minimum Value[b]		0.099%	0.071%
				Maximum Value[b]		1.84%	1.03%

Sources: BSC 2004 [DIRS 169990], Table 17; and BSC 2004 [DIRS 171717] for Realization 11.

[a] Only 14 realizations are presented in this table. Results for realization 2 are not presented because the kinematics of the waste package are such that the impacts between package and pallet occur outside the finely meshed region of the OCB.

[b] Mean, standard deviation, minimum and maximum damage calculated in Appendix B.

[c] = outer surface of waste package.

[d] The mean value of % damaged area for end-to-end impacts is 0.788 percent and 0.333 percent at stress thresholds of 80 percent and 90 percent of yield strength, respectively. These values represent 76.0 percent and 63.5 percent, of the total mean cumulative mean damage for the two residual stress thresholds.

WP = waste package

5.3.3 Ground Motions at the 0.384 m/s PGV Level

Two calculations have been performed to evaluate the damaged areas for single ground motions at the 0.19 m/s PGV level and at the 0.384 m/s PGV level. Both calculations demonstrate that there is no damage to the waste package from either waste package-pallet interactions or from waste package-to-waste package interactions. In fact, the static load from the weight on the waste package on the pallet generates the observed stresses in the waste package and pallet. Given this similarity, the results for the calculation at the 0.384 m/s PGV level are described here because they are most relevant to damage abstractions for the seismic scenario class (the largest amplitude ground motion that does not damage the waste package or its internals is most relevant to the damage abstractions). The results for the calculation at the 0.19 m/s PGV level are available in the original calculation report (BSC 2004 [DIRS 167083], Section 6.3).

5.3.3.1 Results for the 0.384 m/s PGV Level

The single calculation with the 0.384 m/s PGV level ground motion is based on the FE representation previously used for most of the ground motions at the 2.44 m/s PGV level. The single simulation is performed with material properties based on a temperature of 150°C. The simulation started at 9.7 *s* of the ground motion time history (corresponding to the 5 percent

energy point of the ground motion), and the ending time was 34.9 *s* (corresponding to 65 percent of the energy of the ground motion) (BSC 2004 [DIRS 167083], Section 6.4). This duration covered the most intense period of this ground motion time history. Further extension of the simulation is considered unnecessary based on the results presented in this section (see, as an example, Figures 5.3-4 and 5.3-5).

The ground motion for 0.384 m/s PGV level is much less intense than for the 2.44 m/s PGV level. Consequently, the resulting rigid-body motion is very small. Specifically, the relative motion of the waste package with respect to the pallet in longitudinal (Y) and vertical (Z) direction is practically nonexistent. Figure 5.3-3 indicates that once the initial gap between waste package and pallet is closed (Section 5.3.3.2) the relative displacement of two typical waste package and pallet nodes (the locations of nodes number 20 and 18007 are depicted in *Structural Calculations of Waste Package Exposed to Vibratory Ground Motion* (BSC 2004 [DIRS 167083], Figure 17) is less than ±0.07 mm even for the unfiltered data. The filtered plot is more meaningful since the high-frequency noise - very pronounced due to the high-frequency excitation and the absence of damping is eliminated. A low pass filter with cutoff frequency of 1000 *Hz* is used for that purpose throughout this section.

The relative displacement in vertical (Z) direction of the waste package with respect to the pallet is also small, as indicated in Figure 5.3-4. Most of the time, it varies within the range from 0 mm to 0.03 mm (Note the spikes in Figures 5.3-3 and 5.3-4 at the onset of simulations, which are discussed in Section 5.3.3.2.).

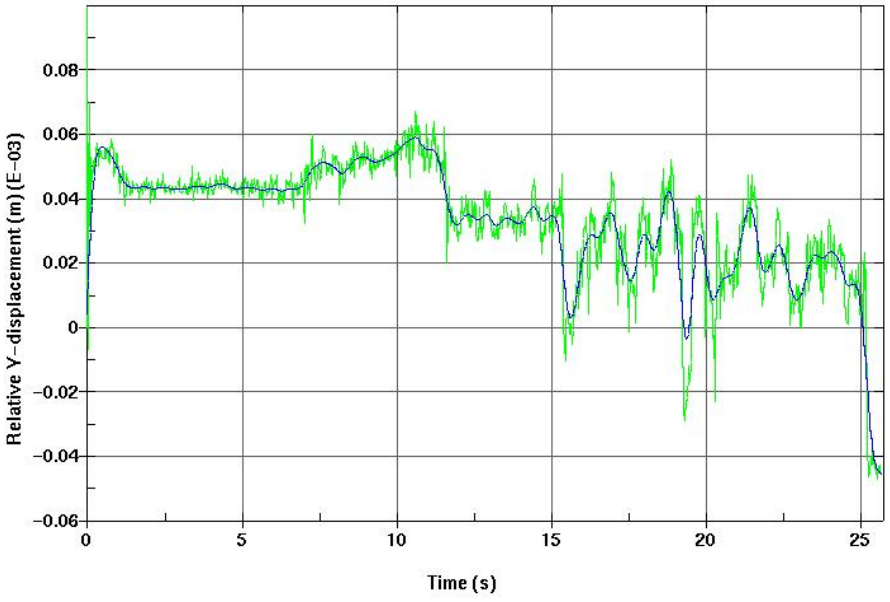

Source: BSC 2004 [DIRS 167083], Figure 20.

Figure 5.3-3. Relative Longitudinal (Y) Displacement (Raw and Filtered) of Waste Package With Respect to the Pallet for the 0.384 m/s PGV Level

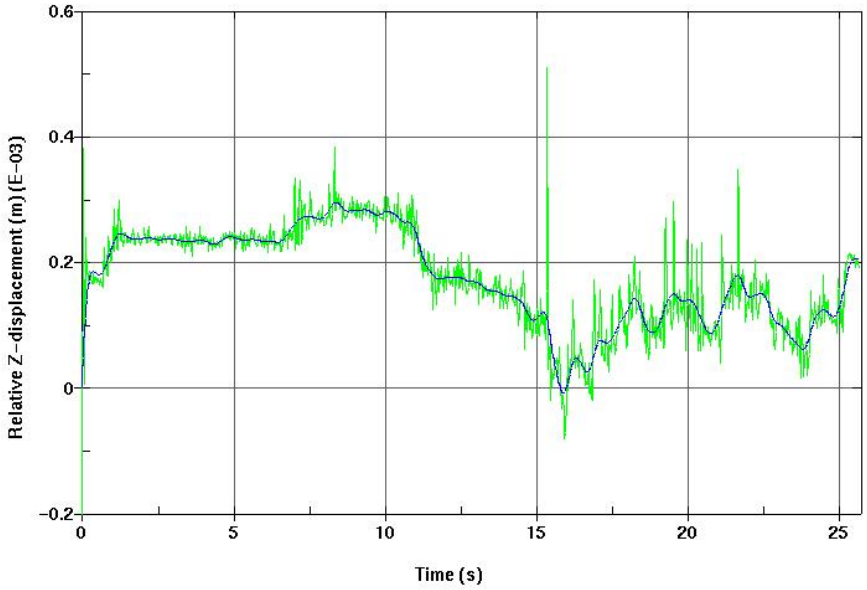

Source: BSC 2004 [DIRS 167083], Figure 21.

Figure 5.3-4. Relative Vertical (Z) Displacement (Raw and Filtered) of Waste Package with Respect to the Pallet for the 0.384 m/s PGV Level

As a consequence of the limited rigid-body motion, there is no contact between the waste package and the longitudinal boundary or between the waste package and the drip shield during the simulation for the 0.384 m/s PGV level. The only remaining interaction that is relevant for this analysis is that between the waste package and the pallet.

The waste package-pallet interactions for this simulation are characterized by extremely small impact velocities due to the limited rigid-body motion in the vertical direction. As shown in Figure 5.3-5, the impact velocity between the waste package and the pallet rarely exceeds 0.005 m/s (for the filtered data; see blue curve in Figure 5.3-5) and the maximum impact velocity for the filtered data is less than 0.006 m/s. It seems appropriate to emphasize that the vibratory part of the simulation is performed without system damping or contact damping (Section 5.2.1.4). The statement that the rigid-body motion is negligible for this simulation is well supported by the results presented in Figures 5.3-3 through 5.3-5.

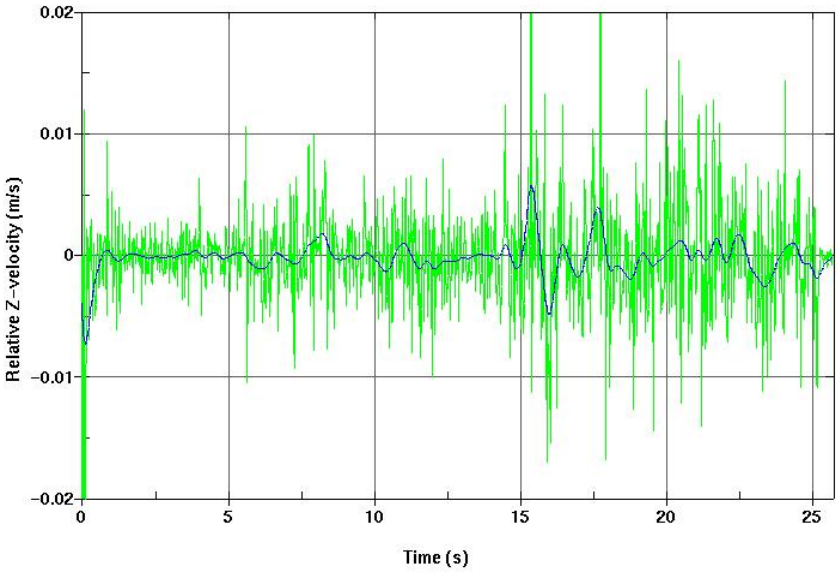

Source: BSC 2004 [DIRS 167083], Figure 22.

Figure 5.3-5. Relative Vertical (Z) Velocity (Raw and Filtered) of Waste Package with Respect to the Pallet for the 0.384 m/s PGV Level

Figure 5.3-6 presents the residual first principal stress intensity plot for the vibratory part of the simulation. The maximum residual first principal stress (87 *MPa*) is below the stress limit (80 percent to 90 percent of yield strength) by a large margin. Note that the stress unit in Figure 5.3-6 is Pascals. The maximum residual stress is not caused by the dynamic response to the ground motion. The deformation of the waste package OCB is elastic during the transient, so the residual stress is zero from the ground motion. Rather, this residual stress results from the static load of the waste package on the emplacement pallet.

In summary, it can be concluded that the waste package OCB remains undamaged throughout the dynamic response to the 0.384 m/s PGV level ground motion; that is, the OCB area exceeding the residual stress thresholds is zero.

5.3.3.2 Initial Settling of the Waste Package on the Pallet

As observed in Figures 5.3-3 through 5.3-5, an indication that an initial spike in the waste package response during the first 0.1 seconds of the transient simulation was seen. A detailed analysis (BSC 2004 [DIRS 167083], Section 6.3.1) demonstrates that the behavior at the onset of the simulation is a numerical artifact from small gaps in the FE representation, and is unrelated to the physics of vibratory ground motion. The results from this analysis are briefly summarized here.

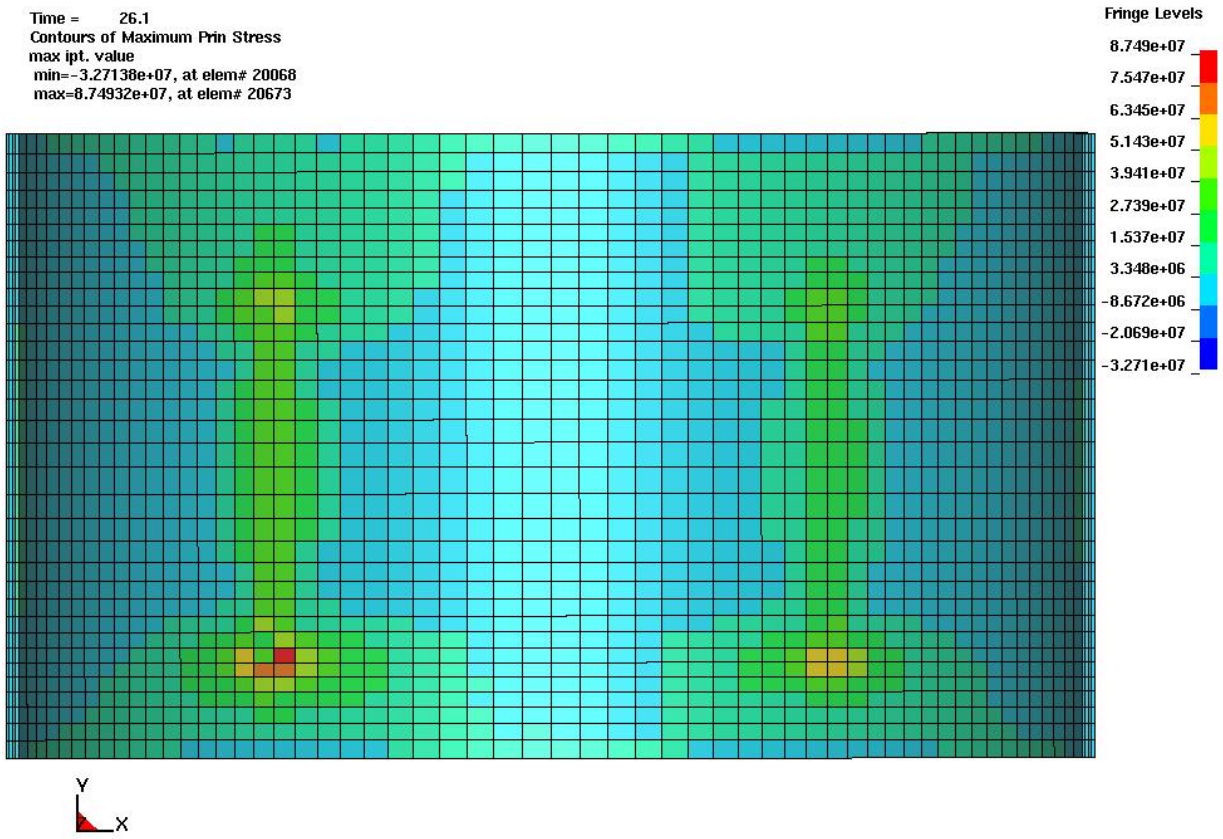

Source: BSC 2004 [DIRS 167083], Figure 23.

NOTE: Units in Pascals.

Figure 5.3-6. Residual First Principal Stress Plot in OCB (Top View) for the 0.384 m/s PGV Level

The cause of the singular behavior at the onset of the simulation is the existence of an initial gap between the waste package OCB and the pallet. This gap is introduced to avoid accidental merging of nodes for the components, and is a consequence of the FE mesh. The actual gap is quite small, on the order of 0.3 mm. The contact gaps could be minimized, or even eliminated, but this was considered unnecessary. These gaps are completely irrelevant for the dynamic calculations with ground motions at the 2.44 m/s or 5.35 m/s PGV levels. For low intensity events, such as the 0.384 m/s PGV level, the initial gap results in a small initial impact velocity that – in the absence of damping – is sufficient to cause the stress intensity and effective stress to exceed the yield strength (BSC 2004 [DIRS 167083], Figures 13 and 18), resulting in a small plastic deformation.

It has been verified (BSC 2004 [DIRS 167083], Section 6.3.1) that once the initial gap is closed and the waste package is settled on the pallet:

- Relative (rigid-body) motion of waste package with respect to pallet becomes negligible (Figures 5.3-3 and 5.3-4 in this report)
- Waste package-pallet impact velocity becomes extremely small (Figure 5.3-5 in this report)
- Stress intensity and effective (von Mises) stress (BSC 2004 [DIRS 167083], Figures 13 and 18, respectively) are significantly below the yield strength
- Effective plastic strain remains constant (BSC 2004 [DIRS 167083], Figure 19), implying the deformation is elastic.

In summary, the behavior at the onset of the simulation is due a numerical effect caused by small gaps closing in the initial FE mesh as the waste package settles down on the pallet. It follows that the results at the onset of this simulation (roughly the first 0.1 seconds) are not representative of the deformation from transient ground motion effects and have been disregarded in developing damage abstractions for the seismic scenario.

5.3.4 Damaged Areas for Side and End Impacts

Based on the results documented in *21-PWR Waste Package Side and End Impacts* (BSC 2003 [DIRS 162293]), Tables 5.3-56 through 5.3-60 list the damaged area and the angle defining its circumferential extension for the side and end impacts at 150°C and 200°C for residual stress thresholds of 80 percent, 90 percent, and 100 percent of the yield strength.

Table 5.3-56. Damaged Area (m^2) and Associated Angle (degrees) at 150°C, Stress Limit = 80 Percent of Yield Strength

		End Impacts: Angle between the axis of the WP and the Vertical (degree)				Side Impacts: Angle between the axis of the WP and the Horizontal (degree)		
		0	1	5	8	0	1	8
Initial Velocity (m/s)	1	0	0.0033 ±17	0.0017 ±10	0.0011 ±8	0	0	0
	2	0	0.0221 ±41	0.0109 ±25	0.0113 ±23	0.0013 ±5	0.0020 ±5	0
	4	0.0244 ±180	0.0734 ±75	0.0850 ±42	0.0716 ±37	0.0156 ±15	0.0063 ±13	0.0068 ±15
	6	0.0276 ±180	0.1665 ±108	0.1556 ±53	0.1082 ±46	0.0379 ±20	0.0204 ±17	0.0153 ±22
	10	0.0254 ±180	0.0834 ±171	0.1280 ±75	0.1061 ±61	0.0715 ±32	0.0283 ±24	0.0508 ±26
	20	0.0542 ±180	0.0698 ±180	0.1916 ±62	0.2332 ±72	0.6232 ±90	0.1560 ±37	0.2193 ±90

Source: BSC 2003 [DIRS 162293], Table 4.

Table 5.3-57. Damaged Area (m^2) and Associated Angle (*degree*) at 150°C, Stress Limit = 90 Percent of Yield Strength

		End Impacts: Angle between the axis of the WP and the Vertical (degree)				Side Impacts: Angle between the axis of the WP and the Horizontal (degree)		
		0	**1**	**5**	**8**	**0**	**1**	**8**
Initial Velocity (m/s)	**1**	0	0.0018 ±13	0.0011 ±8	0.0009 ±6	0	0	0
	2	0	0.0112 ±39	0.0056 ±25	0.0066 ±23	0.0004 ±3	0.0011 ±5	0
	4	0.0244 ±180	0.0212 ±75	0.0508 ±42	0.0367 ±37	0.0046 ±13	0.0015 ±11	0.0006 ±13
	6	0.0244 ±180	0.0549 ±103	0.0767 ±53	0.0501 ±44	0.0176 ±20	0.0092 ±17	0.0081 ±21
	10	0.0254 ±180	0.0264 ±164	0.0610 ±75	0.0379 ±61	0.0257 ±30	0.0157 ±22	0.0160 ±24
	20	0.0278 ±180	0.0403 ±180	0.1008 ±64	0.1279 ±68	0.3103 ±64	0.0404 ±30	0.1040 ±67

Source: BSC 2003 [DIRS 162293], Table 5. WP = waste package

Table 5.3-58. Damaged Area (m^2) and Associated Angle (degree) at 150°C, Stress Limit = 100 Percent of Yield Strength

		End Impacts: Angle between the axis of the WP and the Vertical (degree)			
		0	**1**	**5**	**8**
Initial Velocity (m/s)	**1**	0	0.0016 ±11	0.0009 ±6	0.0006 ±5
	2	0	0.0051 ±37	0.0037 ±23	0.0044 ±21
	4	0	0.0103 ±72	0.0217 ±39	0.0143 ±35
	6	0.0244 ±180	0.0185 ±101	0.0302 ±51	0.0273 ±44
	10	0.0254 ±180	0.0211 ±149	0.0227 ±73	0.0150 ±59
	20	0	0.0120 ±74	0.0444 ±55	0.0734 ±61

Source: BSC 2003 [DIRS 162293], Table 6. WP = waste package

Table 5.3-59. Damaged Area (m^2) and Associated Angle (degree) at 200°C, Stress Limit = 80 Percent of Yield Strength

		End Impacts: Angle between the axis of the WP and the Vertical (degree)				Side Impacts: Angle between the axis of the WP and the Horizontal (degree)		
		0	**1**	**5**	**8**	**0**	**1**	**8**
Initial Velocity (m/s)	**1**	0	0.0038 ±17	0.0022 ±11	0.0017 ±10	0.0002 ±2	0	0
	2	0	0.0221 ±41	0.0123 ±26	0.0116 ±23	0.0034 ±5	0.0023 ±5	0
	4	0.0244 ±180	0.0885 ±78	0.0968 ±42	0.0714 ±37	0.0187 ±15	0.0072 ±13	0.0092 ±25
	6	0.0244 ±180	0.1822 ±108	0.1489 ±54	0.1038 ±46	0.0430 ±26	0.0238 ±17	0.0153 ±22
	10	0.0476 ±180	0.0846 ±180	0.1287 ±75	0.1163 ±64	0.0910 ±35	0.0409 ±30	0.0585 ±46
	20	0.0595 ±180	0.1219 ±180	0.2668 ±66	0.2525 ±72	0.7443 ±67	0.2351 ±54	0.2451 ±90

Source: BSC 2003 [DIRS 162293], Table 7. WP = waste package

Table 5.3-60. Damaged Area (m^2) and Associated Angle (degree) at 200°C, Stress Limit = 90 Percent of Yield Strength

		End Impacts: Angle between the axis of the WP and the Vertical (degree)				Side Impacts: Angle between the axis of the WP and the Horizontal (degree)		
		0	**1**	**5**	**8**	**0**	**1**	**8**
Initial Velocity (m/s)	**1**	0	0.0021 ±15	0.0013 ±10	0.0011 ±8	0	0	0
	2	0	0.0138 ±42	0.0064 ±25	0.0057 ±23	0.0004 ±3	0.0010 ±5	0
	4	0.0244 ±180	0.0242 ±75	0.0571 ±42	0.0416 ±37	0.0051 ±25	0.0025 ±13	0.0006 ±24
	6	0.0244 ±180	0.0602 ±106	0.0815 ±54	0.0517 ±46	0.0205 ±21	0.0128 ±17	0.0089 ±20
	10	0.0254 ±180	0.0257 ±171	0.0594 ±75	0.0518 ±62	0.0373 ±30	0.0210 ±28	0.0202 ±39
	20	0.0262 ±180	0.0536 ±180	0.1707 ±90	0.1403 ±68	0.4153 ±64	0.0904 ±49	0.1283 ±50

Source: BSC 2003 [DIRS 162293], Table 8. WP = waste package

The damaged area distribution on the OCB surface is illustrated in Figure 5.3-7(a) and 5.3-7(b), based on end impact calculations with a finely zoned FE grid (BSC 2004 [DIRS 170844], Attachment I, Figures I-3 and I-4). Figure 5.3-7 presents plots of the first principal stress with the number of stress fringe levels reduced to three and adjusted to emphasize the amount and distribution of the damaged area; the stress unit in Figure 5.3-7 is Pascal [Pa = N/m^2]. The stress thresholds of 248 MPa and 279 MPa correspond, respectively, to the residual stress thresholds for 80 percent and 90 percent of yield strength of Alloy 22 at 150 ºC. All elements with residual first principal stress below 248 MPa are blue. All elements with residual first principal stress from 248 MPa to 279 MPa are green. Finally, all elements with residual first principal stress exceeding 279 MPa are red. All other colors, if present, outline the waste package parts other than the OCB (most importantly, the trunnion collar sleeve is brown) to improve the clarity of the figure.

Figure 5.3-7 illustrates two important points regarding the damage from end impacts. First, the majority of the damaged area is covered by the trunnion sleeve. In this situation, the sleeve helps to prevent radionuclide transport out of the waste package, although the damage abstraction for TSPA does not take credit for this effect. Second, residual stress in the OCB is transferred from the trunnion sleeve via the trunnion sleeve welds during the impact process. In effect, the trunnion sleeve acts to spread the deformation over a much larger area than would occur with a point impact on the OCB. Stress fields in the OCB are also presented in *21-PWR Waste Package Side and End Impacts* (BSC 2003 [DIRS 162293], Attachment VI) for some of these cases. These stress fields illustrate the extent of damage in the axial direction, and present the first principal stress in the OCB – bottom lid junction.

Tables 5.3-61 through 5.3-63 list the damaged area and the angle defining its circumferential extension for end impacts at 100°C for residual stress thresholds of 80 percent, 90 percent, and 100 percent of the yield strength.

Finally, Table 5.3-64 shows the damaged area for the OCB at 150°C, obtained by comparing the residual stress intensity to the damage threshold (= 80 percent of Yield Strength in this case). The drop results for 100°C and 200°C indicate that, in general, an increase in temperature results in an increase in the damaged area, which can be explained by increased ductility of Alloy 22 on elevated temperature. The stress intensity is defined in Section 5.3.

This table is added for information only. Its purpose is to illustrate the difference in damage induced by two different residual stress measures, the first principal stress versus the stress intensity. The difference in results for Table 5.3-56 versus Table 5.3-64 illustrates the influence of the third principal stress.

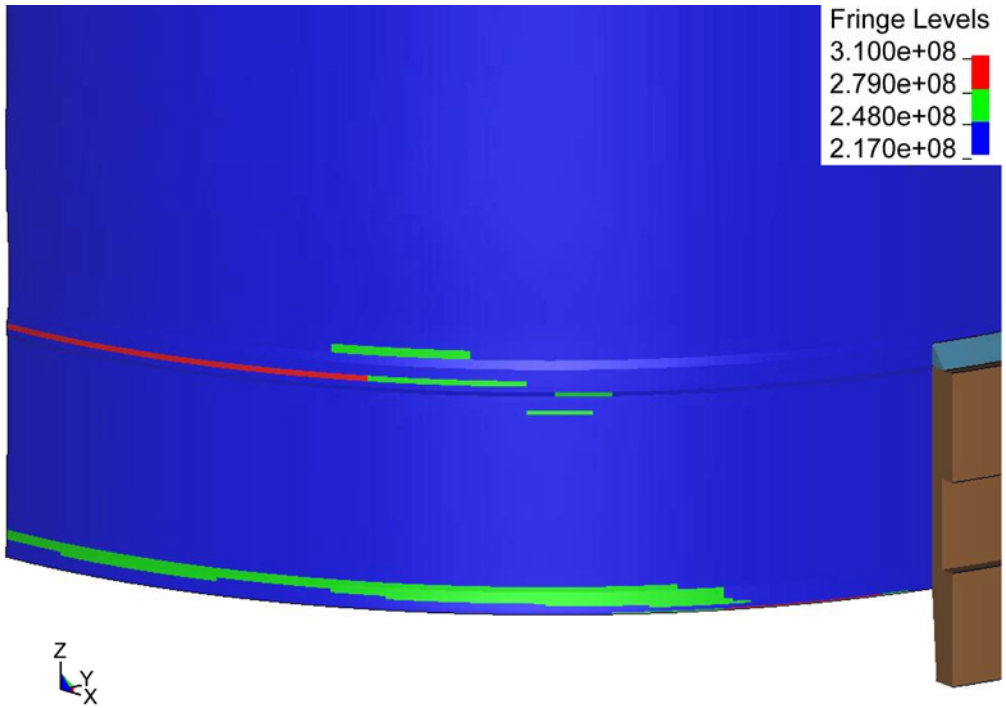

(a) Residual First Principal Stress Plot (in Pa) for 1-degree 4-m/s End Impact

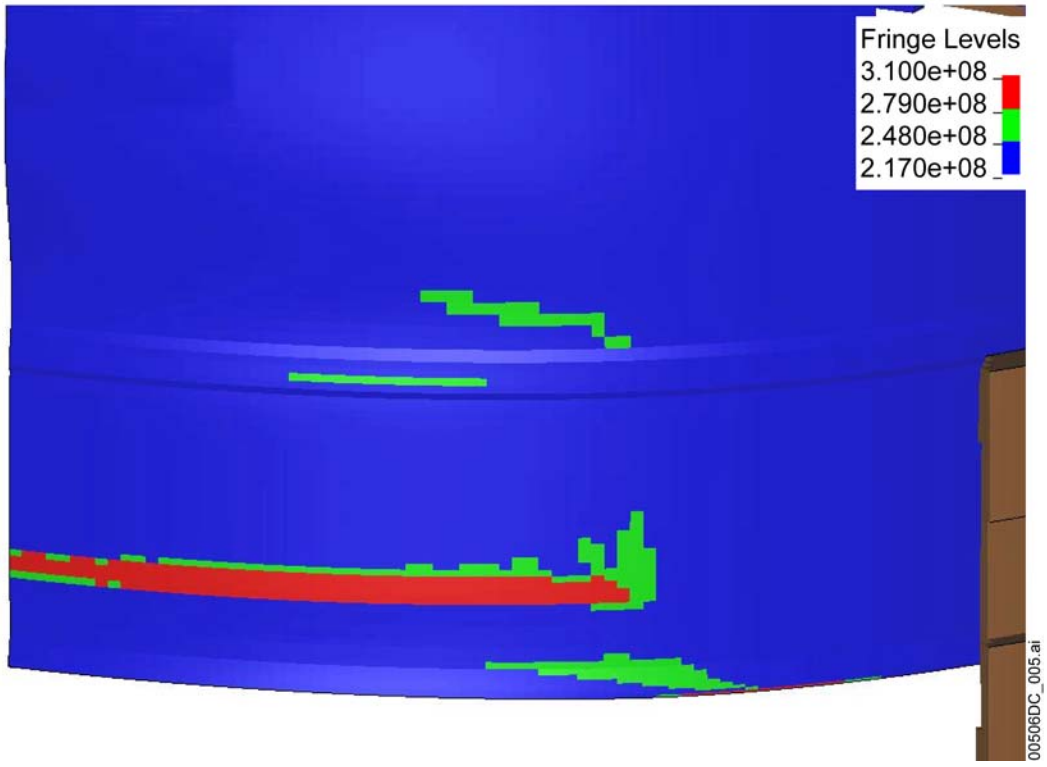

(b) Residual First Principal Stress Plot (in Pa) for 8-degree 6-m/s End Impact

Source: BSC 2004 [DIRS 170844], Attachment I, Figures I-3 and I-4.

Figure 5.3-7. Spatial Distribution of Residual First Principal Stress

Table 5.3-61. Damaged Area (m^2) and Associated Angle (degree) at 100°C, Stress Limit = 80 Percent of Yield Strength

		End Impacts: Angle between the axis of the WP and the Vertical (degree)			
		0	**1**	**5**	**8**
Initial Velocity (m/s)	**1**	0	0.0027 ±15	0.0011 ±8	0.0009 ±6
	2	0	0.0203 ±39	0.0113 ±25	0.0102 ±21
	4	0.0300 ±180	0.0576 ±66	0.0770 ±42	0.0676 ±37
	6	0.0266 ±180	0.1466 ±99	0.1474 ±53	0.1021 ±46
	10	0.0251 ±180	0.0969 ±162	0.1262 ±72	0.0807 ±61

Source: BSC 2003 [DIRS 162293], Table 9. WP = waste package

Table 5.3-62. Damaged Area (m^2) and Associated Angle (degree) at 100°C, Stress Limit = 90 Percent of Yield Strength

		End Impacts: Angle between the axis of the WP and the Vertical (degree)			
		0	**1**	**5**	**8**
Initial Velocity (m/s)	**1**	0	0.0016 ±11	0.0009 ±6	0.0006 ±5
	2	0	0.0071 ±37	0.0069 ±23	0.0065 ±21
	4	0.0193 ±143	0.0173 ±72	0.0424 ±39	0.0349 ±35
	6	0.0244 ±180	0.0566 ±101	0.0737 ±51	0.0510 ±44
	10	0.0254 ±180	0.0254 ±158	0.0628 ±72	0.0413 ±59

Source: BSC 2003 [DIRS 162293], Table 10. WP = waste package

Table 5.3-63. Damaged Area (m^2) and Associated Angle (degree) at 100°C, Stress Limit = 100 Percent of Yield Strength

		End Impacts: Angle between the axis of the WP and the Vertical (degree)			
		0	**1**	**5**	**8**
Initial Velocity (m/s)	**1**	0	0.0011 ±8	0.0006 ±5	0.0004 ±3
	2	0	0.0051 ±37	0.0031 ±23	0.0037 ±19
	4	0	0.0112 ±69	0.0170 ±39	0.0171 ±35
	6	0.0244 ±180	0.0173 ±99	0.0346 ±51	0.0258 ±44
	10	0.0251 ±180	0.0220 ±151	0.0183 ±74	0.0180 ±59

Source: BSC 2003 [DIRS 162293], Table 11. WP = waste package

Table 5.3-64. Damaged Area (m^2) and Associated Angle (degree) at 150°C, Stress Limit = 80 Percent of Yield Strength, for Residual Stress Intensity

		End Impacts: Angle between the axis of the WP and the Vertical (degree)			
		0	**1**	**5**	**8**
Initial Velocity (m/s)	**1**	0	0.0044 ±21	0.0026 ±13	0.0022 ±11
	2	0.0075 ±180	0.0240 ±44	0.0155 ±26	0.0160 ±25
	4	0.0502 ±180	0.1238 ±78	0.1419 ±44	0.1089 ±39
	6	0.0445 ±180	0.2572 ±112	0.2763 ±59	0.2229 ±48
	10	0.0926 ±180	0.1944 ±180	0.6018 ±90	0.6126 ±72
	20	0.5711 ±180	0.8137 ±180	1.747 ±90	1.675 ±106

Source: BSC 2003 [DIRS 162293], Table 12. WP = waste package

NOTE: Damaged area based on the residual stress intensity, rather than residual stress.

The information in these tables is not used directly in abstractions for the seismic scenario class. Rather, the information in Tables 5.3-56 and 5.3-57 is used to estimate the damaged areas from multiple waste package-to-waste package impacts. These damaged areas are then incorporated into Table 5.3-22 and Table 5.3-55 that become the direct input to the waste package damage abstractions for the seismic scenario.

5.3.5 Maximum Accelerations of Fuel Rod Assemblies

As seen in Table 5.3-65, it presents the maximum peak acceleration (in the axial direction of the fuel assemblies) experienced by any of the fuel assemblies for material properties evaluated at 150°C. Table 5.3-66 presents the average peak acceleration for each impact. The average peak acceleration is obtained by averaging the peak values of acceleration time histories of all fuel assemblies. Details of these calculations and supporting figures are provided in *Maximum Accelerations on the Fuel Assemblies of a 21-PWR Waste Package During End Impacts* (BSC 2003 [DIRS 162602]), Attachment V). A low pass filter with three different cutoff frequencies has been used to remove the high frequency response for all the results presented in this document. The choice of cutoff frequencies is discussed in *Maximum Accelerations on the Fuel Assemblies of a 21-PWR Waste Package During End Impacts* (BSC 2003 [DIRS 162602], Attachment VII).

Table 5.3-65. Maximum Peak Acceleration (*g*) for the Fuel Assemblies with Three Different Cutoff Frequencies

	Initial Velocity (m/s)				
Cutoff Frequency (*Hz*)	**0.5**	**1**	**2**	**4**	**6**
450	75 (See Figure V-1)	144 (See Figure V-4)	263 (See Figure V-8)	323 (See Figure V-11)	506 (See Figure V-14)
600	101 (See Figure V-2)	192 (See Figure V-6)	347 (See Figure V-9)	369 (See Figure V-12)	567 (See Figure V-15)
1000	136 (See Figure V-3)	343 (See Figure V-7)	502 (See Figure V-10)	479 (See Figure V-13)	701 (See Figure V-16)

Source: Modified from BSC 2003 [DIRS 162602], Table 4 and Attachment V.

Table 5.3-66. Average Peak Acceleration (*g*) for the Fuel Assemblies with Three Different Cutoff Frequencies

	Initial Velocity (m/s)				
Cutoff Frequency (*Hz*)	**0.5**	**1**	**2**	**4**	**6**
450	35 (Corresponds to Figure V- 1)	72 (Corresponds to Figure V- 4)	115 (Corresponds to V-Figure 8)	155 (Corresponds to. Figure V- 11)	194 (Corresponds to Figure V- 14)
600	48 (Corresponds to Figure V- 2)	99 (Corresponds to Figure V- 6)	147 (Corresponds to Figure V- 9)	180 (Corresponds to Figure V- 12)	219 (Corresponds to Figure V- 15)
1000	78 (Corresponds to Figure. V- 3)	160 (Corresponds to Figure V-7)	215 (Corresponds to Figure V-10)	244 (Corresponds to Figure V- 13)	278 (Corresponds to Figure V- 16)

Source: Modified from BSC 2003 [DIRS 162602], Table 5 and Attachment V.

Two additional cases were run at 200°C, one with an initial velocity of 1 *m/s* and the second with an initial velocity of 4 *m/s*. The results are presented in *Maximum Accelerations on the Fuel Assemblies of a 21-PWR Waste Package During End Impacts* (BSC 2003 [DIRS 162602], Attachment VI). The variation of 50°C for material properties has only a minor effect on the results.

The data in Tables 5.3-65 and 5.3-66 is used directly in defining a bounding abstraction for cladding damage that is used in the seismic scenario class. The rationale for this abstraction is explained in the *Seismic Consequence Abstraction* report (BSC 2004 [DIRS 169183], Section 6.5.7).

5.3.6 Mesh Refinement Study for End Impacts

Table 5.3-67 shows the results of the mesh refinement study for the lower residual stress threshold (i.e., 80 percent of the yield strength = (0.8)(310 MPa) = 248 MPa for Alloy 22 at 150°C). The values presented in red and blue correspond to the results in Table 5.3-56 for the original calculations and the new results for the refined mesh, respectively. The percentage

differences in the volume of a typical element (δ_V[7]) and the damaged area (δ_{DA}) are presented in black. Negative percentage values correspond to a decrease of the volume or the damaged area compared to the results in Table 5.3-56.

The results presented in Table 5.3-67 indicate that, on average, a mesh refinement of 595 percent results in a 29 percent decrease in the damaged area. The one exception is for the 0 degree results that are discussed separately in Section 5.3.6.1. Only one end impact calculation resulted in an increase (16 percent) of damaged area compared to the values in Table 5.3-56. Although a comparison based on the averages is useful, it should also be noted that the difference in damaged area is less than 20 percent in four out of seven cases.

The results clearly indicate a tendency for the coarser mesh (BSC 2003 [DIRS 162293]) to overestimate the damaged area for low-angle impacts more than for high-angle impacts. This is reasonable because the deformation energy for low-angle end impacts is distributed over a larger portion of the waste package in comparison to the more localized deformation due for high-angle end impacts. The low-angle impacts are, compared to the corresponding high-angle impacts, characterized by the damaged area shapes that are generally more elongated (i.e., spread more in the circumferential direction and less in the axial direction). Consequently, the coarser mesh has tendency to overestimate the damaged area for low-angle impacts more than for the high-angle impacts due to the relatively small area-to-boundary length ratio of damaged areas in the former case. The stress averaging within the relatively coarse constant-stress elements for *21-PWR Waste Package Side and End Impacts* (BSC 2003 [DIRS 162293]) is, consequently, more likely to overestimate damaged area for low-angle impacts than for high-angle impacts. It is also important to recognize that a coarse mesh is inherently less capable of accommodating localized deformation. That is, the coarse mesh is inherently stiffer numerically because it represents fewer degrees of freedom in comparison to a refined mesh. Consequently, the impact energy delivered to a structure is smeared over a larger area by the coarse mesh. In other words, the impact energy is redistributed over a larger area because of the inherent inability of the (less flexible) coarse mesh to capture the localized-deformation. This leads to a consistent bias in the coarse mesh to overestimates damaged area, particularly for relatively low residual stress thresholds.

Table 5.3-68 presents, in the same manner as Table 5.3-67, the results corresponding to the upper damage threshold (i.e., 90 percent of the yield strength = (0.9)(310 MPa) = 279 MPa for Alloy 22 at 150°C).

[7] The typical element is selected from the region of the OCB characterized by the most pronounced contribution to the damaged area.

Table 5.3-67. Damaged Areas for the Lower Residual Stress Threshold of 80 Percent of Yield Strength

		Angle between the Waste Package Centerline and the Vertical (degree)			
		0	1	5	8
Impact Velocity (m/s)	1	—	—	—	—
	2	—	—	V=8.29e-7 m^3 (e# 22386) V=1.31e-7 m^3 (e# 116590) δ_V=-533%	V=8.29e-7 m^3 (e# 22386) V=1.31e-7 m^3 (e# 116590) δ_V=-533%
				DA=0.0109 m^2 DA=0.0130 m^2 δ_{DA}=+16%	DA=0.0113 m^2 DA=0.0105 m^2 δ_{DA}=-8%
	4	V=4.47e-7 m^3 (e# 15556) V=4.80e-8 m^3 (e# 270687) δ_V=-831%	V=1.11e-6 m^3 (e# 22426) V=1.46e-7 m^3 (e# 214246) δ_V=-660%	V=2.02e-6 m^3 (e# 23219) V=3.02e-7 m^3 (e# 18230) δ_V=-569%	—
		DA=0.0244 m^2 DA=0.0122 m^2 δ_{DA}=-100%	DA=0.0734 m^2 DA=0.0421 m^2 δ_{DA}=-74%	DA=0.0850 m^2 DA=0.0651 m^2 δ_{DA}=-31%	
	6	V=4.47e-7 m^3 (e# 15556) V=4.80e-8 m^3 (e# 270687) δ_V=-831%	—	V=9.52e-7 m^3 (e# 22666) V=1.78e-7 m^3 (e# 9014) δ_V=-435%	V=1.11e-6 m^3 (e# 22626) V=1.78e-7 m^3 (e# 8774) δ_V=-524%
		DA=0.0276 m^2 DA=0.0264 m^2 δ_{DA}=-5%		DA=0.1556 m^2 DA=0.1466 m^2 δ_{DA}=-6%	DA=0.1082 m^2 DA=0.0967 m^2 δ_{DA}=-12%
	10	—	V=6.44e-7 m^3 (e# 17982) V=6.38e-8 m^3 (e# 212565) δ_V=-909%	—	—
			DA=0.0834 m^2 DA=0.0571 m^2 δ_{DA}=-46%		
	20	—	—	—	—

Source: BSC 2004 [DIRS 170844], Table 2.

NOTE 1: DA designates the damaged area and V designates the volume of a typical element (e#) of the waste package OCB. Subscript ('0') refers to the base mesh. Subscript ('1') refers to the refined yield. δDA and δV are changes in damaged area and volume respectively, for base case and mesh refinement study.

NOTE 2: Blank fields correspond to cases from (BSC 2003 [DIRS 162293]) that are not rerun in this study.

WP = waste package

Table 5.3-68. Damaged Area for the Upper Residual Stress Threshold of 90 Percent of Yield Strength

		Angle between the Waste Package Centerline and the Vertical (degree)			
		0	1	5	8
Impact Velocity (m/s)	1	—	—	—	—
	2	—	—	V=8.29e-7 m^3 (e# 22386) V=1.31e-7 m^3 (e# 116590) δ_V=-533%	V=8.29e-7 m^3 (e# 22386) V=1.31e-7 m^3 (e# 116590) δ_V=-533%
				DA=0.0056 m^2 DA=0.0052 m^2 δ_{DA}=-8%	DA=0.0066 m^2 DA=0.0051 m^2 δ_{DA}=-29%
	4	V=4.47e-7 m^3 (e# 15556) V=4.80e-8 m^3 (e# 270687) δ_V=-831%	V=1.11e-6 m^3 (e# 22426) V=1.46e-7 m^3 (e# 214246) δ_V=-660%	V=2.02e-6 m^3 (e# 23219) V=3.02e-7 m^3 (e# 18230) δ_V=-569%	—
		DA=0.0244 m^2 DA=0.0122 m^2 δ_{DA}=-100%	DA=0.0212 m^2 DA=0.0126 m^2 δ_{DA}=-68%	DA=0.0508 m^2 DA=0.0288 m^2 δ_{DA}=-76%	
	6	V=4.47e-7 m^3 (e# 15556) V=4.80e-8 m^3 (e# 270687) δ_V=-831%	—	V=9.52e-7 m^3 (e# 22666) V=1.78e-7 m^3 (e# 9014) δ_V=-435%	V=1.11e-6 m^3 (e# 22626) V=1.78e-7 m^3 (e# 8774) δ_V=-524%
		DA=0.0244 m^2 DA=0.0124 m^2 δ_{DA}=-97%		DA=0.0767 m^2 DA=0.0655 m^2 δ_{DA}=-17%	DA=0.0501 m^2 DA=0.0335 m^2 δ_{DA}=-50%
	10	—	V=6.44e-7 m^3 (e# 17982) V=6.38e-8 m^3 (e# 212565) δ_V=-909%	—	—
			DA=0.0264 m^2 DA=0.0259 m^2 δ_{DA}=-2%		
	20	—	—	—	—

Source: BSC 2004 [DIRS 170844], Table 3.

NOTE 1: DA designates the damaged area. V designates the volume of a typical element (e#) of the waste package OCB. Subscript ('$_0$') refers to the base mesh. Subscript ('$_1$') refers to the refined yield. δ_{DA} and δ_V are changes in damaged area and volume respectively, for base case and mesh refinement study.

NOTE 2: The blank table fields correspond to the simulations documented in the source document that are not rerun in this study.

The results presented in Table 5.3-68 (with exception of 0 degree results that are discussed separately in Section 5.3.6.1) indicate that, on average, a mesh refinement of 595 percent results in a 36 percent decrease of the damaged area in comparison to the results in Table 5.3-57. The differences in the damaged areas are consistently on the conservative side in comparison to the results with a coarse mesh. An explanation for the somewhat more pronounced damaged area reduction for the upper damage threshold (Table 5.3-68) compared to those for the lower damage threshold (Table 5.3-67) is in the damaged area size. The damaged area for the upper residual stress threshold is typically at least two times smaller then for the lower residual stress threshold (see Tables 5.3-56 and 5.3-57). Consequently, the same absolute difference in damaged area would cause a relative difference that is twice as large. Stated differently, the damage area for the upper residual stress threshold is intrinsically more mesh sensitive.

The damaged areas (especially those corresponding to the upper residual stress threshold) are of irregular, often elongated, shape (for example, BSC 2004 [DIRS 170844], Figure I-3 and Figure I-4 or Figure 5-37); the accuracy of the estimated damage area is inherently limited by the size of the affected elements for these types of shapes. Since the typical element minimum dimensions in this calculation are 2 mm to 3 mm, and since the affected region of the waste package OCB is almost three orders of magnitude larger, it is obvious that there is a resolution limit for a reasonable damaged area evaluation. This is acceptable since the use of larger elements in a coarser mesh results in a consistent overestimate of the damaged area. Thus, the tradeoff between accuracy of the FE mesh and computational tractability is inherently more pronounced for damaged area evaluation than for stress evaluation. However, it is important to recognize that the results with the coarser mesh are on the conservative side.

This conclusion is supported by the results for three additional FE calculations with a further refined mesh, which are presented in Tables 5.3-69 and 5.3-70[8]. Three end impacts are defined by the impact parameters presented in the first column of Tables 5.3-69 and 5.3-70. These calculations are performed by using LS-DYNA V970 D MPP-00 for massively parallel processing because of the large number of elements. As an illustration of the rapid increase of the computational load, the number of elements in the base FE representation used in *21-PWR Waste Package Side and End Impacts* (BSC 2003 [DIRS 162293]) for an end impact with one degree impact angle and initial velocity of 4 m/s was 50,726. The corresponding number of elements in the first and second refined-mesh calculations is 335,102 (BSC 2004 [DIRS 170844], Attachment II, Mesh 1 (SMP) \ a1v4 \ d3hsp) and 1,198,942 (BSC 2004 [DIRS 170844], Attachment II, Mesh 2 (MPP) \ a1v4 \ d3hsp), respectively.

The values corresponding to the results obtained from the base calculation (BSC 2003 [DIRS 162293]) and from the first refined mesh are again presented as red and blue, respectively. In addition, the values are designated by subscripts "0" and "1", respectively. The values corresponding to the FE representation with the largest mesh density are presented as green with a subscript "2." For example, δ_{V12} refers to the change of the typical element volume between the first refined mesh ("1") and the second refined mesh ("2");δ_{DA02} refers to the change of the damaged area value between the base mesh ("0") and the second ("2") refined mesh; and so on.

[8] Throughout Section 5.3.6, the "refined mesh" refers to the first refined mesh and the "very refined mesh" refers to the second refined mesh.

Table 5.3-69. Damaged Areas for the Lower Residual Stress Threshold of 80 Percent of Yield Strength for the Base Case, the Refined Mesh, and the Very Refined Mesh

	Volume (m3Number (e#) of Typical Element	Damaged Area (m^2)	Difference in Volume (%)	Difference in Damaged Area (%)
Angle = 5 degree Velocity = 2 m/s	V_0=8.29·10^{-7} (e# 22386) V_1=1.31·10^{-7} (e# 116590) V_2=2.37·10^{-8} (e# 366764)	DA_0=0.0109 DA_1=0.0130 DA_2=0.0128	δ_{V01}=-533 δ_{V12}=-453 δ_{V02}=-3402	δ_{DA01}=+16 δ_{DA12}=-2 δ_{DA02}=+15
Angle = 1 degree Velocity = 4 m/s	V_0=1.11·10^{-6} (e# 22426) V_1=1.31·10^{-7} (e# 214006) V_2=2.36·10^{-8} (e# 658212)	DA_0=0.0734 DA_1=0.0421 DA_2=0.0406	δ_{V01}=-747 δ_{V12}=-455 δ_{V02}=-4603	δ_{DA01}=-74 δ_{DA12}=-4 δ_{DA02}=-81
Angle = 5 degree Velocity = 4 m/s	V_0=2.02·10^{-6} (e# 23219) V_1=3.02·10^{-7} (e# 18230) V_2=8.43·10^{-8} (e# 68834)	DA_0=0.0850 DA_1=0.0651 DA_2=0.0602	δ_{V01}=-569 δ_{V12}=-258 δ_{V02}=-2296	δ_{DA01}=-30 δ_{DA12}=-8 δ_{DA02}=-41

Source: BSC 2004 [DIRS 170844], Table 4.

NOTE: $_0$ = base mesh; $_1$ = 1st refined mesh; $_2$ = 2nd refined mesh. V = volume of element (e#); DA = Damaged Area; δ_V or δ_{DA} = Changed in Volume or Damaged Area.

Table 5.3-70. Damaged Areas for the Lower Residual Stress Threshold of 90 Percent of Yield Strength For the Base Case, the Refined Mesh, and the Very Refined Mesh

	Volume (m^3) and Number (e#) of Typical Element	Damaged Area (m^2)	Difference in Volume (%)	Difference in Damaged Area (%)
Angle = 5 degree Velocity = 2 m/s	V_0=8.29·10^{-7} (e# 22386) V_1=1.31·10^{-7} (e# 116590) V_2=2.37·10^{-8} (e# 366764)	DA_0=0.0056 DA_1=0.0052 DA_2=0.0066	δ_{V01}=-533 δ_{V12}=-453 δ_{V02}=-3402	δ_{DA01}=-8 δ_{DA12}=+21 δ_{DA02}=+15
Angle = 1 degree Velocity = 4 m/s	V_0=1.11·10^{-6} (e# 22426) V_1=1.31·10^{-7} (e# 214006) V_2=2.36·10^{-8} (e# 658212)	DA_0=0.0212 DA_1=0.0126 DA_2=0.0104	δ_{V01}=-747 δ_{V12}=-455 δ_{V02}=-4603	δ_{DA01}=-68 δ_{DA12}=-21 δ_{DA02}=-104
Angle = 5 degree Velocity = 4 m/s	V_0=2.02·10^{-6} (e# 23219) V_1=3.02·10^{-7} (e# 18230) V_2=8.43·10^{-8} (e# 68834)	DA_0=0.0508 DA_1=0.0288 DA_2=0.0244	δ_{V01}=-569 δ_{V12}=-258 δ_{V02}=-2296	δ_{DA01}=-76 δ_{DA12}=-18 δ_{DA02}=-108

Source: BSC 2004 [DIRS 170844], Table 5.

NOTE: 0 = base mesh; 1 = 1st refined mesh; 2 = 2nd refined mesh. V = volume of element (e#); DA = Damaged Area; δV or δDA = Changed in Volume or Damaged Area.

The results presented in Tables 5.3-69 and 5.3-70 indicated that the mesh refinement between the (first) refined mesh and the (second) very refined mesh results (average of δ_{V12}) in an average reduction of the typical-element volume by 389 percent. The corresponding average change of the damaged area value for the lower and upper damage threshold is 5 percent and 20 percent, respectively[9]. This indicates that the results obtained for the (first) refined mesh are reasonably mesh-insensitive. Furthermore, it confirms that the results corresponding to the upper residual stress threshold are more mesh-sensitive.

[9] Note that absolute values of δ_{DA} are used to calculate the average change of damage area. This approach is used to avoid "compensation" of the decrease of the damaged area in one case by the increase in other, which may be misleading. Nonetheless, the use of absolute values can also cause confusion. Hence, note that if the signs were taken into account, the average change of the upper-threshold damaged area value would be –6%.

The average mesh-density increase of 35 times between the base calculation (BSC 2003 [DIRS 162293]) and the second refined mesh results in an overestimate of the damaged area by factor of approximately two. It cannot be overemphasized that, based on the results presented in Tables 5.3-71 and 5.3-72, the factor of two is likely to be a bounding value. This statement is based on the following rationale: 1) two out of three of the cases with the very refined mesh are selected based on the largest damaged area difference, and 2) the first refined mesh results are practically mesh insensitive.

The damaged area values presented in Tables 5.3-67 through 5.3-70 are based on a value of 0.21 for the Poisson's ratio of A 516 CS, instead of 0.3. This latter value is the accurate value that is also used in *21-PWR Waste Package Side and End Impacts* (BSC 2003 [DIRS 162293]). A 516 CS is the material used for the basket guides and stiffeners and the fuel basket plates and tubes. These internal components are enclosed in the IV; consequently, their Poisson's ratio has negligible effect on the deformation of the OCB and the resulting damaged areas. This is confirmed by two calculations that are redone with the correct value of Poisson's ratio for A 516 CS. A 5 degree impact angle and 4 m/s impact velocity; the damaged areas are 0.0658 m^2 and 0.0288 m^2 for the lower and upper residual stress thresholds, respectively. These values correspond to 1.1 percent and 0 percent difference from the corresponding values in Tables 5.3-67 and 5.3-68. Additionally, for an 8 degree impact angle and 6 m/s impact velocity, the damaged areas are 0.0957 m^2 and 0.0333 m^2 for the lower and upper residual stress thresholds, respectively. These values correspond to 1.0 percent and 0.6 percent difference from the corresponding values in Tables 5.3-67 and 5.3-68. Since the difference in damaged area is on the order of 1 percent or less, from the input error for A 516 CS Poisson's ratio, it is unnecessary to redo the other calculations with a refined or very refined mesh.

5.3.6.1 Discussion of Results for Zero-Degree Impact Angle

The results for zero-degree impact angle merit a separate discussion for the following reasons:

- The level of approximation inherent in achieving an ideal, zero-degree end impact between two waste packages is larger than that for oblique impact angles.
  - The ideal zero-degree end impact is a limiting case that is extremely unlikely to occur because of the irregularities of the invert surface and because of the complexity of the applied loads (i.e., the seismic excitation)
  - The ideal zero-degree end impact implies not only an absence of relative inclination between the two waste packages but also a perfect alignment of their centerlines at the time of collision. In other words, the waste package centerlines have to be not only parallel but also collinear
  - The ideal zero-degree end impact requires two identical waste packages.
- The damaged area for ideal zero-degree impacts is contained within a very narrow axially symmetric ring, located at the end surface of the OCB, close to its outer edge (BSC 2004 [DIRS 170844], Figure I-2). Thus, it is overlapped by the lower trunnion sleeve weld, as

illustrated in *21-PWR Waste Package End Impacts - A Mesh Study* (BSC 2004 [DIRS 170844], Figure I-1).

The ideal zero-degree end impact is not only an extremely unlikely event but its damaged area estimate is dominantly, if not exclusively, governed by the OCB discretization across the wall thickness. In other words, the across-wall-thickness element size is the resolution length for the calculation of the damaged area.

The results for the 4 m/s end impact presented in Tables 5.3-67 and 5.3-68 indicate that the base mesh (BSC 2003 [DIRS 162293]) overestimates the damaged area by a factor of two compared to the refined mesh. A detailed analysis of the refined-mesh results reveals that the reduction is due to axial distribution of the residual first principal stress. According to *21-PWR Waste Package End Impacts - A Mesh Study* (BSC 2004 [DIRS 170844], Figure I-1), most of the elements whose residual first principal stress exceeds the damage thresholds are located slightly off of the OCB surface (layer 1)[10]. If the elements corresponding to layer 1 on *21-PWR Waste Package End Impacts - A Mesh Study* (BSC 2004 [DIRS 170844], Figure I-1) are on the OCB surface (i.e., if they belong to layer 0), then the 100-percent damaged area difference in Table 5.3-68 would be reduced to zero (compare BSC 2004 [DIRS 170844] Figure I-2a with Figure I-2b). In the case of the coarser base mesh (BSC 2003 [DIRS 162293]), the surface layer of elements (layer 0) encompasses the elements belonging to layers 0 and 1 of the refined mesh (BSC 2004 [DIRS 170844], Figures I-1 and I-2), and the corresponding stress averaging results in the overestimate of the damaged area by a factor of two.

A similar trend is evident for the 6 m/s ideal zero-degree end impact. The increase of deformation energy at 6 m/s compared to 4 m/s results in a "catch up" of the damaged area at the lower residual stress threshold, so the difference is only 5 percent. At the same time, the increase of deformation energy is not sufficient to result in an increase in damaged area at the upper residual stress threshold, so the difference is still approximately a factor of two.

5.3.6.2 Summary and Conclusions

Based on the results in Tables 5.3-67 through 5.3-70, it is reasonable to claim that mesh-insensitive results for damaged area are achieved with the refined mesh. On the other hand, the damaged areas for the base calculations are generally conservative. The average overestimate, according to results presented in Tables 5.3-67 and 5.3-68, is approximately 30 percent, although in a few outliers it can reach 100 percent. Only one out of nine end impacts resulted in a small increase of damaged area value (16 percent) (Tables 5.3-67 and 5.3-68). The use of results from the base case calculations in developing abstractions for the seismic scenario is justified by the computational efficiency of the base mesh and by the modest conservatism in the damaged areas.

The results from this study support the data in Tables 5.3-22 and 5.3-55 that are the basis for the waste package damage abstraction in the seismic scenario class. The results from this supplemental study are not used directly in the abstraction process.

[10] Recall that the damaged area is, by definition, defined by the surfaces of the OCB.

5.3.7 Alternate Ground Motions at 2.44 m/s PGV Level

The original set of calculations for the 2.44 m/s PGV level (BSC 2004 [DIRS 167083]) used ground motion time history that do not preserve intercomponent variability. In other words, the variability between the three velocity components of a given ground motion is limited because each velocity component is scaled to a target value, rather than maintaining the intercomponent variability in the original ground motion records. In addition, the ground motions records were not spectrally conditioned to earthquake spectra typical of the western United States.

The four additional calculations at the 2.44 m/s PGV level have been performed with ground motions that do preserve intercomponent variability and do condition response spectra to be more typical of those found in the western United States. These time histories were spectrally conditioned to have response spectra more typical of the Yucca Mountain site prior to being scaled.

The four additional calculations correspond to realizations 3, 4, 6, and 15. Realizations 3, 6, and 4 are characterized by the largest damaged areas (in the descending order) among the calculations documented in Table 5.3-22. The changes in the PGV between the ground motion sets are illustrated in Table 5.3-71 for the longitudinal (along the tunnel; H2) and vertical (V) directions. The input data and results labeled hereinafter as "Old" and "New" refer to the original ground motion time histories and the modified ground motion time histories, respectively.

Table 5.3-71. Change of PGV between Two Ground Motion Sets

Realization	Ground Motion	Longitudinal (H2) PGV			Vertical (V) PGV		
		Old	New	Change	Old	New	Change
3	4	2.43 *m/s*	2.60 *m/s*	+7%	2.28 *m/s*	2.97 *m/s*	+30%
4	8	2.44 *m/s*	4.02 *m/s*	+65%	2.30 *m/s*	1.54 *m/s*	-33%
6	1	2.43 *m/s*	1.95 *m/s*	-20%	2.30 *m/s*	1.11 *m/s*	-52%
15	3	2.43 *m/s*	6.43 *m/s*	+165%	2.28 *m/s*	6.09 *m/s*	+167%

Realizations 3, 6, and 4, in addition to being characterized by the largest damaged areas, are also typical regarding the ground motion change between the two sets. Ground motion 4 (realization 3) is representative of a small PGV increase in the longitudinal and a moderate PGV increase in the vertical direction. (Table 5.3-71). Ground motion 1 (realization 6) is representative of a moderate decrease in the PGV in both the longitudinal and vertical directions. Ground motion 8 (realization 4) is representative of a moderate PGV increase in the longitudinal and a moderate PGV decrease in the vertical direction. Finally, ground motion 3 (realization 15) is characterized by a dramatic PGV increase in both directions.

5.3.7.1 Investigation of Damage from Waste Package-Waste Package Interactions

This section presents the damaged area on the OCB resulting from impacts between adjacent waste packages in the longitudinal (along the tunnel) direction. This damaged area is based on (1) the kinematic data that define the speed, location and angle of end impacts from the simulations of vibratory ground motion, with (2) the damaged areas from individual end impact calculations presented in Tables 5.3-56 and 5.3-57.

The kinematic parameters for end impacts with the four alternate ground motions at the 2.44 m/s PGV level are presented in Tables 5.3-72 through 5.3-75. The "time" presented in the second column is the time of impact. The impact speed (the third column) is the relative speed between the longitudinal boundary (representing the neighboring waste package) and the waste package node (i.e., its trunnion sleeve) in the impact region. The impact angle presented in the fourth column defines inclination of the waste package with respect to the longitudinal boundary; an angle of zero would correspond to ideal end impact.

Table 5.3-72. End-Impact Parameters and Damaged Area for Realization 3

Impact Location	Time (s)	Speed (m/s)	Angle (degree)	Damaged Area (m^2)	
				80% Yield Strength	90% Yield Strength
F 1	2.7250	2.4	0.3	0.0131	0.0074
F 3	3.3000	1.4	1.6	0.0100	0.0052
F 9	3.1250	2.7	1.1	0.0400	0.0149
F 9	3.1625	1.1	1.2	0.0051 NC	0.0027 NC
C 3	3.5250	1.2	2.1	0.0061	0.0032
C 4	0.5375	1.5	1.2	0.0124	0.0063
C 5	4.1125	1.2	0.2	0.0014	0.0007
C 9	2.8625	3.6	0.3	0.0326	0.0194
C 9	2.1625	1.7	0.4	0.0066 NC	0.0034 NC
C 10	2.2250	2.3	0.2	0.0089 NC	0.0055 NC
Total				0.12	0.057

Source: BSC 2004 [DIRS 168385], Table 6.1-1.

Table 5.3-73. End-Impact Parameters and Damaged Area for Realization 4

Impact Location	Time (s)	Speed (m/s)	Angle (degree)	Damaged Area (m^2)	
				80% Yield Strength	90% Yield Strength
F 3	3.7625	1.6	0.8	0.0117	0.0060
F 11	2.2250	2.2	0.2	0.0074	0.0044
C 3	2.5375	3.5	0.3	0.0310	0.0184
C 4	3.3375	1.9	2.9	0.0154 NC	0.0078 NC
C 11	2.5750	3.2	0.6	0.0376	0.0162
Total				0.088	0.045

Source: BSC 2004 [DIRS 168385], Table 6.1-2.

Table 5.3-74. End-Impact Parameters and Damaged Area for Realization 6

Impact Location	Time (s)	Speed (m/s)	Angle (degree)	Damaged Area (m^2)	
				80% Yield Strength	90% Yield Strength
F 2	2.1750	2.6	1.1	0.0374	0.0143
F 3	0.6375	1.9	0.2	0.0040 NC	0.0021 NC
F 6	2.6125	2.3	0.2	0.0089X0.5	0.0055X0.5
F 7	1.4625	1.8	1.7	0.0167X0.5	0.0085X0.5
F 8	1.5250	2.1	1.6	0.0232	0.0111
F 9	0.6625	1.4	0.2	0.0022X0.5	0.0011X0.5
C 3	1.0000	1.2	0.4	0.0028	0.0015
C 9	1.6750	1.2	1.7	0.0064X0.5	0.0034X0.5
C 10	2.3250	1.7	1.3	0.0158	0.0081
C 11	0.8875	1.8	0.5	0.0092X0.5	0.0047X0.5
Total				0.10	0.047

Source: BSC 2004 [DIRS 168385], Table 6.1-3.

Table 5.3-75. End-Impact Parameters and Damaged Area for Realization 15

Impact Location	Time (s)	Speed (m/s)	Angle (degree)	Damaged Area (m^2)	
				80% Yield Strength	90% Yield Strength
F 7	0.775	2.1	5.9	0.0145	0.0079
F 9	0.100	1.1	0.3	0.0016	0.0008
C 3	0.250	2.6	0.6	0.0254	0.0114
C 10	0.575	1.0	5.7	0.0016 NC	0.0011 NC
C 10	0.600	1.5	5.6	0.0063	0.0034
C 10	0.725	1.2	5.6	0.0035 NC	0.0020 NC
Total				0.048	0.024

Source: BSC 2004 [DIRS 168385], Table 6.1-4.

A summary of damaged areas in Tables 5.3-72 through 5.3-75 is presented in Table 5.3-76.

Table 5.3-76. Damaged Area from Waste Package-Waste Package Interaction (End Impacts)

Realization	Ground Motion	Damaged Area (m^2)	
		80% Yield Strength	90% Yield Strength
3	4	0.12	0.057
4	8	0.088	0.045
6	1	0.10	0.047
15	3	0.048	0.024

Source: BSC 2004 [DIRS 168385], Table 6.1-5.

5.3.7.2 Damage from Waste Package-Pallet Interactions

The damaged area resulting from the waste package-pallet interaction during the vibratory ground motion is presented in Table 5.3-77.

Table 5.3-77. Damaged Area from Waste Package-Pallet Interaction

Realization	Ground Motion	Damaged Area (m^2)	
		80% Yield Strength	90% Yield Strength
3	4	0.0014	0.0
4	8	0.0032	0.0
6	1	0.0081	0.0014
15	3	0.043	0.010

Source: BSC 2004 [DIRS 168385], Table 6.2-1.

The damaged-area from waste package-pallet interactions is illustrated in Figures 5.3-8 through 5.3-11. These figures present the first principal stress plots with the number of stress fringe levels reduced to three and adjusted to emphasize the amount and distribution of the damaged area. The stress unit in Figures 5.3-8 through 5.3-11 is *Pascal* ($Pa = N/m^2$). Note that the stress thresholds of 248 *MPa* and 279 *MPa* correspond, respectively, to 80 percent and 90 percent of the yield strength for Alloy 22 at 150°C.) Thus, all elements with residual first principal stress below 248 *MPa* are blue and are not damaged. All elements with residual first principal stress from 248 *MPa* to 279 *MPa* are green. Finally, all elements with residual first principal stress exceeding 279 *MPa* are red and are always damaged.

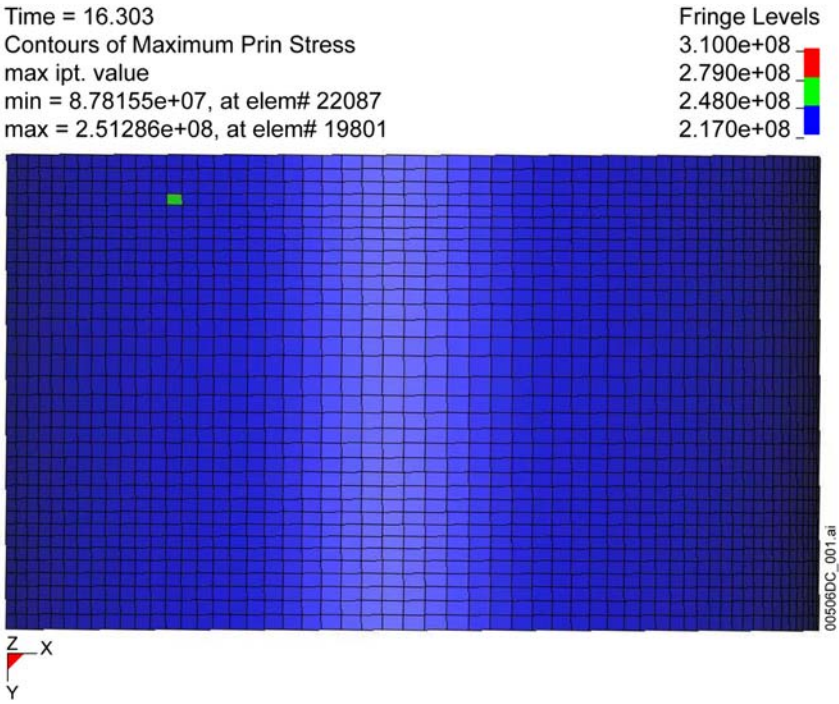

Source: BSC 2004 [DIRS 168385], Figure 6.2-1.

NOTE: Units in Pascals

Figure 5.3-8. Residual First Principal Stress Plot in OCB (Bottom View) for Realization 3

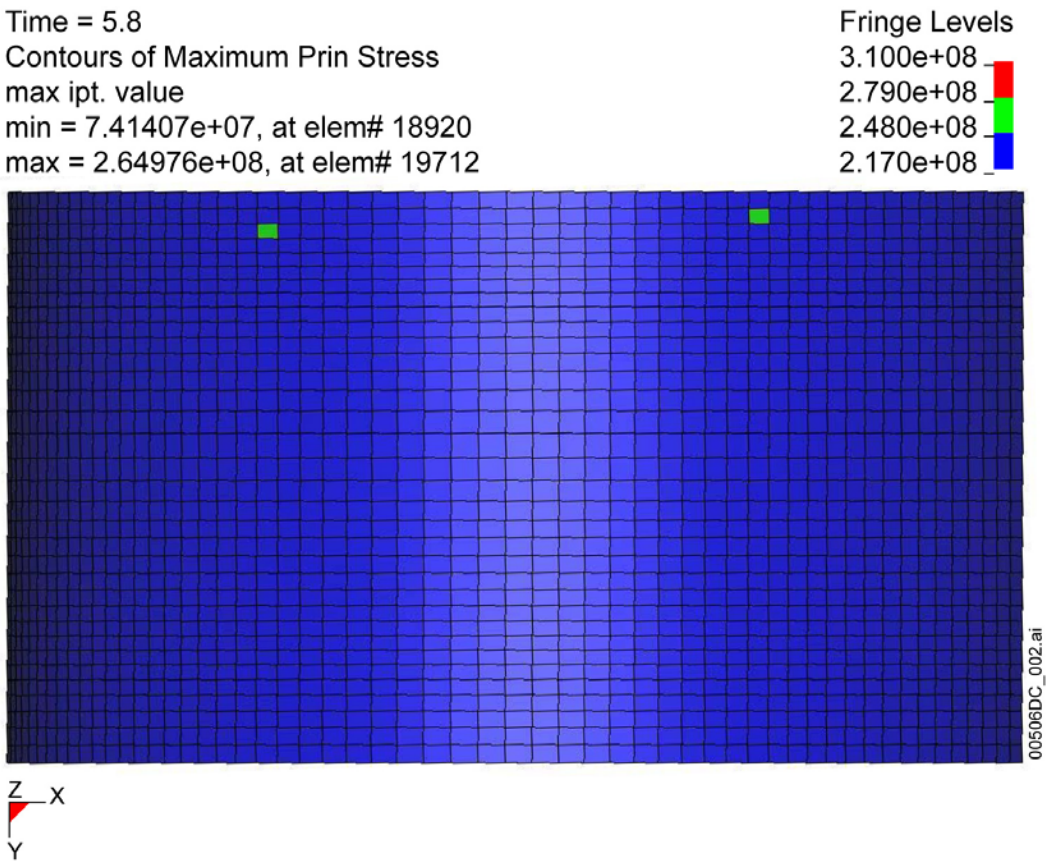

Source: BSC 2004 [DIRS 168385], Figure 6.2-2.

NOTE: Units in Pascals.

Figure 5.3-9. Residual First Principal Stress Plot in OCB (Bottom View) for Realization 4

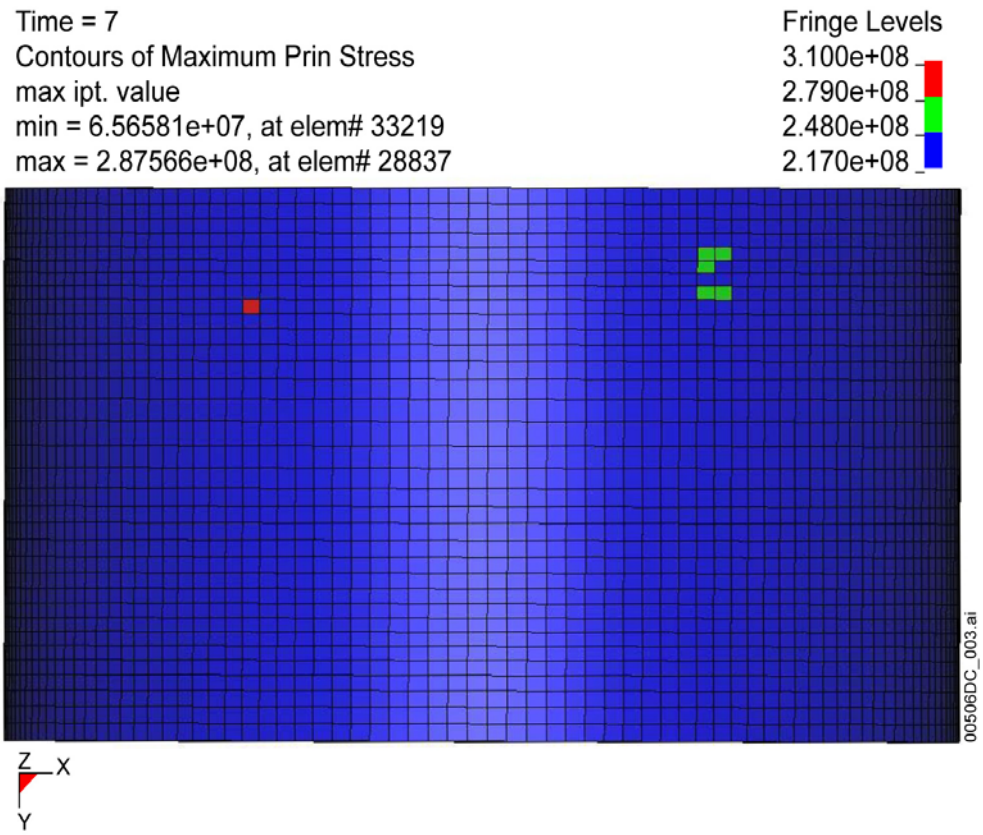

Source: BSC 2004 [DIRS 168385], Figure 6.2-3.

NOTE: Units in Pascals.

Figure 5.3-10. Residual First Principal Stress Plot in OCB (Bottom View) for Realization 6

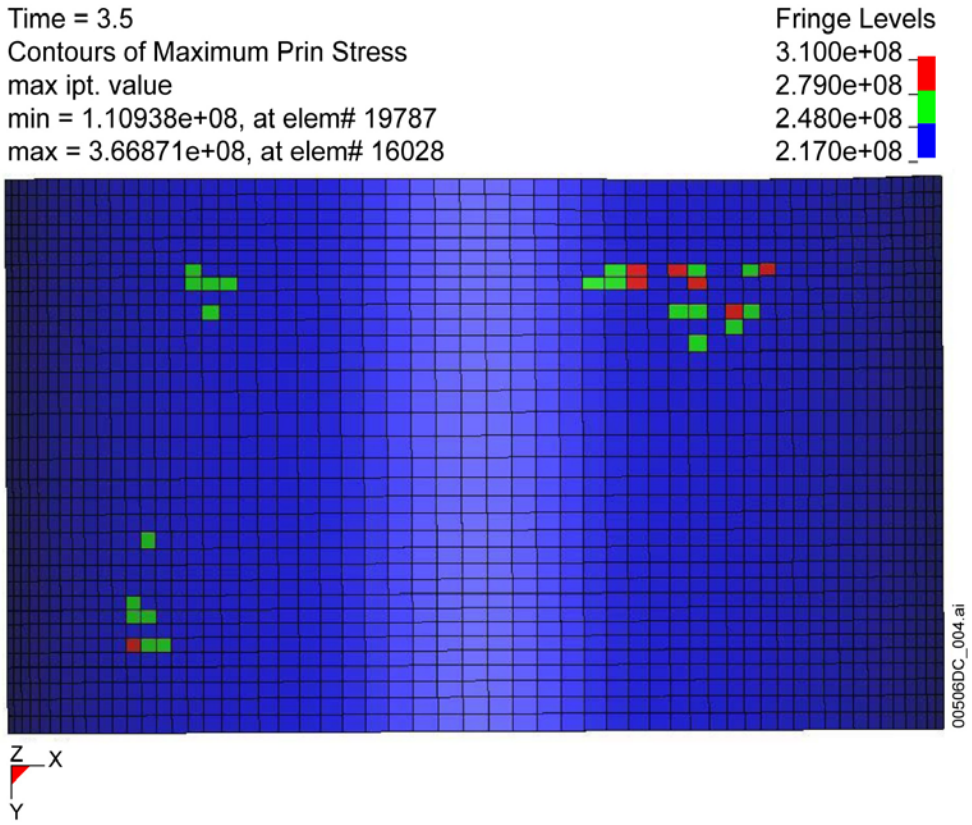

Source: BSC 2004 [DIRS 168385], Figure 6.2-4.
NOTE: Units in Pascals.

Figure 5.3-11. Residual First Principal Stress in OCB (Bottom View) for Realization 15

5.3.7.3 Discussion and Summary

The damaged areas characterizing the four supplemental calculations with modified ground motions at the 2.44 m/s PGV level are summarized in Table 5.3-78.

Table 5.3-78. Cumulative Damaged Area for Modified Ground Motions at the 2.44 m/s PGV Level

Realization	Ground Motion	Damaged Area					
		WP-Pallet Interaction (m^2; % of total OCB area)		WP-WP Interaction (m^2; % of total OCB area)		Cumulative (m^2; % of total OCB area)	
		80% Yield Strength	90% Yield Strength	80% Yield Strength	90% Yield Strength	80% Yield Strength	90% Yield Strength
3	4	0.0014; 0.0050%	0.0; 0.0	0.12; 0.43%	0.057; 0.20%	0.12; 0.43%	0.057; 0.20%
4	8	0.0032; 0.011%	0.0; 0.0	0.088; 0.31%	0.045; 0.16%	0.091; 0.32%	0.045; 0.16%
6	1	0.0081; 0.029%	0.0014; 0.0050%	0.10; 0.35%	0.047; 0.17%	0.11; 0.39%	0.048; 0.17%
15	3	0.043; 0.15%	0.010; 0.035%	0.048; 0.17%	0.024; 0.085%	0.091; 0.32%	0.034; 0.12%

Source: BSC 2004 [DIRS 168385], Table 6.3-1.
NOTE: OCB stands for the OCB; total OCB area is 28.2 m2.
WP = waste package

The cumulative damaged areas for the four 2.44 m/s realizations obtained by using the two different ground motion sets are presented in Table 5.3-79. The "Old" results are obtained from Table 5.3-22, and the alternate or "New" results are obtained from Table 5.3-79.

Table 5.3-79. Cumulative Damaged Area from Two 2.4 m/s Per Year Ground Motion Sets

Realization	Ground Motion	Damaged Area (m^2; % of total OCB area)			
		80% Yield Strength		90% Yield Strength	
		Old	New	Old	New
3	4	0.20; 0.71%	0.12; 0.43%	0.083; 0.29%	0.057; 0.20%
4	8	0.15; 0.53%	0.091; 0.32%	0.067; 0.24%	0.045; 0.16%
6	1	0.18; 0.64%	0.11; 0.39%	0.066; 0.23%	0.048; 0.17%
15	3	0.028; 0.099%	0.091; 0.32%	0.012; 0.043%	0.034; 0.12%

Source: BSC 2004 [DIRS 168385], Table 6.3-2.

NOTE: Total OCB is 28.2 m^2 (Section 5.3).

The results from Table 5.3-79 are schematically illustrated in Figure 5.3-12. The damage data for all realizations in Table 5.3-22 are included in Figure 5.3-12 to illustrate the variability of damaged area versus the new data points.

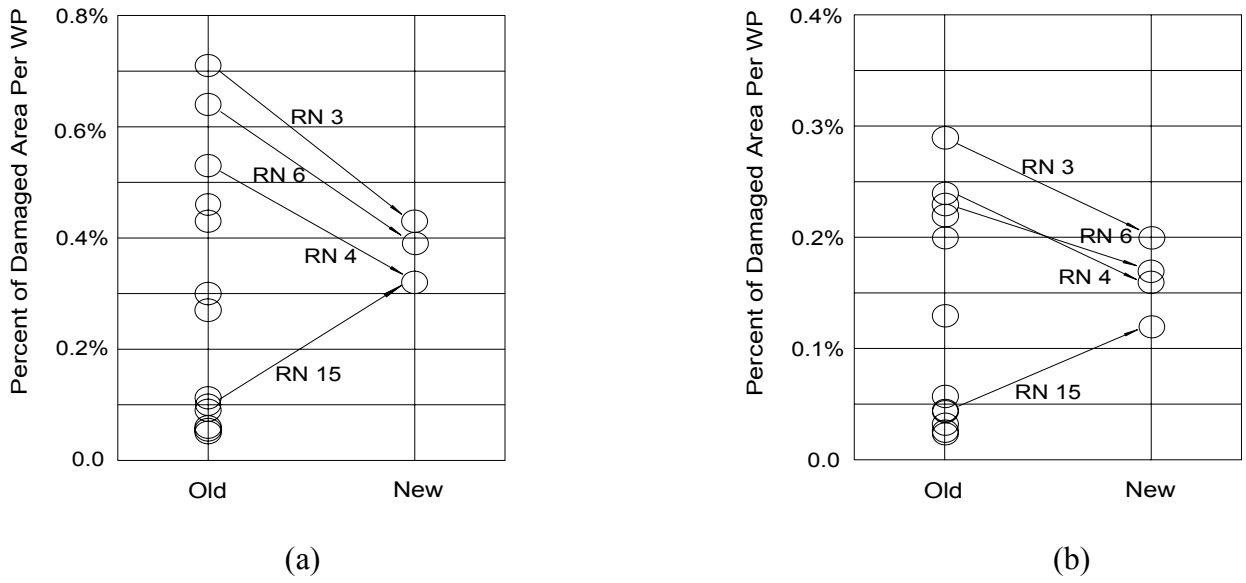

Source: BSC 2004 [DIRS 168385], Figure 6.3-1.

NOTE: (a) 80 percent of yield strength; (b) 90 percent of yield strength; RN = realization number.

Figure 5.3-12. Schematic Representation of Scatter and Change of Damaged Area for Two Stress Thresholds

Keeping in mind the changes in the PGV values for components H2 and V between the old and new ground motions, the changes in damaged areas for realizations 6 and 15 are as expected, in the sense that damaged area increases or decreases with the corresponding changes in PGV for the longitudinal and vertical components. On the other hand, a more detailed examination is necessary to explain the changes of damaged areas for realizations 3 and 4.

As indicated in Table 5.3-71, the PGV changes in ground motion 4 (realization 3) are characterized by a 7 percent increase in the longitudinal (H2) direction and a 30 percent increase in vertical (V) direction. The PGV changes in ground motion 8 (realization 4) are characterized by a 65 percent increase in the longitudinal direction and a 33 percent decrease in the vertical direction. Since the majority of the damaged areas in Table 5.3-22 is usually contributed by end impacts, the velocity time history in the longitudinal direction should be a primary influence on damaged area. Nonetheless, the damaged areas decreased for both realizations. This apparent inconsistency can be explained by a detailed examination of the velocity time histories (Figures 5.3-13 and 5.3-14) and end impact parameters (Tables 5.3-72 and 5.3-73).

As shown in Figure 5.3-13, indications that despite the seven percent PGV increase in the longitudinal direction, the ground motion velocity time histories in that direction are similar it terms of the number and magnitude of the velocity peaks (Note that the old and new ground motions generally have different 5 percent time, 95 percent time, and duration.). This is consistent with the number and speed of the end impacts for the old and new realization 3 (Table 5.3-4 and Table 5.3-72, respectively). The most important difference between the end-impact parameters for the two realization 3 simulations is not in the impact speed but in the impact angle. The new realization 3 is (in a sharp contrast to the old one) characterized by a proportionally large number of small-angle impacts, generally less than 0.5 degree. Moreover, all the high-speed impacts (with one exception) are small-angle impacts (Table 5.3-72). The reason for this is that in spite of the 30 percent PGV increase in the vertical direction, the new vertical ground motion time history is more favorable to small-angle impacts. For example, the new ground motion 4 has only two vertical velocity peaks exceeding 2 *m/s*, while the old one has six (Figure 5.3-13).

The similar arguments are applicable for realization 4. According to Figure 5.3-14, the ground motion in the longitudinal direction is more intense for the new realization 4, which is consistently accompanied with a somewhat larger number of high-speed impacts (Table 5.3-5 and Table 5.3-73). Nonetheless, the new vertical ground motion time history (contrary to the old one) rarely exceeds 1 *m/s*. Consequently, almost all high-speed end impacts for the new realization 4 are small-angle impacts.

This has important repercussions on the contribution to damaged area from waste package-waste package impacts. Waste package-waste package impacts are the dominant contribution to damaged area and damaged area decreases significantly between the 0 and 1 degree impact angles (Tables 5.3-56 and 5.3-57). For example, according to Table 5.3-56, the damaged area corresponding to a 3.5 *m/s* end impact at 0.2 degree and 0.8 degree is 0.0268 m^2 and 0.0521 m^2, respectively. The damaged areas corresponding to small-angle impacts are also characterized by a larger extension in the circumferential direction (see Tables 5.3-56 and 5.3-57), which results in more damage areas that are either not taken into account ("NC") or not fully taken into account ("X 0.5") (see discussion in Section 5.3.1.2). The sensitivity of damaged area to small

impact angles leads to a conservative approach in the impact-angle estimate to ensure a reasonable conservatism of the results: impact angles are rounded up with 0.1 degree accuracy. Finally, this discussion elucidates a subtle interaction between the longitudinal and vertical ground motions that affects the magnitude of the damaged area change and that is not obvious from the data in Table 5.3-71.

The sensitivity of damaged area to small impact angle also led to an investigation of an alternate interpolation scheme that is discussed in the next Section (5.3.8). This alternate interpolation scheme uses the damage for 1-degree impacts as the basis for determining damaged area from small angle impacts. More specifically, if the impact angle is between 0 degrees and 1 degree, then the damaged area is (conservatively) set equal to the damaged area for a 1-degree impact. The damaged areas for Realizations 3, 4, 6, and 15 have been reanalyzed with this new interpolation scheme (BSC 2004 [DIRS 170843], Attachment II). A comparison of Table II-8 in *Alternative Damaged Area Evaluation for Waste Package Exposed to Vibratory Ground Motion* (BSC 2004 [DIRS 170843]) with Table 5.3-79 confirms the assertion that the low impact angles for the high-speed impacts are the main factor behind changes in damaged areas caused by the new ground motions at the 2.44 m/s PGV level.

The results from this study support the data in Tables 5.3-24 and 5.3-25 that are the basis for the waste package damage abstraction in the seismic scenario class. The results from this supplemental study are not used directly in the abstraction process.

5.3.8 Alternate Interpolation for Waste Package-to-Waste Package Damage

5.3.8.1 Alternate Interpolation for the 2.44 m/s PGV Level

This section presents the damaged area on the OCB resulting from impacts between adjacent waste packages in the longitudinal (along the tunnel) direction. This damaged area is based on (1) the kinematic data that define the speed, location and angle of end impacts from the simulations of vibratory ground motion, with (2) the damaged areas from individual end impact calculations presented in Tables 5.3-56 and 5.3-57, and (3) the alternate interpolation scheme for small angle impacts.

The calculation of damaged area for multiple end impacts is summarized in Tables 5.3-80 through 5.3-94. The "time" presented in the second column is the time of impact. The impact speed (the third column) is the relative speed between the longitudinal boundary (representing the neighboring waste package) and the waste package (i.e., its trunnion sleeve) node in the impact region. The impact angle presented in the fourth column defines inclination of the waste package with respect to the longitudinal boundary; the change in the definition of the angles between zero and one degree (Assumption 3.18) is indicated by the arrow in the fourth column. For example, see the notation "0.5→1.0" in Table 5.3-81.

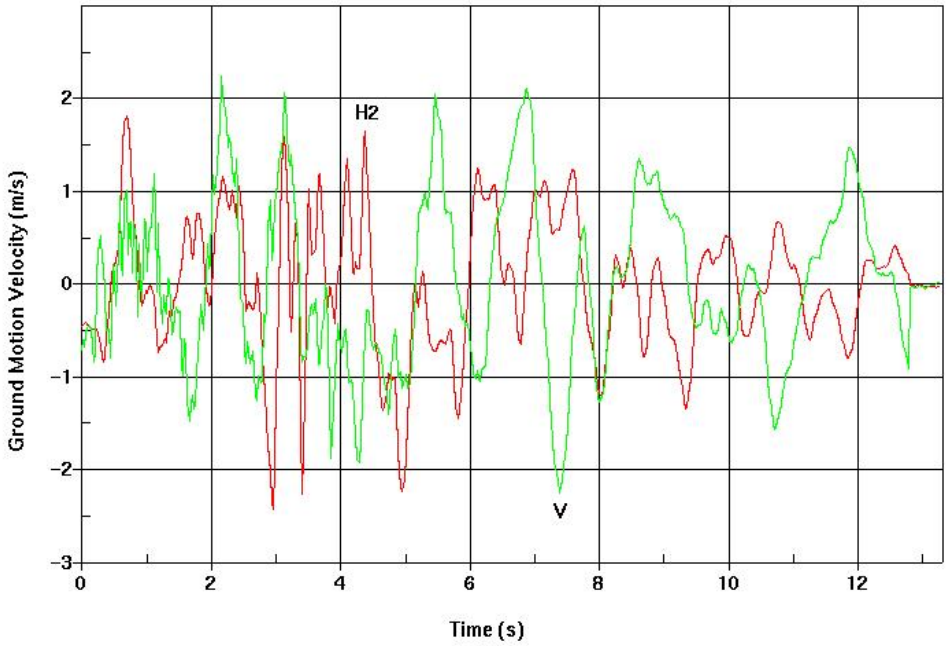

(a)

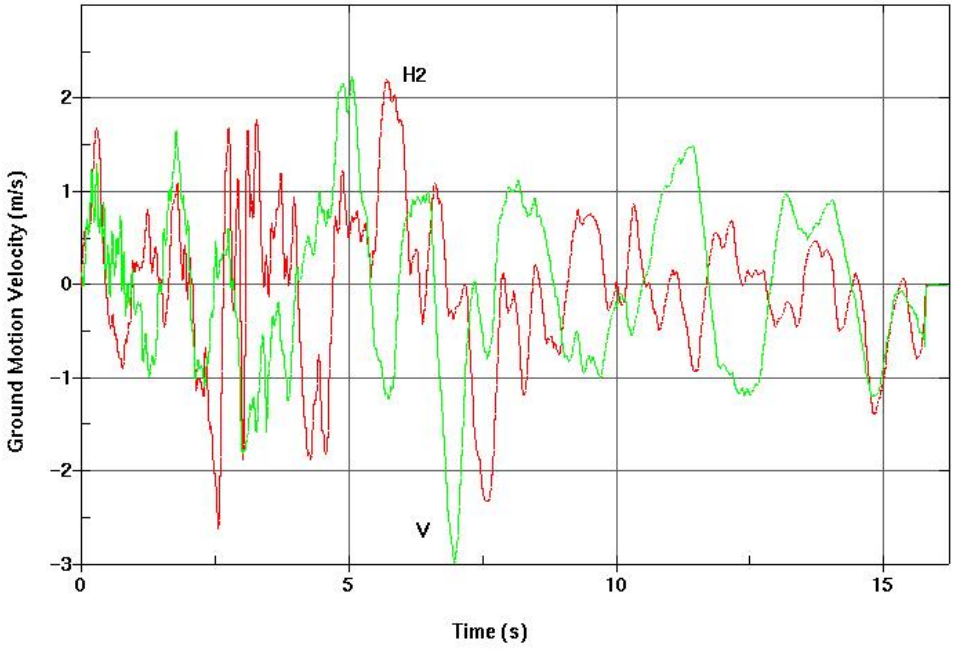

(b)

Source: BSC 2004 [DIRS 168385], Figure 6.3-2.

NOTE: (a) old; (b) new; Time in seconds.

Figure 5.3-13. Velocity Time History of Ground Motion 4 (from Realization 3) For Two Ground Motion Sets

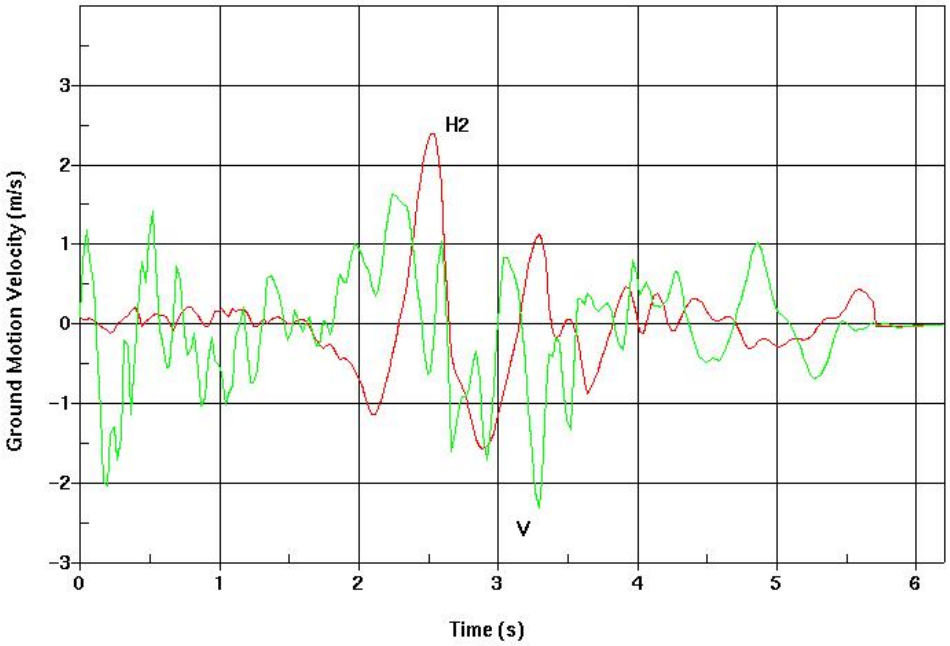

(a)

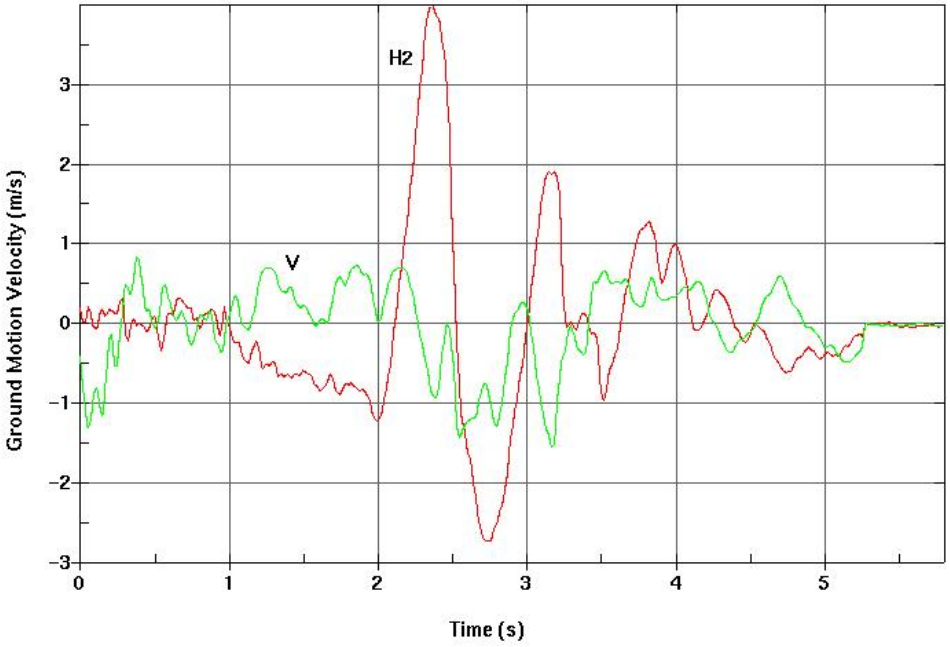

(b)

Source: BSC 2004 [DIRS 168385], Figure 6.3-3.

NOTE: (a) old; (b) new; time in seconds.

Figure 5.3-14. Velocity Time History of Ground Motion 8 (from Realization 4) For Two Ground Motion Sets

Table 5.3-80. End-Impact Parameters and Damaged Area for Realization 1 at the 2.44 m/s PGV Level

Impact Location	Time (s)	Speed (m/s)	Angle (degree)	Damaged Area (m^2)	
				80% Yield Strength	90% Yield Strength
F 8	6.025	1.3	1.0	0.0089	0.0046
C 10	4.750	1.0	1.5	0.0031X0.5	0.0017X0.5
C 11	4.875	1.5	1.3	0.0122	0.0063
Total				0.023	0.012

Source: BSC 2004 [DIRS 170843], Table 6.1.2-1.

Table 5.3-81. End-Impact Parameters and Damaged Area for Realization 2 at 2.44 m/s PGV Level

Impact Location	Time (s)	Speed (m/s)	Angle (degree)	Damaged Area (m^2)	
				80% Yield Strength	90% Yield Strength
F	0.750	1.2	0	0	0
F 8	3.150	1.8	0.5→1.0	0.0183	0.0093
F 9	5.000	1.5	1.0	0.0127X0.5	0.0065X0.5
Total				0.025	0.013

Source: BSC 2004 [DIRS 170843], Table 6.1.2-2.

Table 5.3-82. End-Impact Parameters and Damaged Area for Realization 3 at 2.44 m/s PGV Level

Impact Location	Time (s)	Speed (m/s)	Angle (degree)	Damaged Area (m^2)	
				80% Yield Strength	90% Yield Strength
F 1	6.050	1.3	1.3	0.0086	0.0045
F 6	3.500	3.9	3.4	0.0771	0.0374
F 9	0.675	1.5	1.1	0.0125	0.0064
F 11	3.100	2.4	0.9→1.0	0.0324	0.0132
C 4	0.975	1.1	1.6	0.0048	0.0026
C 6	2.625	1.1	1.6	0.0048 NC	0.0026 NC
C 7	3.225	3.6	0.9→1.0	0.0631	0.0192
C 8	4.575	1.5	1.6	0.0117 NC	0.0060 NC
C 8	7.350	1.1	1.1	0.0051 NC	0.0027 NC
Total				0.20	0.083

Source: BSC 2004 [DIRS 170843], Table 6.1.2-3.

Table 5.3-83. End-Impact Parameters and Damaged Area for Realization 4 at 2.44 m/s PGV Level

Impact Location	Time (s)	Speed (m/s)	Angle (degree)	Damaged Area (m^2)	
				80% Yield Strength	90% Yield Strength
F 3	2.400	1.9	1.0	0.0202	0.0103
F 9	2.775	2.5	4.1	0.0307	0.0162
C 9	2.650	2.6	2.9	0.0354 NC	0.0166 NC
C 9	2.700	3.5	4.0	0.0650	0.0343
Total				0.12	0.061

Source: BSC 2004 [DIRS 170843], Table 6.1.2-4.

Table 5.3-84. End-Impact Parameters and Damaged Area for Realization 5 at 2.44 m/s PGV Level

Impact Location	Time (s)	Speed (m/s)	Angle (degree)	Damaged Area (m^2)	
				80% Yield Strength	90% Yield Strength
F 2	0.425	1.6	1.2	0.0142 NC	0.0073 NC
F 2	2.025	2.0	1.7	0.0201 NC	0.0102 NC
F 2	2.075	4.2	1.4	0.0836 NC	0.0275 NC
F 3	3.425	1.3	2.9	0.0068 NC	0.0036 NC
F 3	5.025	1.8	3.0	0.0137 NC	0.0070 NC
F 3	5.075	4.4	2.5	0.0947	0.0385
F 3	5.900	1.3	1.0	0.0089 NC	0.0046 NC
F 9	1.325	1.2	1.7	0.0064	0.0034
F 9	2.500	1.0	3.8	0.0022 NC	0.0013 NC
C 2	3.125	1.2	0.2→1.0	0.0071	0.0037
C 3	0.800	1.2	1.7	0.0064X0.5	0.0034X0.5
C 4	1.650	1.7	2.9	0.0125	0.0064
C 9	2.325	2.4	4.7	0.0262	0.0145
C 11	0.200	1.4	0.2→1.0	0.0108	0.0056
Total				0.16	0.074

Source: BSC 2004 [DIRS 170843], Table 6.1.2-5.

Table 5.3-85. End-Impact Parameters and Damaged Area for Realization 6 at 2.44 m/s PGV Level

Impact Location	Time (s)	Speed (m/s)	Angle (degree)	Damaged Area (m^2)	
				80% Yield Strength	90% Yield Strength
F 4	1.950	2.5	1.4	0.0344	0.0140
F 4	2.600	2.4	0.5→1.0	0.0324 NC	0.0132 NC
F 8	1.525	1.9	1.0	0.0202X0.5	0.0103X0.5
F 9	1.100	2.4	1.5	0.0315	0.0134
F 9	3.025	1.9	1.6	0.0187 NC	0.0095 NC
C 9	3.125	4.0	2.7	0.0692	0.0300
C 9	2.750	2.9	0.9→1.0	0.0452 NC	0.0157 NC
Total				0.15	0.063

Source: BSC 2004 [DIRS 170843], Table 6.1.2-6.

Table 5.3-86. End-Impact Parameters and Damaged Area for Realization 7 at 2.44 m/s PGV Level

Impact Location	Time (s)	Speed (m/s)	Angle (degree)	Damaged Area (m^2)	
				80% Yield Strength	90% Yield Strength
F 2	2.350	1.4	0.4→1.0	0.0108	0.0056
F 9	3.700	2.7	0.5→1.0	0.0401	0.0147
F 10	2.925	2.1	2.5	0.0209 NC	0.0103 NC
C	3.150	2.2	0	0.0024	0.0024
C 3	4.150	1.2	0.8	0.0056 NC	0.0029 NC
C 3	4.200	4.5	0.4	0.0538	0.0265
C 8	2.775	2.4	3.0	0.0290	0.0139
Total				0.14	0.063

Source: BSC 2004 [DIRS 170843], Table 6.1.2-7.

The initial velocity components were not specified properly for Realization 8 (see discussion in Section 5.3.2). Consequently, the results from this realization are not included in Tables 5.3-16, 5.3-22, 5.3-94, 5.3-95, and 5.3-96 that summarize the results at the 2.44 m/s PGV level.

Table 5.3-87. End-Impact Parameters and Damaged Area for Realization 9 at 2.44 m/s PGV Level

Impact Location	Time (s)	Speed (m/s)	Angle (degree)	Damaged Area (m2)	
				80% Yield Strength	90% Yield Strength
F 3	0.800	1.5	1.7	0.0116	0.0059
F 3	7.075	1.0	2.4	0.0027 NC	0.0016 NC
F 5	2.625	1.7	2.7	0.0129	0.0066
F 8	1.575	2.8	4.5	0.0408	0.0226
F 9	2.250	1.6	5.0	0.0072 NC	0.0038 NC
F 9	2.325	1.1	4.1	0.0021 NC	0.0013 NC
F 10	3.950	1.8	1.4	0.0174	0.0089
C 8	1.375	1.4	2.6	0.0086	0.0045
C 9	1.925	1.7	4.2	0.0098X0.5	0.0051X0.5
C 10	2.450	2.2	3.8	0.0210	0.0107
Total				0.12	0.062

Source: BSC 2004 [DIRS 170843], Table 6.1.2-9.

Table 5.3-88. End-Impact Parameters and Damaged Area for Realization 10 at 2.44 m/s PGV Level

Impact Location	Time (s)	Speed (m/s)	Angle (degree)	Damaged Area (m^2)	
				80% Yield Strength	90% Yield Strength
F 3	5.425	1.1	2.7	0.0041	0.0022
C 3	5.050	1.5	0.3→1.0	0.0127	0.0065
C 3	5.175	1.6	3.8	0.0094 NC	0.0049 NC
Total				0.017	0.0087

Source: BSC 2004 [DIRS 170843], Table 6.1.2-10.

Table 5.3-89. End-Impact Parameters and Damaged Area for Realization 11 at 2.44 m/s PGV Level

Impact Location	Time (s)	Speed (m/s)	Angle (degree)	Damaged Area (m^2)	
				80% Yield Strength	90% Yield Strength
F 6	4.150	1.7	1.5	0.0154	0.0079
F 10	1.275	1.5	0.3→1.0	0.0127 NC	0.0065 NC
F 10	2.125	1.6	1.7	0.0133	0.0068
C 3	0.975	1.1	0.5→1.0	0.0052	0.0027
C 8	3.400	1.6	1.9	0.0129 NC	0.0066 NC
C 9	2.000	1.7	1.6	0.0152 NC	0.0078 NC
C 9	2.225	2.8	1.3	0.0425	0.0158
Total				0.076	0.033

Source: BSC 2004 [DIRS 170843], Table 6.1.2-11.

Table 5.3-90. End-Impact Parameters and Damaged Area for Realization 12 at 2.44 m/s PGV Level

Impact Location	Time (s)	Speed (m/s)	Angle (degree)	Damaged Area (m^2)	
				80% Yield Strength	90% Yield Strength
F 3	6.400	1.1	0.7→1.0	0.0052	0.0027
F 8	5.950	3.0	0.4→1.0	0.0478	0.0162
F 9	3.575	1.1	0.8→1.0	0.0052 NC	0.0027 NC
C 3	1.025	2.2	0.5→1.0	0.0272	0.0122
C 4	5.825	2.2	0.2→1.0	0.0272X0.5	0.0122X0.5
C 4	6.175	1.0	1.7	0.0030 NC	0.0017 NC
C 9	3.775	2.3	0.8→1.0	0.0298	0.0127
Total				0.12	0.050

Source: BSC 2004 [DIRS 170843], Table 6.1.2-12.

Table 5.3-91. End-Impact Parameters and Damaged Area for Realization 13 at 2.44 m/s PGV Level

Impact Location	Time (s)	Speed (m/s)	Angle (degree)	Damaged Area (m^2)	
				80% Yield Strength	90% Yield Strength
F 4	2.300	1.9	0.6→1.0	0.0202	0.0103
C 3	2.025	1.2	0.5→1.0	0.0071 NC	0.0037 NC
C 3	2.450	2.0	3.2	0.0159	0.0081
C 3	7.625	1.1	0.9→1.0	0.0052 NC	0.0027 NC
C 9	9.875	1.1	0.7→1.0	0.0052	0.0027
Total				0.041	0.021

Source: BSC 2004 [DIRS 170843], Table 6.1.2-13.

Table 5.3-92. End-Impact Parameters and Damaged Area for Realization 14 at 2.44 m/s PGV Level

Impact Location	Time (s)	Speed (m/s)	Angle (degree)	Damaged Area (m^2)	
				80% Yield Strength	90% Yield Strength
F 2	2.775	1.4	0.2→1.0	0.0108	0.0056
F 3	3.925	1.0	0.6→1.0	0.0033	0.0018
C 10	4.450	1.2	0.2→1.0	0.0071	0.0037
Total				0.021	0.011

Source: BSC 2004 [DIRS 170843], Table 6.1.2-14.

Table 5.3-93. End-Impact Parameters and Damaged Area for Realization 15 at 2.44 m/s PGV Level

Impact Location	Time (s)	Speed (m/s)	Angle (degree)	Damaged Area (m^2)	
				80% Yield Strength	90% Yield Strength
F 8	1.125	2.0	1.7	0.0201	0.0102
Total				0.020	0.010

Source: BSC 2004 [DIRS 170843], Table 6.1.2-15.

Table 5.3-94 presents a summary of Tables 5.3-83 through 5.3-94, except for Realization 8.

Table 5.3-94. Damaged Area from End Impacts (Waste Package-Waste Package Interaction) at 2.44 m/s PGV Level

Realization	Ground Motion	Damaged Area (m^2; % of total OCB area)	
		80% Yield Strength	90% Yield Strength
1	7	0.023; 0.082%	0.012; 0.043%
2	16	0.025; 0.089%	0.013; 0.046%
3	4	0.20; 0.71%	0.083; 0.29%
4	8	0.12; 0.43%	0.061; 0.22%
5	11	0.16; 0.57%	0.074; 0.26%
6	1	0.15; 0.53%	0.063; 0.22%
7	2	0.14; 0.50%	0.063; 0.22%

Table 5.3-94. Damaged Area from End Impacts (Waste Package-Waste Package Interaction) at 2.44 m/s PGV Level (Continued)

Realization	Ground Motion	Damaged Area (m^2; % of total OCB area)	
		80% Yield Strength	90% Yield Strength
9	10	0.12; 0.43%	0.062; 0.22%
10	9	0.017; 0.060%	0.0087; 0.031%
11	5	0.076; 0.27%	0.033; 0.12%
12	6	0.12; 0.43%	0.050; 0.18%
13	12	0.041; 0.15%	0.021; 0.074%
14	14	0.021; 0.074%	0.011; 0.039%
15	3	0.020; 0.071%	0.010; 0.035%

Source: BSC 2004 [DIRS 170843], Table 6.1.2-16.

NOTE: OCB stands for the OCB; total OCB area is 28.2 m^2 (see calculation in Section 5.3.1.1 of this report).

5.3.8.2 Cumulative Damage with the Alternate Interpolation

The waste package-to-waste package, waste package-pallet, and cumulative damaged areas characterizing the 14 different realizations for the 2.44 m/s PGV level ground motions are summarized in Table 5.3-95, based on the alternate interpolation scheme. The waste package-pallet damaged areas are identical with those in Table 5.3-96.

A summary of the cumulative damaged areas presented in Table 5.3-94 and is provided in Table 5.3-96) (labeled "New" in Table 5.3-96) and Table 5.3-22 (labeled "Old" in Table 5.3-96). Comparing the results reveals that while the change in the cumulative damaged area is significant in some low-damage realizations (most notably realizations 2, 12, 13, and 14), the increase of the mean damaged area due to Assumption 3.18 is 10 percent and 7 percent for the lower and upper damage threshold, respectively. The maximum damaged area is changed only for the lower damage threshold, and even that increase (from 0.20 percent to 0.21 percent of the total OCB surface area) is somewhat exaggerated due to the rounding off to two significant digits. In conclusion, the alternate interpolation technique has little impact on the cumulative damaged areas at the 2.44 m/s PGV level.

Table 5.3-95. Damaged Area from Vibratory Ground Motion at the 2.44 m/s PGV Level Based on Alternate Interpolation Scheme

Realization	Ground Motion	Damaged Area (m^2; % of total OCB area)					
		WP-Pallet Interaction		WP-WP Interaction		Cumulative	
		80% Yield Strength	90% Yield Strength	80% Yield Strength	90% Yield Strength	80% Yield Strength	90% Yield Strength
1	7	0.0029; 0.010%	0.0014; 0.0050%	0.023; 0.082%	0.012; 0.043%	0.026; 0.092%	0.013; 0.046%
2	16	0; 0	0; 0	0.025; 0.089%	0.013; 0.046%	0.025; 0.089%	0.013; 0.046%
3	4	0.0050; 0.018%	0; 0	0.20; 0.71%	0.083; 0.29%	0.21; 0.74%	0.083; 0.29%
4	8	0.030; 0.11%	0.0064; 0.023%	0.12; 0.43%	0.061; 0.22%	0.15; 0.53%	0.067; 0.24%
5	11	0.0015; 0.0053	0; 0	0.16; 0.57%	0.074; 0.26%	0.16; 0.57%	0.074; 0.26%
6	1	0.025; 0.089%	0.0028; 0.0099%	0.15; 0.53%	0.063; 0.22%	0.18; 0.64%	0.066; 0.23%
7	2	0.017; 0.060%	0; 0	0.14; 0.50%	0.063; 0.22%	0.16; 0.57%	0.063; 0.22%
9	10	0.0035; 0.012%	0; 0	0.12; 0.43%	0.062; 0.22%	0.12; 0.43%	0.062; 0.22%
10	9	0; 0	0; 0	0.017; 0.060%	0.0087; 0.031%	0.017; 0.060%	0.0087; 0.031%
11	5	0.012; 0.043%	0.0037; 0.013%	0.076; 0.27%	0.033; 0.12%	0.088; 0.31%	0.037; 0.13%
12	6	0.0039; 0.014%	0; 0	0.12; 0.43%	0.050; 0.18%	0.12; 0.43%	0.050; 0.18%
13	12	0; 0	0; 0	0.041; 0.15%	0.021; 0.074%	0.041; 0.15%	0.021; 0.074%
14	14	0.010; 0.035%	0.0043; 0.015%	0.021; 0.074%	0.011; 0.039%	0.031; 0.11%	0.015; 0.053%
15	3	0.0078; 0.028%	0.0015; 0.0053%	0.020; 0.071%	0.010; 0.035%	0.028; 0.099%	0.012; 0.043%

Source: BSC 2004 [DIRS 170843], Table 6.1.3-1.

NOTE: OCB stands for the OCB; total OCB area is 28.2 m^2 (Section 5.3.1.1 of this report).

WP = waste package

Table 5.3-96. Comparison of Cumulative Damaged Areas for Two Interpolation Schemes at 2.44 m/s PGV Level

Realization	Ground Motion	Cumulative Damaged Area (m^2; % of total OCB area)					
		80% Yield Strength			90% Yield Strength		
		Old	New	Increase (%)	Old	New	Increase (%)
1	7	0.026; 0.092%	0.026; 0.092%	0.	0.013; 0.046%	0.013; 0.046%	0.
2	16	0.017; 0.060%	0.025; 0.089%	47.	0.0089; 0.032%	0.013; 0.046%	46.
3	4	0.20; 0.71%	0.21; 0.74%	5.	0.083; 0.29%	0.083; 0.29%	0.
4	8	0.15; 0.53%	0.15; 0.53%	0.	0.067; 0.24%	0.067; 0.24%	0.
5	11	0.15; 0.53%	0.16; 0.57%	7.	0.066; 0.23%	0.074; 0.26%	12.
6	1	0.18; 0.64%	0.18; 0.64%	0.	0.066; 0.23%	0.066; 0.23%	0.
7	2	0.13; 0.46%	0.16; 0.57%	23.	0.057; 0.20%	0.063; 0.22%	11.
9	10	0.12; 0.43%	0.12; 0.43%	0.	0.062; 0.22%	0.062; 0.22%	0.
10	9	0.014; 0.050%	0.017; 0.060%	21.	0.0071; 0.025%	0.0087; 0.031%	6.
11	5	0.086; 0.30%	0.088; 0.31%	2.	0.036; 0.13%	0.037; 0.13%	3.
12	6	0.077; 0.27%	0.12; 0.43%	56.	0.036; 0.13%	0.050; 0.18%	39.
13	12	0.032; 0.11%	0.041; 0.15%	28.	0.016; 0.057%	0.021; 0.074%	31.
14	14	0.016; 0.057%	0.031; 0.11%	94.	0.0072; 0.026%	0.015; 0.053%	108.
15	3	0.028; 0.099%	0.028; 0.099%	0.	0.012; 0.043%	0.012; 0.043%	0.

Source: BSC 2004 [DIRS 170843], Table 6.1.3-2.

NOTE: OCB stands for the OCB; total OCB area is 28.2 m^2 (Section 5.3.1.1 of this report).

5.3.8.3 Alternate Interpolation for the 5.35 m/s PGV Level

This section presents the damaged area on the OCB resulting from impacts between adjacent waste packages in the longitudinal (along the tunnel) direction. This damaged area is based on (1) the kinematic data at the 5.35 m/s PGV level that define the speed, location and angle of end impacts from the simulations of vibratory ground motion, (2) the damaged areas from individual end impact calculations presented in Tables 5.3-56 and 5.3-57, and (3) the alternate interpolation scheme for small angle impacts (Assumption 3.18). The calculation of damaged area for multiple end impacts is summarized in Tables 5.3-97 through 5.3-110.

Table 5.3-97. End-Impact Parameters and Damaged Area for Realization 1 at 5.35 m/s PGV Level

Impact Location	Time (s)	Speed (m/s)	Angle (degree)	Damaged Area (m^2)	
				80% Yield Strength	90% Yield Strength
F 3	4.825	2.0	2.6	0.0176	0.0090
F 7	2.725	1.4	2.7	0.0085	0.0044
F 8	4.025	1.0	7.2	0.0013 NC	0.0010 NC
F 8	7.100	1.2	3.7	0.0047	0.0025
F 9	2.350	1.0	3.9	0.0021	0.0013
C 2	4.900	4.5	5.3	0.1005	0.0556
C 3	5.400	1.8	1.0	0.0183 NC	0.0093 NC
C 7	2.100	1.8	2.1	0.0158	0.0080
C 10	4.525	1.2	6.6	0.0033	0.0020
C 11	6.900	1.3	4.0	0.0056	0.0030
Total				0.16	0.086

Source: BSC 2004 [DIRS 170843], Table 6.2.2-1.

Table 5.3-98. End-Impact Parameters and Damaged Area for Realization 2 at 5.35 m/s PGV Level

Impact Location	Time (s)	Speed (m/s)	Angle (degree)	Damaged Area (m^2)	
				80% Yield Strength	90% Yield Strength
F 2	3.500	1.1	2.8	0.0040X0.5	0.0022X0.5
F 3	4.975	1.9	1.0	0.0202	0.0103
F 9	0.500	1.6	0.3→1.0	0.0146	0.0074
F 12	2.300	1.1	1.0	0.0052	0.0027
C 1	1.600	1.4	0.2→1.0	0.0108	0.0056
C 3	4.675	1.3	0.6→1.0	0.0089	0.0046
C 7	3.725	1.3	1.0	0.0089	0.0046
Total				0.071	0.036

Source: BSC 2004 [DIRS 170843], Table 6.2.2-2.

Table 5.3-99. End-Impact Parameters and Damaged Area for Realization 3 at 5.35 m/s PGV Level

Impact Location	Time (s)	Speed (m/s)	Angle (degree)	Damaged Area (m^2)	
				80% Yield Strength	90% Yield Strength
F 1	1.225	1.3	1.7	0.0082 NC	0.0042 NC
F 1	2.650	2.4	1.4	0.0317	0.0133
F 4	5.600	3.4	1.3	0.0584	0.0196
F 5	0.925	1.7	2.2	0.0140 NC	0.0071 NC
F 5	2.900	3.7	2.5	0.0688 NC	0.0288 NC
F 7	3.100	4.0	3.6	0.0809	0.0404
F 8	6.600	1.5	0.3→1.0	0.0127 NC	0.0065 NC
F 8	8.450	1.7	1.4	0.0156 NC	0.0080 NC
F 9	1.700	2.2	1.7	0.0257X0.5	0.0118X0.5
F 9	4.725	2.2	0.2→1.0	0.0272 NC	0.0122 NC
F 9	9.000	1.1	5.0	0.0026 NC	0.0016 NC
F 10	3.975	2.3	3.2	0.0255	0.0125
F 10	10.275	1.7	3.1	0.0121 NC	0.0062 NC
C 2	1.875	2.7	0.8→1.0	0.0401	0.0147 NC
C 3	0.375	2.5	2.8	0.0325 NC	0.0151
C 3	3.825	2.5	0.4→1.0	0.0349 NC	0.0137 NC
C 3	8.650	2.0	1.3	0.0177 NC	0.0090 NC
C 4	6.750	1.7	5.2	0.0081 NC	0.0043 NC
C 5	6.075	1.5	0.6→1.0	0.0127 NC	0.0065 NC
C 6	6.950	1.3	1.9	0.0079 NC	0.0041 NC
C 7	1.350	1.1	1.8	0.0047 NC	0.0025 NC
C 7	2.825	4.7	1.4	0.1064	0.0357
C 7	7.300	1.8	4.8	0.0095 NC	0.0049 NC
C 8	1.525	1.0	1.4	0.0031 NC	0.0017 NC
C 8	5.425	1.4	1.0	0.0108 NC	0.0056 NC
C 8	9.825	1.5	2.4	0.0105 NC	0.0054 NC
C 9	4.125	2.4	2.5	0.0299 NC	0.0137 NC
C 10	2.150	1.3	1.9	0.0079 NC	0.0041 NC
C 10	3.200	2.2	1.5	0.0261 NC	0.0119 NC
C 10	4.100	2.1	2.6	0.0206 NC	0.0098 NC
C 11	2.225	1.2	2.2	0.0060 NC	0.0031 NC
C 11	3.000	3.8	2.4	0.0715	0.0293
C 11	5.900	1.2	4.7	0.0038 NC	0.0021 NC
C 11	6.150	1.8	0.6→1.0	0.0183 NC	0.0093 NC
Total				0.43	0.17

Source: BSC 2004 [DIRS 170843], Table 6.2.2-3.

Table 5.3-100. End-Impact Parameters and Damaged Area for Realization 4 at 5.35 m/s PGV Level

Impact Location	Time (s)	Speed (m/s)	Angle (degree)	Damaged Area (m^2)	
				80% Yield Strength	90% Yield Strength
F 3	2.125	3.0	2.5	0.0478	0.0207
F 5	2.875	1.5	2.4	0.0105	0.0054
F 6	2.925	1.6	3.0	0.0109 NC	0.0056 NC
F 7	3.000	1.4	2.0	0.0095 NC	0.0049 NC
F 7	3.725	2.2	1.3	0.0266	0.0120
F 12	3.325	1.2	7.0	0.0033	0.0020
C 2	1.250	1.2	0.4→1.0	0.0071	0.0037
C 5	2.475	1.9	4.6	0.0110	0.0057
C 5	3.250	1.7	6.1	0.0082 NC	0.0045 NC
C 6	**2.575**	**1.2**	**3.6**	**0.0048X0.5**	**0.0026X0.5**
C 8	**1.150**	**1.3**	**0.2→1.0**	**0.0089**	**0.0046**
Total				0.12	0.055

Source: BSC 2004 [DIRS 170843], Table 6.2.2-4.

Table 5.3-101. End-Impact Parameters and Damaged Area for Realization 5 at 5.35 m/s PGV Level

Impact Location	Time (s)	Speed (m/s)	Angle (degree)	Damaged Area (m^2)	
				80% Yield Strength	90% Yield Strength
F	3.675	1.8	0	0	0
F 1	1.925	2.0	4.1	0.0134	0.0069
F 1	4.850	1.4	1.6	0.0100 NC	0.0052 NC
F 5	1.300	2.7	0.9→1.0	0.0401	0.0147
F 6	2.700	1.8	1.7	0.0167 NC	0.0085 NC
F 6	5.000	1.2	0.4→1.0	0.0071 NC	0.0037 NC
F 7	3.425	1.4	2.6	0.0086	0.0045
F 10	0.350	2.1	1.6	0.0232	0.0111
F 12	5.900	1.3	3.0	0.0067X0.5	0.0035X0.5
C 2	0.525	1.6	1.3	0.0140X0.5	0.0072X0.5
C 3	5.375	1.7	0.1→1.0	0.0165	0.0084
C 4	0.825	1.2	0.7→1.0	0.0071 NC	0.0037 NC
C 4	3.950	1.2	1.0	0.0071X0.5	0.0037X0.5
C 5	3.000	1.9	2.4	0.0166	0.0085
C 8	1.650	3.4	0.8→1.0	0.0580	0.0182
C 8	2.300	1.5	1.3	0.0122 NC	0.0063 NC
C 11	6.225	1.3	2.0	0.0078	0.0041
C 12	0.100	1.4	0.2→1.0	0.0108	0.0056
C 12	3.125	1.4	0.2→1.0	0.0108 NC	0.0056 NC
Total				0.21	0.089

Source: BSC 2004 [DIRS 170843], Table 6.2.2-5.

Table 5.3-102. End-Impact Parameters and Damaged Area for Realization 6 at 5.35 m/s PGV Level

Impact Location	Time (s)	Speed (m/s)	Angle (degree)	Damaged Area (m^2)	
				80% Yield Strength	90% Yield Strength
F 2	0.950	4.0	1.7	0.0754 NC	0.0264 NC
F 2	2.325	4.4	1.7	0.0933	0.0328
F 3	3.225	1.3	0.1→1.0	0.0089 NC	0.0046 NC
F 6	3.075	2.0	2.0	0.0193	0.0098
F 8	1.775	3.2	2.9	0.0541 NC	0.0246 NC
F 9	1.275	4.4	6.9	0.0863 NC	0.0455 NC
F 9	1.425	1.4	3.3	0.0077 NC	0.0040 NC
F 9	2.125	1.6	1.5	0.0137 NC	0.0070 NC
F 10	0.600	2.9	0.9→1.0	0.0452 NC	0.0157 NC
F 10	2.725	5.0	2.0	0.1200	0.0445
C 1	1.575	3.2	1.1	0.0529 NC	0.0176 NC
C 1	2.650	4.6	1.9	0.1024 NC	0.0374 NC
C 1	2.875	2.5	1.2	0.0347 NC	0.0139 NC
C 3	2.250	6.4	1.7	0.1572	0.0563
C 6	0.700	3.7	0.7→1.0	0.0657X0.5	0.0197X0.5
C 7	4.275	1.3	0.1→1.0	0.0089 NC	0.0046 NC
Total				0.42	0.15

Source: BSC 2004 [DIRS 170843], Table 6.2.2-6.

Table 5.3-103. End-Impact Parameters and Damaged Area for Realization 7 at 5.35 m/s PGV Level

Impact Location	Time (s)	Speed (m/s)	Angle (degree)	Damaged Area (m^2)	
				80% Yield Strength	90% Yield Strength
F	0.325	1.9	0	0	0
F 1	2.400	6.0	8.4	0.1019 NC	0.0466 NC
F 1	4.150	1.8	0.7→1.0	0.0183 NC	0.0093 NC
F 2	4.350	2.3	2.2	0.0275X0.5	0.0126X0.5
F 6	1.700	1.5	1.2	0.0124 NC	0.0063 NC
F 7	4.075	3.4	1.3	0.0584	0.0196
F 9	3.250	3.8	3.7	0.0746 NC	0.0378 NC
F 11	2.175	5.4	1.4	0.1382	0.0472
F 12	2.225	3.1	3.2	0.0511 NC	0.0243 NC
C	2.100	2.0	0	0	0
C 3	2.700	3.3	2.5	0.0568 NC	0.0242
C 3	2.900	1.9	3.3	0.0143 NC	0.0073 NC
C 4	2.000	4.0	0.5→1.0	0.0734	0.0212 NC
C 4	3.675	1.6	0.3→1.0	0.0146 NC	0.0074 NC
C 6	2.325	1.5	8.0	0.0062	0.0038
C 9	3.375	2.3	1.9	0.0280	0.0126
C 10	4.550	2.0	1.5	0.0207 NC	0.0105 NC
C 11	0.900	1.7	1.3	0.0158	0.0081
Total				0.33	0.12

Source: BSC 2004 [DIRS 170843], Table 6.2.2-7.

Table 5.3-104. End-Impact Parameters and Damaged Area for Realization 8 at 5.35 m/s PGV Level

Impact Location	Time (s)	Speed (m/s)	Angle (degree)	Damaged Area (m^2)	
				80% Yield Strength	90% Yield Strength
F	12.075	1.2	0	0	0
F 1	2.925	1.7	6.2	0.0082X0.5	0.0045X0.5
F 2	1.100	1.2	1.9	0.0063 NC	0.0033X0.5
F 3	7.025	1.9	4.0	0.0125 NC	0.0064 NC
F 3	9.300	2.0	1.5	0.0207	0.0105
F 4	1.975	1.7	2.5	0.0133 NC	0.0068 NC
F 4	1.550	1.7	1.6	0.0152 NC	0.0077 NC
F 4	5.375	2.2	6.2	0.0179 NC	0.0099X0.5
F 6	3.425	2.6	3.2	0.0351 NC	0.0169 NC
F 7	2.675	3.5	2.9	0.0634	0.0286
F 8	9.350	2.1	0.3→1.0	0.0247 NC	0.0117 NC
F 9	11.325	1.0	1.5	0.0031 NC	0.0017 NC
F 10	6.475	1.5	0.6→1.0	0.0127 NC	0.0065 NC
F 10	6.775	2.1	1.7	0.0229	0.0110
F 11	4.325	1.6	0.8→1.0	0.0146 NC	0.0074 NC
F 12	3.825	2.0	3.2	0.0159 NC	0.0081
F 12	9.900	1.7	0.2→1.0	0.0165	0.0084 NC
C 1	2.375	2.0	1.3	0.0213 NC	0.0108 NC
C 2	4.450	1.7	2.5	0.0071 NC	0.0038 NC
C 2	5.225	1.2	3.5	0.0049 NC	0.0026 NC
C 2	5.450	1.2	6.5	0.0033 NC	0.0020 NC
C 2	6.900	2.3	1.6	0.0286	0.0127
C 3	2.275	1.2	0.4→1.0	0.0071 NC	0.0037 NC
C 4	2.825	2.2	4.9	0.0185 NC	0.0102 NC
C 4	3.050	3.0	3.2	0.0479	0.0228
C 5	3.075	2.1	3.0	0.0196 NC	0.0098 NC
C 6	4.625	1.2	1.3	0.0068	0.0036
C 8	3.700	3.4	0.6→1.0	0.0580 NC	0.0182 NC
C 9	1.850	4.1	1.2	0.0786	0.0243
C 9	9.500	1.6	2.0	0.0127 NC	0.0065 NC
C 10	2.100	2.2	1.4	0.0263 NC	0.0120 NC
C 10	11.725	1.5	1.6	0.0117 NC	0.0060 NC
C 12	3.375	2.3	1.1	0.0296	0.0127
Total				0.32	0.14

Source: BSC 2004 [DIRS 170843], Table 6.2.2-8.

Table 5.3-105. End-Impact Parameters and Damaged Area for Realization 9 at 5.35 m/s PGV Level

Impact Location	Time (s)	Speed (m/s)	Angle (degree)	Damaged Area (m^2)	
				80% Yield Strength	90% Yield Strength
F 1	1.725	1.7	0.3→1.0	0.0165	0.0084
F 8	3.425	1.1	1.0	0.0052	0.0027
C 4	1.475	1.2	0.1→1.0	0.0071 NC	0.0037 NC
C 4	3.100	1.4	1.3	0.0104	0.0054
C 11	1.900	1.8	3.2	0.0132	0.0068
Total				0.045	0.023

Source: BSC 2004 [DIRS 170843], Table 6.2.2-9.

Table 5.3-106. End-Impact Parameters and Damaged Area for Realization 10 at 5.35 m/s PGV Level

Impact Location	Time (s)	Speed (m/s)	Angle (degree)	Damaged Area (m^2)	
				80% Yield Strength	90% Yield Strength
F 2	1.250	6.5	8.0	0.1079	0.0486
F 4	4.950	2.1	8.0	0.0143 NC	0.0081 NC
F 5	2.450	2.4	1.5	0.0315	0.0134
F 6	0.600	2.5	3.7	0.0312 NC	0.0159 NC
F 12	0.875	3.6	5.8	0.0673	0.0388
F 12	1.675	2.7	6.2	0.0241 NC	0.0132 NC
C 1	1.475	3.8	1.8	0.0701	0.0254
C 1	5.200	3.7	8.0	0.0626 NC	0.0322 NC
C 4	0.475	1.3	0.1→1.0	0.0089 NC	0.0046 NC
C 4	1.300	1.3	8.0	0.0042	0.0026
C 5	0.825	1.8	4.0	0.0114 NC	0.0057 NC
C 5	1.200	2.5	7.1	0.0273	0.0150
C 5	2.200	1.2	4.3	0.0042 NC	0.0023 NC
C 6	0.975	1.0	7.2	0.0013	0.0010
C 11	4.775	2.8	1.8	0.0422X0.5	0.0169X0.5
Total				0.33	0.15

Source: BSC 2004 [DIRS 170843], Table 6.2.2-10.

Table 5.3-107. End-Impact Parameters and Damaged Area for Realization 12 at 5.35 m/s PGV Level

Impact Location	Time (s)	Speed (m/s)	Angle (degree)	Damaged Area (m^2)	
				80% Yield Strength	90% Yield Strength
F	0.275	1.8	0	0	0
F 1	5.775	2.1	4.8	0.0151X0.5	0.0081X0.5
F 1	6.225	1.5	5.9	0.0063 NC	0.0035 NC
F 2	3.750	1.9	4.2	0.0120 NC	0.0062 NC
F 2	5.350	1.4	1.4	0.0103 NC	0.0053 NC
F 2	6.750	1.8	3.4	0.0128X0.5	0.0065X0.5
F 10	1.425	1.2	1.3	0.0068	0.0036
F 12	3.450	2.0	0.6→1.0	0.0221	0.0112
C 3	3.875	1.6	7.2	0.0072	0.0042
C 5	5.600	1.3	5.4	0.0044 NC	0.0025 NC
C 6	1.150	3.5	0.9→1.0	0.0606	0.0187
C 6	3.650	2.2	1.5	0.0261 NC	0.0119 NC
C 7	0.875	2.2	1.5	0.0261 NC	0.0119 NC
C 10	5.125	1.1	2.3	0.0043	0.0024
Total				0.11	0.047

Source: BSC 2004 [DIRS 170843], Table 6.2.2-11.

Table 5.3-108. End-Impact Parameters and Damaged Area for Realization 13 at 5.35 m/s PGV Level

Impact Location	Time (s)	Speed (m/s)	Angle (degree)	Damaged Area (m^2)	
				80% Yield Strength	90% Yield Strength
F 1	7.125	1.2	5.1	0.0035X0.5	0.0020X0.5
F 3	1.075	1.5	0.5→1.0	0.0127 NC	0.0065 NC
F 3	2.275	2.2	3.1	0.0225 NC	0.0111 NC
F 3	4.950	1.1	2.8	0.0040 NC	0.0022 NC
F 4	1.625	2.4	1.4	0.0317	0.0133
F 11	6.350	1.2	0.8→1.0	0.0071X0.5	0.0037X0.5
F 12	9.375	1.7	3.8	0.0106	0.0055
C 2	9.175	1.8	0.2→1.0	0.0183	0.0093
C 3	1.900	1.5	3.9	0.0081	0.0042
C 6	2.475	2.2	2.2	0.0246	0.0116
C 6	2.550	1.0	2.9	0.0025 NC	0.0015 NC
C 6	3.950	2.0	1.2	0.0215 NC	0.0109 NC
C 7	3.900	1.6	1.3	0.0140 NC	0.0072 NC
C 9	0.750	1.1	0.2→1.0	0.0052 NC	0.0027 NC
C 9	1.300	2.2	0.7→1.0	0.0272 NC	0.00122 NC
C 9	1.350	1.4	0.6→1.0	0.0108 NC	0.0056 NC
C 9	2.975	2.4	0.8→1.0	0.0324	0.0132
C 12	10.325	1.4	0.5→1.0	0.0108	0.0056
Total				0.14	0.066

Source: BSC 2004 [DIRS 170843], Table 6.2.2-12.

Table 5.3-109. End-Impact Parameters and Damaged Area for Realization 14 at 5.35 m/s PGV Level

Impact Location	Time (s)	Speed (m/s)	Angle (degree)	Damaged Area (m^2)	
				80% Yield Strength	90% Yield Strength
F 1	7.150	1.3	2.1	0.0077	0.0040
Total				0.0077	0.0040

Source: BSC 2004 [DIRS 170843], Table 6.2.2-13.

Table 5.3-110. End-Impact Parameters and Damaged Area for Realization 15 at 5.35 m/s PGV Level

Impact Location	Time (s)	Speed (m/s)	Angle (degree)	Damaged Area (m^2)	
				80% Yield Strength	90% Yield Strength
F 4	1.075	4.3	3.3	0.0921	0.0426
F 4	0.850	1.5	0.6→1.0	0.0127 NC	0.0065 NC
F 7	0.750	1.5	7.2	0.0062	0.0036
F 7	1.225	1.1	10.0	0.0018 NC	0.0014 NC
F 11	0.025	2.8	0.1→1.0	0.0426	0.0152
C 3	0.150	3.5	0.4→1.0	0.0606	0.0187
C 4	0.500	2.2	0.6→1.0	0.0272 NC	0.0122 NC
C 6*	1.400	8.6	5.2	0.0332	0.0133
C 9	0.925	4.1	2.7	0.0825	0.0353
C 11	0.600	1.6	0.8→1.0	0.0146 NC	0.0074 NC
C 11	1.200	2.4	7.8	0.0235X0.5	0.0128X0.5
C 12	0.325	1.6	1.9	0.0129	0.0066
Total				0.34	0.14

Source: BSC 2004 [DIRS 170843], Table 6.2.2-14.

* NOTE: Trunnion sleeve impacts the invert not the longitudinal boundary

Table 5.3-111 presents a summary of Tables 5.3-97 through 5.3-110. Note that the results for realization 11 are not presented herein since ground motion 5 was not correctly generated.

Table 5.3-111. Damaged Area from End Impacts (Waste Package-Waste Package Interaction) at 5.35 m/s PGV Level Based on Alternate Interpolation Scheme

Realization	Ground Motion	Damaged Area (m^2; % of total OCB area)	
		80% Yield Strength	90% Yield Strength
1	7	0.16; 0.57%	0.086; 0.30%
2	16	0.071; 0.25%	0.036; 0.13%
3	4	0.43; 1.52%	0.17; 0.60%
4	8	0.12; 0.43%	0.055; 0.20%
5	11	0.21; 0.74%	0.089; 0.32%
6	1	0.42; 1.49%	0.15; 0.53%
7	2	0.33; 1.17%	0.12; 0.43%
8	13	0.32; 1.13%	0.14; 0.50%
9	10	0.045; 0.16%	0.023; 0.082%
10	9	0.33; 1.17%	0.15; 0.53%
12	6	0.11; 0.39%	0.047; 0.17%

Table 5.3-111. Damaged Area from End Impacts (Waste Package-Waste Package Interaction) at 5.35 m/s PGV Level Based on Alternate Interpolation Scheme (Continued)

Realization	Ground Motion	Damaged Area (m^2; % of total OCB area)	
		80% Yield Strength	90% Yield Strength
13	12	0.14; 0.50%	0.066; 0.23%
14	14	0.0077; 0.027%	0.0040; 0.014%
15	3	0.34; 1.21%	0.14; 0.50%

Source: BSC 2004 [DIRS 170843], Table 6.2.2-15.

NOTE: OCB stands for the OCB; total OCB area is 28.2 m2 (Section 5.3.1.1 of this report).

5.3.8.4 Cumulative Damage with the Alternate Interpolation

The waste package-to-waste package, waste package-pallet, and cumulative damaged areas characterizing the 13 realizations for the 5.35 m/s PGV level ground motions are summarized in Table 5.3-112, based on the alternate interpolation scheme. The waste package-pallet damaged areas are identical with those in Table 5.3-113.

Shown in Table 5.3-113, it provides a summary of the cumulative damaged areas presented in Table 5.3-111 (labeled "New" in Table 5.3-113) and in Table 5.3-112 (labeled "Old" in Table 5.3-113). Comparing the results reveals that while the change in the cumulative damaged area is significant in some low-damage realizations (most notably realization 9), the increase of the mean damaged area due to Assumption 3.18 is 4 percent and 2 percent for the lower and upper damage threshold, respectively. The maximum damaged area is changed only for the lower damage threshold, from 1.84 percent to 1.88 percent of the total OCB surface area. In conclusion, the alternate interpolation technique has little impact on the cumulative damaged areas at the 5.35 m/s PGV level.

Table 5.3-112. Damaged Area from Vibratory Ground Motion at 5.35 m/s PGV Level Based on Alternate Interpolation Scheme

Realization	Ground Motion	Damaged Area (m^2; % of total OCB area)					
		WP-Pallet Interaction		WP-WP Interaction		Cumulative	
		80% Yield Strength	90% Yield Strength	80% Yield Strength	90% Yield Strength	80% Yield Strength	90% Yield Strength
1	7	0.20; 0.71%	0.17; 0.60%	0.16; 0.57%	0.086; 0.30%	0.36; 1.28%	0.26; 0.92%
3	4	0.096; 0.34%	0.083; 0.29%	0.43; 1.52%	0.17; 0.60%	0.53; 1.88%	0.25; 0.89%
4	8	0.12; 0.43%	0.096; 0.34%	0.12; 0.43%	0.055; 0.20%	0.24; 0.85%	0.15; 0.53%
5	11	0.093; 0.33%	0.071; 0.25%	0.21; 0.74%	0.089; 0.32%	0.30; 1.06%	0.16; 0.57%
6	1	0.046; 0.16%	0.024; 0.085%	0.42; 1.49%	0.15; 0.53%	0.47; 1.67%	0.17; 0.60%
7	2	0.038; 0.13%	0.028; 0.099%	0.33; 1.17%	0.12; 0.43%	0.37; 1.31%	0.15; 0.53%

Table 5.3-112. Damaged Area from Vibratory Ground Motion at 5.35 m/s PGV Level Based on Alternate Interpolation Scheme (Continued)

Realization	Ground Motion	Damaged Area (m^2; % of total OCB area)					
		WP-Pallet Interaction		WP-WP Interaction		Cumulative	
		80% Yield Strength	90% Yield Strength	80% Yield Strength	90% Yield Strength	80% Yield Strength	90% Yield Strength
8	13	0.095; 0.34%	0.068; 0.24%	0.32; 1.13%	0.14; 0.50%	0.42; 1.49%	0.21; 0.74%
9	10	0.0052; 0.018%	0.0035; 0.012%	0.045; 0.16%	0.023; 0.082%	0.050; 0.18%	0.027; 0.096%
10	9	0.16; 0.57%	0.14; 0.50%	0.33; 1.17%	0.15; 0.53%	0.49; 1.74%	0.29; 1.03%
12	6	0.062; 0.22%	0.041; 0.15%	0.11; 0.39%	0.047; 0.17%	0.17; 0.60%	0.088; 0.31%
13	12	0.027; 0.096%	0.018; 0.064%	0.14; 0.50%	0.066; 0.23%	0.17; 0.60%	0.084; 0.30%
14	14	0.020; 0.071%	0.016; 0.057%	0.0077; 0.027%	0.0040; 0.014%	0.028; 0.099%	0.020; 0.071%
15	3	0.0045; 0.016%	0; 0	0.34; 1.21%	0.14; 0.50%	0.34; 1.21%	0.14; 0.50%

Source: BSC 2004 [DIRS 170843], Table 6.2.3-1.

NOTES: OCB stands for the OCB; total OCB area is 28.2 m2 (Section 5.1).

Accuracy of the results (damaged area) due to the waste package-pallet interaction is doubtful (see discussion in BSC 2004 [DIRS 167083], Section 6.5).

WP = waste package

Table 5.3-113. Comparison of Cumulative Damaged Areas from Vibratory Ground Motion at the 5.35 m/s PGV Level

Realization	Ground Motion	Cumulative Damaged Area (m^2; % of total OCB area)					
		80% Yield Strength			90% Yield Strength		
		Old	New	Increase (%)	Old	New	Increase (%)
1	7	0.36; 1.28%	0.36; 1.28%	0.	0.26; 0.92%	0.26; 0.92%	0.
3	4	0.52; 1.84%	0.53; 1.88%	2.	0.25; 0.89%	0.25; 0.89%	0.
4	8	0.23; 0.82%	0.24; 0.85%	4.	0.15; 0.53%	0.15; 0.53%	0.
5	11	0.27; 0.96%	0.28; 1.00%	4.	0.15; 0.53%	0.16; 0.57%	7.
6	1	0.47; 1.67%	0.47; 1.67%	0.	0.17; 0.60%	0.17; 0.60%	0.
7	2	0.36; 1.28%	0.37; 1.31%	2.	0.15; 0.53%	0.15; 0.53%	0.

Table 5.3-113. Comparison of Cumulative Damaged Areas from Vibratory Ground Motion at the 5.35 m/s PGV Level (Continued)

Realization	Ground Motion	Cumulative Damaged Area (m^2; % of total OCB area)					
		80% Yield Strength			90% Yield Strength		
		Old	New	Increase (%)	Old	New	Increase (%)
8	13	0.42; 1.49%	0.42; 1.49%	0.	0.21; 0.74%	0.21; 0.74%	0.
9	10	0.039; 0.14%	0.050; 0.18%	29.	0.021; 0.074%	0.027; 0.096%	29.
10	9	0.49; 1.74%	0.49; 1.74%	0.	0.29; 1.03%	0.29; 1.03%	0.
12	6	0.16; 0.57%	0.17; 0.60%	5.	0.085; 0.30%	0.088; 0.31%	3.
13	12	0.15; 0.53%	0.17; 0.60%	13.	0.071; 0.25%	0.084; 0.30%	4.
14	14	0.028; 0.099%	0.028; 0.099%	0.	0.020; 0.071%	0.020; 0.071%	0.
15	3	0.29; 1.03%	0.34; 1.21%	17.	0.14; 0.50%	0.14; 0.50%	0.

Source: BSC 2004 [DIRS 170843], Table 6.2.3-2.

NOTE: OCB stands for the OCB; total OCB area is 28.2 m2 (Section 5.1).

5.3.8.5 Alternate Interpolation for the 0.384 m/s PGV Level

For the single calculation performed at the 0.384 m/s PGV level of ground motion, there was no contact between the waste package and longitudinal boundary. Consequently, the results of these this calculation are not affected by the alternative interpolation scheme for damage as a function of impact angle.

5.4 CONCLUSIONS

This document provides an integrated overview of the six calculation reports that define the response of the waste package and/or its internals to the vibratory ground motion hazard at the proposed geologic repository at Yucca Mountain, Nevada. This report describes the interrelationship between the various calculations for waste package damage and the use of this information in the seismic scenario class for TSPA. Three key calculation reports describe the potential for mechanical damage to the waste package, fuel assemblies, and cladding from a seismic event (see Table 1-1). Three supporting documents have also been published to investigate sensitivity of damage to various assumptions for the calculations (see Table 1-1).

The purpose of the first two key reports in Table 1-1 is to determine the damaged areas on the waste package from impacts between the waste package and emplacement pallet and from impacts between adjacent waste packages in response to vibratory ground motion. The purpose of the third key report in Table 1-1 is to determine the average and maximum g-loads on the fuel rod assemblies due to impacts between adjacent waste packages. These g-loads define the axial loads on fuel rod cladding, providing the basis for definition of cladding failure during end-to-end impacts of adjacent waste packages.

The calculation of damaged areas on the waste package from impacts between the waste package and emplacement pallet and from impacts between adjacent waste packages is discussed in Sections 5.3.1 through 5.3.4 of this report. At the 2.44 m/s PGV level, the mean cumulative damage to the waste package is 0.310 percent and 0.139 percent of the total surface area for the 80 percent and 90 percent residual stress thresholds, respectively (see Table 5.3-22). At 5.35 m/s PGV level, the mean cumulative damage to the waste package is 1.01 percent and 0.52 percent of the total surface area for the 80 percent and 90 percent residual stress thresholds, respectively (see Table 5.3-55). The mean damaged area at the 80 percent residual stress threshold is approximately twice that at the 90 percent residual stress threshold. All calculations are performed with material properties based on 150°C.

On the other hand, there is an order of magnitude difference in the minimum and maximum damaged areas for a given PGV level and residual stress threshold, as shown in Tables 5.3-22 or 5.3-55. In this situation, the variation in ground motion time history and friction coefficients dominates the uncertainty in damaged area, rather than the variation in residual stress threshold.

There is no damage to the waste package at the 0.384 m/s PGV level, as discussed in Section 5.3.3.

The third key report in Table 1-1 determines the average peak acceleration and the maximum peak acceleration on the fuel rod assemblies in the axial direction due to impacts between adjacent waste packages, as discussed in Section 5.3.5. The average peak acceleration is obtained by averaging the peak values of acceleration time histories of all fuel assemblies. The maximum peak acceleration varies between 75 g's and 701 g's (Table 5.3-65). The average peak acceleration varies between 35 g's to 278 g's (Table 5.3-66). These accelerations form the basis for estimating buckling failure of the cladding due to end-to-end impacts of adjacent waste packages for the seismic scenario class.

The three supplemental analyses in Table 1-1 support the results and conclusions in the three key reports. The rationale and results from the supplemental analyses are as follows:

- It is always necessary to demonstrate that the results from a FE analysis are insensitive to the level of mesh refinement. The mesh refinement study described in Section 5.3.6 provides a supporting document that reports on a detailed mesh refinement study for end-to-end impacts of adjacent waste packages, and demonstrates that the original damaged area calculations in Sections 5.3.1 and 5.3.2 are almost always conservative. This mesh refinement study is described in Section 5.3.6.

  The results presented in Table 5.3-68 (with exception of 0 degree results that are discussed separately in Section 5.3.1.1) indicate that, on average, a mesh refinement of 595 percent (in volume) results in a 36 percent decrease of the damaged area in comparison to the results in Table 5.3-57. The differences in the damaged areas are consistently on the conservative side (larger) in comparison to the results with a coarse mesh. This conclusion is supported by the results for three additional FE calculations with a further refined mesh, which are presented in Tables 5.3-69 and 5.3-70. The results presented in Tables 5.3-69 and 5.3-70 indicated that the mesh refinement between the (first) refined mesh and the (second) very refined mesh results in an average change of

the damaged area value for the lower and upper damage thresholds of 5 percent and 20 percent, respectively. This indicates that the results obtained for the (first) refined mesh are reasonably mesh-insensitive, and that the original damage area calculations are conservative.

- Structural response calculations were based on the most current ground motions available at the time the analyses were performed. However, two aspects of the ground motions (intercomponent variability and spectral conditioning) have changed over time, as explained in Section 1.3.4. Section 5.3.7 evaluates the effect of intercomponent variability and spectral conditioning for ground motions at the 2.44 m/s PGV level, and again demonstrates that the range of damaged area in the original calculations in Section 5.3.1 is conservative.

- The damaged area calculations for end-to-end impacts incorporate a simple interpolation scheme on impact velocity and impact angle. Damage at an impact angle of 0 degrees is substantially less than damage at an impact angle of 1 degree because the impact load is uniformly distributed around the circumference, rather than concentrated at a point. In practice, a 0 degree impact is very unlikely because it requires perfect alignment of waste package centerlines. Section 5.3.8 reanalyzes the damaged areas for end-to-end impacts with an alternate interpolation scheme. This alternate scheme holds damaged area constant at the 1-degree value for impact angles greater than 0 degrees and less than 1 degree.

  This change in interpolation scheme produces only minor changes in total damaged area, in part because multiple impacts at angles greater than 1 degree tend to dominate the total damaged area. For example, a comparison of the cumulative damaged areas presented in Table 5.3-96 reveals that while the change in the cumulative damaged area is significant in some low-damage realizations (most notably realizations 2, 12, 13, and 14), the increase of the mean damaged area due to Assumption 3.18 is 10 percent and 7 percent for the lower and upper damage threshold, respectively. The maximum damaged area is changed only for the lower damage threshold, and even that increase (from 0.20 percent to 0.21 percent of the total OCB surface area) is somewhat exaggerated due to the rounding off to two significant digits. In conclusion, the alternate interpolation technique has little impact on the cumulative damaged areas at the 2.44 m/s PGV level or at the 5.35 m/s PGV level.

INTENTIONALLY LEFT BLANK

6. REFERENCES

6.1 DOCUMENTS CITED

Avallone, E.A. and Baumeister, T., III, eds. 1987. *Marks' Standard Handbook for Mechanical Engineers.* 9th Edition. New York, New York: McGraw-Hill. TIC: 206891. 103508

BSC (Bechtel SAIC Company) 2001. *Repository Design, Waste Package Project 21-PWR Waste Package with Absorber Plates, Sheet 1 of 3, Sheet 2 of 3, and Sheet 3 of 3*. DWG-UDC-ME-000001 REV A. Las Vegas, Nevada: Bechtel SAIC Company. ACC: MOL.20020102.0174. 157812

BSC 2003. *21-PWR Waste Package Side and End Impacts.* 000-00C-DSU0-01000-000-00B. Las Vegas, Nevada: Bechtel SAIC Company. ACC: ENG.20030227.0067. 162293

BSC 2003. *Drop of Waste Package on Emplacement Pallet - A Mesh Study.* 000-00C-DSU0-02200-000-00A. Las Vegas, Nevada: Bechtel SAIC Company. ACC: ENG.20030915.0001. 165497

BSC 2003. *Emplacement Pallet.* 000-MW0-TEP0-00101-000-00A, and -00102-000-00A. 2 Sheets. Las Vegas, Nevada: Bechtel SAIC Company. ACC: ENG.20030205.0007; ENG.20030205.0008. 161520

BSC 2003. *Maximum Accelerations on the Fuel Assemblies of a 21-PWR Waste Package During End Impacts.* 000-00C-DSU0-01100-000-00A. Las Vegas, Nevada: Bechtel SAIC Company. ACC: ENG.20030327.0002. 162602

BSC 2003. *Spatial Distribution of Damage to Waste Package in Aftermath of Vibratory Ground Motion.* 000-00C-WIS0-01100-000-00A. Las Vegas, Nevada: Bechtel SAIC Company. ACC: ENG.20031113.0001. 166247

BSC 2004. *21-PWR Waste Package End Impacts - A Mesh Study.* 000-00C-WIS0-02100-000-00A. Las Vegas, Nevada: Bechtel SAIC Company. ACC: ENG.20040617.0005. 170844

BSC 2004. *Additional Structural Calculations of Waste Package Exposed to Vibratory Ground Motion.* 000-00C-WIS0-01700-000-00A. Las Vegas, Nevada: Bechtel SAIC Company. ACC: ENG.20040318.0011. 168385

BSC 2004. *Additional Structural Calculations of Waste Package Exposed to Vibratory Ground Motion.* 000-00C-WIS0-01700-000-00B. Las Vegas, Nevada: Bechtel SAIC Company. TBV-6834. 171717

BSC 2004. *Alternative Damaged Area Evaluation for Waste Package Exposed to Vibratory Ground Motion.* 000-00C-WIS0-01900-000-00A. Las Vegas, Nevada: Bechtel SAIC Company. ACC: ENG.20040420.0010. 170843

BSC 2004. *D&E / PA/C IED Emplacement Drift Configuration and Environment.* 800-IED-MGR0-00201-000-00B. Las Vegas, Nevada: Bechtel SAIC Company. ACC: ENG.20040326.0001. 168489

BSC 2004. *D&E / PA/C IED Typical Waste Package Components Assembly.* 800-IED-WIS0-00201-000-00E. Las Vegas, Nevada: Bechtel SAIC Company. ACC: ENG.20040517.0007. 169480

BSC 2004. *D&E / PA/C IED Typical Waste Package Components Assembly.* 800-IED-WIS0-00205-000-00D. Las Vegas, Nevada: Bechtel SAIC Company. ACC: ENG.20040518.0001. 169990

BSC 2004. *D&E/PA/C IED Typical Waste Package Components Assembly.* 800-IED-WIS0-00202-000-00C. Las Vegas, Nevada: Bechtel SAIC Company. ACC: ENG.20040517.0008. 169472

BSC 2004. *DOE and Commercial Waste Package System Description Document.* 000-3YD-DS00-00100-000-004. Las Vegas, Nevada: Bechtel SAIC Company. ACC: ENG.20040720.0009. 170803

BSC 2004. *Drift Degradation Analysis.* ANL EBS-MD-000027 REV 03. Las Vegas, Nevada: Bechtel SAIC Company. ACC: DOC.20040915.0010. 166107

BSC 2004. *General Corrosion and Localized Corrosion of WP Outer Barrier.* ANL-EBS-MD-000003, Rev. 02. Las Vegas, Nevada: Bechtel SAIC Company. TBV-6835 169984

BSC 2004. *Multiscale Thermohydrologic Model.* ANL-EBS-MD-000049, Rev. 02. Las Vegas, Nevada: Bechtel SAIC Company. TBV-6420 169565

BSC 2004. *Q-List.* 000-30R-MGR0-00500-000-000 REV 00. Las Vegas, Nevada: Bechtel SAIC Company. ACC: ENG.20040721.0007. 168361

BSC 2004. *Relative Vertical Velocity Between Waste Package and Emplacement Pallet During Vibratory Ground Motion.* 000-00C-WIS0-01800-000-00A. Las Vegas, Nevada: Bechtel SAIC Company. ACC: ENG.20040330.0005. 170850

BSC 2004. *Sampling of Stochastic Input Parameters for Rockfall Calculations and for Structural Response Calculations Under Vibratory Ground Motion.* ANL-EBS-PA-000009 REV 01. Las Vegas, Nevada: Bechtel SAIC Company. ACC: DOC.20040901.0004. 169999

BSC 2004. *Seismic Consequence Abstraction.* MDL-WIS-PA-000003, Rev. 01. Las Vegas, Nevada: Bechtel SAIC Company. 169183

BSC 2004. *Stress Corrosion Cracking of the Drip Shield, the Waste Package Outer Barrier, and the Stainless Steel Structural Material.* ANL-EBS-MD-000005 REV 01 ICN 01. Las Vegas, Nevada: Bechtel SAIC Company. ACC: DOC.20040318.0010. 169042

BSC 2004. *Structural Calculations of Waste Package Exposed to Vibratory Ground Motion.* 000-00C-WIS0-01400-000-00A. Las Vegas, Nevada: Bechtel SAIC Company. ACC: ENG.20040217.0008. 167083

BSC 2004. *Technical Work Plan for: Regulatory Integration Modeling of Drift Degradation, Waste Package and Drip Shield Vibratory Motion and Seismic Consequences.* TWP-MGR-GS-000003 REV 00 ICN 01. Las Vegas, Nevada: Bechtel SAIC Company. ACC: DOC.20040810.0003. 171520

Budnitz, R.J.; Apostolakis, G.; Boore, D.M.; Cluff, L.S.; Coppersmith, K.J.; Cornell, C.A.; and Morris, P.A. 1997. *Recommendations for Probabilistic Seismic Hazard Analysis: Guidance on the Uncertainty and Use of Experts.* NUREG/CR-6372. Two volumes. Washington, D.C.: U.S. Nuclear Regulatory Commission. TIC: 235076; 235074. 103635

Chun, R.; Witte, M.; and Schwartz, M. 1987. *Dynamic Impact Effects on Spent Fuel Assemblies.* UCID-21246. Livermore, California: Lawrence Livermore National Laboratory. ACC: HQX.19881020.0031. 144357

CRWMS (Civilian Radioactive Waste Management) M&O (Management and Operating Contractor) 1998. *Probabilistic Seismic Hazard Analyses for Fault Displacement and Vibratory Ground Motion at Yucca Mountain, Nevada.* Milestone SP32IM3, September 23, 1998. Three volumes. Las Vegas, Nevada: CRWMS M&O. ACC: MOL.19981207.0393. 103731

DeGrassi, G. 1992. Review of the Technical Basis and Verification of Current Analysis Methods Used to Predict Seismic Response of Spent Fuel Storage Racks. NUREG/CR-5912. Washington, D.C.: U.S. Nuclear Regulatory Commission. TIC: 253724. 161539

Dieter, G.E. 1976. *Mechanical Metallurgy.* 2nd Edition. Materials Science and Engineering Series. New York, New York: McGraw-Hill Book Company. TIC: 247879. 118647

Kramer, S.L. 1996. *Geotechnical Earthquake Engineering.* Prentice-Hall International Series in Civil Engineering and Engineering Mechanics. Hall, W.J., ed. Upper Saddle River, New Jersey: Prentice-Hall. TIC: 243891. 103337

McGarr, A. 1984. "Some Applications of Seismic Source Mechanism Studies to Assessing Underground Hazard." *Proceedings of the 1st International Congress on Rockbursts and Seismicity in Mines, Johannesburg, 1982.* Gay, N.C. and Wainwright, E.H., eds. Pages 199-208. Johannesburg, South Africa: South African Institute of Mining and Metallurgy. TIC: 254652. 163996

McGuire, R.K.; Silva, W.J.; and Costantino, C.J. 2001. Technical Basis for Revision of Regulatory Guidance on Design Ground Motions: Hazard- and Risk-Consistent Ground Motion Spectra Guidelines. NUREG/CR-6728. Washington, D.C.: U.S. Nuclear Regulatory Commission. TIC: 251294. 157510

Mecham, D.C., ed. 2004. *Waste Package Component Design Methodology Report.* 000-30R-WIS0-00100-000-002. Las Vegas, Nevada: Bechtel SAIC Company. ACC: ENG.20040713.0003 170673

NRC (U.S. Nuclear Regulatory Commission) 2003. *Yucca Mountain Review Plan, Final Report.* NUREG-1804, Rev. 2. Washington, D.C.: U.S. Nuclear Regulatory Commission, Office of Nuclear Material Safety and Safeguards. TIC: 254568. 163274

Newmark, N.M. and Rosenblueth, E. 1971. *Fundamentals of Earthquake Engineering.* Civil Engineering and Engineering Mechanics Series. Englewood Cliffs, New Jersey: Prentice-Hall. TIC: 2 48548. 151246

Plinski, M.J. 2001. *Waste Package Operations Fabrication Process Report.* TDR-EBS-ND-000003 REV 02. Las Vegas, Nevada: Bechtel SAIC Company. ACC: MOL.20011003.0025. 156800

Punatar, M.K. 2001. *Summary Report of Commercial Reactor Criticality Data for Crystal River Unit 3.* TDR-UDC-NU-000001 REV 02. Las Vegas, Nevada: Bechtel SAIC Company. ACC: MOL.20010702.0087 155635

6.2 CODES, STANDARDS, REGULATIONS, AND PROCEDURES

10 CFR Part 63. Energy: Disposal of High-Level Radioactive Wastes in a Geologic Repository at Yucca Mountain, Nevada. Readily available. 156605

ASME (American Society of Mechanical Engineers) 2001. *2001 ASME Boiler and Pressure Vessel Code (includes 2002 addenda).* New York, New York: American Society of Mechanical Engineers. TIC: 251425.

DOE (U.S. Department of Energy) 2004. *Quality Assurance Requirements and Description.* DOE/RW-0333P, Rev. 16. Washington, D.C.: U.S. Department of Energy, Office of Civilian Radioactive Waste Management. ACC: DOC.20040907.0002.

AP-2.27Q, Rev. 1, ICN 4. *Planning for Science Activities.* Washington, D.C.: U.S. Department of Energy, Office of Civilian Radioactive Waste Management. ACC: DOC.20040610.0006.

AP-3.12Q, Rev. 2, ICN 2. *Design Calculations and Analyses*. Washington, D.C.: U.S. Department of Energy, Office of Civilian Radioactive Waste Management. ACC: DOC.20040318.0002.

LP-SI.11Q-BSC, Rev. 0, ICN 1. *Software Management*. Washington, D.C.: U.S. Department of Energy, Office of Civilian Radioactive Waste Management. ACC: DOC.20041005.0008.

6.3 SOFTWARE CODES

BSC 2002. *Software Code: ANSYS.* V5.6.2. HP-UX 11.00. 10364-5.6.2-01. 159357

BSC 2002. *Software Code: LS-DYNA.* V960.1106. HP9000. 10300-960.1106-00. 158898

BSC 2003. *Software Code: LS-DYNA.* V.970.3858 D MPP. HP Itanium2, HP-UX 11.22. 10300-970.3858 D MPP-00. 166918

BSC 2003. *Software Code: LS-DYNA* V970.3858 D SMP. HP Itanium2 (IA64), HP-UX 11.22. 10300-970.3858 D SMP-00. 166139

CRWMS M&O 1998. *ANSYS.* V5.4. HP-UX 10.20. 30040 5.4. 153710

CRWMS M&O 2000. *Software Code: LS-DYNA.* V950. HP 9000. 10300-950-00. 149714

Hallquist, J.O. 1998. *LS-DYNA, Theoretical Manual.* Livermore, California: Livermore Software Technology Corporation. TIC: 238997. 155373

Livermore Software Technology Corporation. 2001. *LS-DYNA Keyword User's Manual.* Version 960. Two volumes. Livermore, California: Livermore Software Technology Corporation. TIC: 252119. 159166

Livermore Software Technology Corporation. 2003. *LS-DYNA Keyword User's Manual.* Version 970. Livermore, California: Livermore Software Technology Corporation. TIC: 254203. 166841

INTENTIONALLY LEFT BLANK